Offshore Wind Turbine Monopile Foundation Installation with a Dynamic Positioned Vessel

A feasibility study by modeling

Martijn Wittingen - BSc

SDPO.18.031.m





Offshore Wind Turbine Monopile Foundation Installation with a Dynamic Positioned Vessel

A feasibility study by modeling

by

Martijn Wittingen - BSc

to obtain the degree of Master of Science at the Delft University of Technology, to be defended publicly on Monday, October 29, 2018 at 02:00 PM.

Student number: 4334892

Project duration: September, 2017 – October, 2018

Thesis committee: Ir. K. Visser, TU Delft, chairman Dr. Ir. M. Godjevac, TU Delft, supervisor

Ir. J. Ye, TU Delft, supervisor TU Delft, supervisor

Dr. Ir. H.J. de Koning Gans, TU Delft, committee member

Ir. E. El Amam,RH Marine, supervisorIr. A. Breijs,Boskalis, supervisorIr. R. van der Wal,Boskalis, supervisor

An electronic version of this thesis is available at http://repository.tudelft.nl/.



Preface

After years of studying, this thesis is the final work done to receive the Master of Science title. Special thanks to Klaas Visser, Milinko Godjevac and Jun Ye for leading me through this graduation period and to give an inside view in academic research.

I want to thank the companies RH Marine and Boskalis, specially Ehab el Amam, Alexander Breijs and Remmelt van der Wal, for their support, critical notes during the graduation period and for sharing their inside knowledge on this topic.

Last but not least, I really appreciated the support of family and friends, especially of Inge, during this sometimes challenging period.

Martijn Wittingen - BSc Delft, October 2018

Abstract

After years of using fossil fuel, the transition to renewable energy sources need to be made to limit the increase in temperature and to support the future energy demand. To support and speed up the transition phase from fossil fuels to renewables it is necessary to decrease the costs. Offshore Wind Turbines are widely used for the production of renewable energy and several Offshore Wind Turbine projects are planned for the future. Most of the Offshore Wind Turbines are founded by monopile, large steel tube, to support the wind turbine. Nowadays, these monopile be installed by either jack-up vessel or moored floating vessel. However, these installation method come with a major drawback: the installation procedure is time consuming. A new installation method is propose to reduce the installation time. This thesis focus of the feasibility to install the monopile with a dynamically positioned (DP) vessel. The required station keeping situation is faster achieved with a DP vessel. Due to the footprint of the DP vessel relative to an earth fixed position, a vessel motion compensated pile gripper is used to maintain the upright position of the monopile and to decrease the interaction forces between vessel and monopile. Adding the monopile to the vessel is an off-design condition for the DP controller. During the early hammering phase of the monopile, the monopile have limited interaction with the soil and is unstable. The upright position is maintain by the gripper frame. The forces from the gripper frame on the monopile are reaction forces on the vessel. Beside these forces, environmental forces are acting on the monopile and via the gripper frame acting on the vessel. The forces on the vessel could lead to unstable behavior and/or increased vessel footprint.

A simulation model is build to investigate the behavior of the DP vessel during the operation. A industry used DP simulator and a simulation model of the Bokalift1 is used. A model of a typical shallow water and deep water monopile is build. A hydraulic based gripper frame is simulated with an inclination controller and a induced vessel motion controller which need to maintain the upright position of the monopile. The inclination controller is tuned with a higher bandwidth compare to the bandwidth of the DP controller to prevent motions of the monopile is the same frequency range as the linear motions of the vessel. The forces from the gripper frame are fed into the Kalman filter of the DP controller. This is done to prevent a drift of the vessel when the gripper frame starts acting on the vessel.

In all simulation cases with governing environmental conditions, the vessel could maintain stable behavior. The rotations of the monopile are in the same frequency as the first order wave forces on the vessel. This relative high frequency motions to not significantly amplify the position of the DP vessel. However, despite the fact of feeding the Kalman filter, a larger drift is observed in case of the large, deep water monopile in the operation stage when the gripper frame force is introduced to the vessel. This increase the requirement on the envelope of the gripper frame. The requirement on the gripper frame is given in terms of power, force and envelope based on governing environmental conditions. The requirements on the gripper frame are assumed to be within an acceptable magnitude. The operation seams to be promising in the future.

List of Tables

	Distribution of foundation types, [EWEA, 2014-2015]	3
1.2	Comparison	4
1.3	Vessel - pile gripper frame combinations in use	4
2.1	3.3 MW Turbine MP dimensions	12
2.2	8.0 MW Turbine MP dimensions	12
2.3	Rigid/flexible calculation	16
2.4	Dynamic Positioning Pros and Cons relative to Mooring	20
2.5	Specification vessel-gripper-monopile model	34
2.6	Specification control law gripper frame	35
3.1	Output and input DP simulator	40
3.2	Range of equivalent mono-pile parameters	45
3.3	Current moment depended on mono-pile diameter, water depth and current velocity $(kN \cdot m)$	46
3.4	Wind moment depended on mono-pile diameter, water depth and wind velocity $(kN \cdot m) \dots $	47
3.5	Wind moment depended on mono-pile diameter, water depth and wind velocity	
	$(kN\cdot m) \dots \dots$	47
	Block outputs	48
3.7	Block outputs	52
3.8	Constants valve [12]	57
3.9	Required load flow	57
3.10	Overall simulation block out- and inputs	59
3.11	Environmental conditions surge and sway comparison	60
3.12	Environmental conditions roll-pitch comparison	61
3.13	Test 1 roll and pitch (deg) comparison RH marine simulator with Boskalis data	
	Hs 2.5m, Tp 7s	61
3.14	Test 2 roll and pitch (deg) comparison RH marine simulator with Boskalis data	
	Hs 2.5m, Tp 9s	61
3.15	Vessel footprint tests conditions	61
	DP footprint 'clean' vessel under environmental load	61
	Angle error between simulation and Boskalis data in (%), default inclination 0.1°	62
		62
	Variables inverse kinematic test	63
	Load flow as function of load pressure	64
	Motion reduction gripper frame	65
	Assumptions and variables simulation	69
	Environmental conditions	69
4.3	Relative magnitude stationary environmental force direction 330	70
4.4	Simulation steps	70
4.5	Comparison vessel footprint 'clean' vessel and vessel with monopile (m)	71
4.6	Increase in footprint test with monopile compare to base case (%)	72
	and Tp 9 sec	73
₸.0	and Tp 9 sec	74

viii List of Tables

4.9	Surge and sway response for a sinus wave force with an amplitude of 300 kN and Tp 100 sec	74
4.10	Surge and sway response for a sinus wave force with an amplitude of 100 kN	′ ¬
	and Tp 100 sec	74
	Required gripper frame envelope (m)	75
	Relative GF envelope compare to DP vessel footprint	75
4.13	Required hydraulic pump power (kW)	75
	Required hydraulic gripper frame force (kN)	75
4.15	Design specifications gripper frame	76
A.1	Soil parameters [27]	81
	Linear soil stiffness mono-pile, 10m diameter, (kN/m)	82
A.3	Linear soil stiffness mono-pile, 7.4m diameter, (kN/m)	83
B.1	Vessel main particular	85
	Hydrostatic and Mass properties	85
	Thruster and rudder particulars	86
	Environmental conditions roll-pitch comparison	88
	Vessel footprint tests	89
C.1	Gripper frame specifications [Boskalis]	91
D.1	FB24 main specifications	95
	FB16 main specifications	95
F.1	Environmental force direction case 1-4	99
F.2	Overview test cases 1-4	99
	Environmental force direction case 5	99
	Overview test case 5	99

Abbreviations

MCPGF = **M**otion **C**ompensated **P**ile **G**ripper **F**rame

FPGF = **F**ixed **P**ile **G**ripper **F**rame

DP = **D**ynamically **P**ositioned

OWT = **O**ffshore **W**ind **T**urbine

ILT = **I**nternal **L**ifting **T**ool

DoF = **D**egrees **o**f **F**reedom

LAT = **LAT**itude

LON = LONgitude

GF = **G**ripper **F**rame

DNV = **D**et **N**orske **V**eritas

API = **A**merican **P**etroleum **I**nstitute

NED = **N**orth **E**ast **D**own

Contents

Pr	eface		iii
Αk	ostrac	et	٧
Lis	st of ⁻	Tables	vii
Αk	brev	iations	ix
1	1.1 1.2	Need for speed	3 4 4 6
	1.4 1.5 1.6 1.7	Problem description	8 9 10
2		Monopile	11 13
	2.2	DP system	21
	2.3	Hydraulic frame. 2.3.1 Ship motion compensated platforms 2.3.2 Hydraulic system components. Kinematics.	24 27 28
	2.5	2.4.1 Reference frames	29 33 33 33
3	Sim (3.1	Dynamic Positioning simulator. 3.1.1 DP control system 3.1.2 Simulated vessel	39 39 40 40
		3.2.1 Monopile model	47

xii Contents

		N 4l - l	and the second	00
	3.3	3.3.1 3.3.2 3.3.3 3.3.4 3.3.5 3.3.6 3.3.7 3.3.8	verification	. 60 . 61 . 61 . 62 . 62 . 64
4	Sve	tem an	alveie	67
-	4.1 4.2	Grippe Envelo 4.2.1 4.2.2 4.2.3 4.2.4 4.2.5 4.2.6 4.2.7 4.2.8 Conclu	er frame force feed forward ope and capacity requirements by case studies Simulation objectives Variables and assumptions Environmental conditions Direction environmental force Simulation steps Simulation results. Simulation analysis. Gripper frame requirements usion	. 67 . 68 . 68 . 69 . 70 . 71 . 71
5	5.1	Conclu	ns, recommendations and limitations usions nmendations and limitations	
Α	Р-у	curves		81
В	Ves	sel deta	ails	85
_		B.0.1 B.0.2 B.0.3	Vessel specifications	. 85 . 87 . 88
С	Hyd	C.0.1 C.0.2	Gripper Frame details Gripper frame specifications	. 91
D	Mon		details Monopile properties	
Ε	Hyd	ro ham	nmer details	97
F	Sim	ulation	results	99
Bi	bliog	raphy		109

Introduction

This chapter will introduce the reader into the subject and present the relevance of this research. A background on the development of offshore wind and mono-pile installation is given, followed by the problem description, research objective, methodology and a thesis outline.

1.1. Need for speed

Since the industrial revolution, lots of the earth fossil fuel resources are used to make our life easier. Fossil fuels are used for transportation, electrical energy production, for cooling or heating of buildings, the production chain and so on. Fossil fuels are one of the main drivers of the industrial revolution. But it also comes with a drawback.

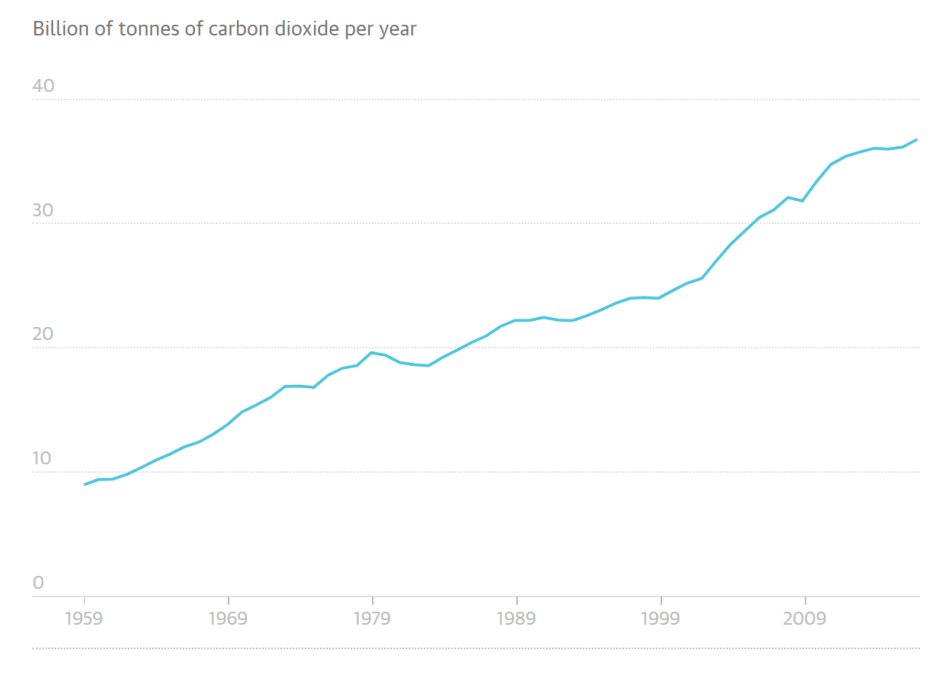


Figure 1.1: Global carbon emission in the last 50 years, [The Gardian 2017]

Figure 1.1 shows the development of global carbon emissions during the last 50 years. The increase of CO2 concentration in the air results in global warming. Some effects of global warming are recognized by National Geographic [21]:

• Melting ice at the poles

2 1. Introduction

- Quick rise of the sea level the last century
- Increase in precipitation, on average, across the globe

To limit the effects of global warming to acceptable consequences, the Paris Agreement in 2015 [33] makes an agreement to accept an increase in temperature with a maximum value of 2 degrees Celsius above pre-industrial levels and to put effort to limit the temperature rise even further to a maximum value of 1.5 degrees Celsius. The parties aim to reach the peak of greenhouse gas emission as soon as possible.

Furthermore, the Dutch government notices the advantage of being less dependent on international energy suppliers and be more self-sufficient [6].

The meet the Paris Agreements and to be independent in the future, countries are forced to invest in sustainable solutions for electrical power generation. The sun is a sustainable and never ending energy source. With the help of solar panels, solar power towers, hydro-electric installations, bio-energy installations or on- and offshore wind turbines, the solar energy can be used for the generation of electrical energy. When dividing the earth surface virtually into parts, for every area, there will be an optimal solution to convert sustainable energy into electrical energy. For example, in the Sahara desert, with high sun strength and low wind speeds, solar panels or solar power towers are preferable solutions above wind turbines. In Europe where the sun strength is lower, countries population density is higher (area's for building installation are not widely available) and wind strength, especially at sea, is higher, offshore wind turbines (OWT) are the solution to contribute to the energy transition. Electrical energy generation by OWT's is a well-developed method in the last 30 years which provide a significant amount of energy compare to other offshore sustainable energy installations such as Tide Energy. As a conclusion: Offshore Wind Energy is the preferable solution in Europe to carry the energy transition in order to retain a livable planet.

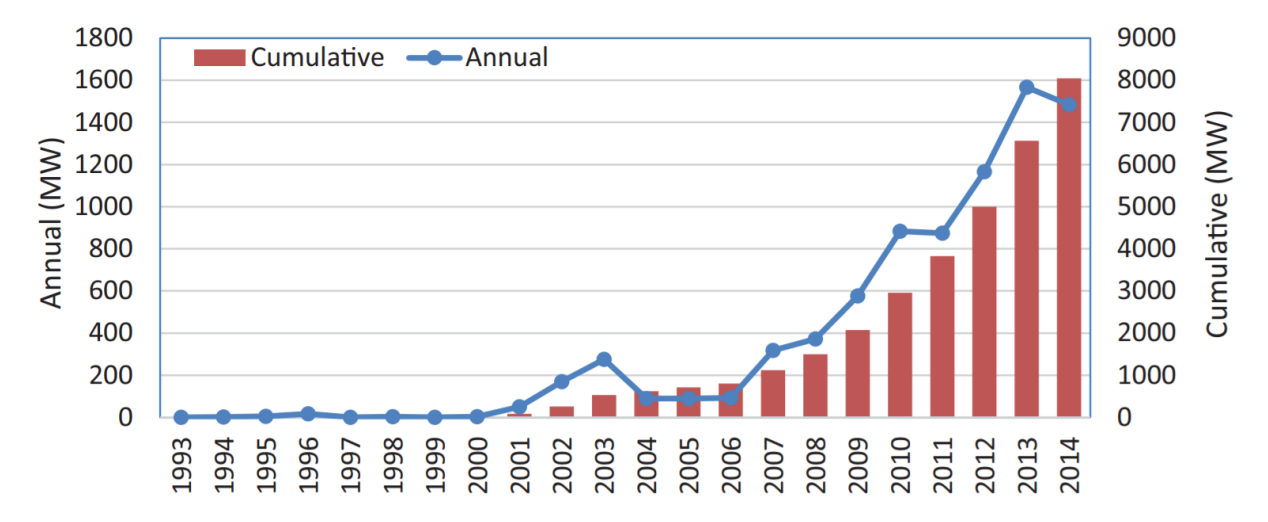


Figure 1.2: Growth offshore wind in Europe, [30]

Large growth Figure 1.2 shows the growth of the offshore wind energy market in Europe of the last 21 years till 2014. An exponential growth can be recognized.

When considering the capacity of approximately 5 MW per turbine, the number of offshore wind turbines installed in 2014 is in order of 300 turbines. The figure for the future is in a completely different order. There is a need for 250 GW installed offshore wind power in the Southern part of the North Sea during the years till 2050 in total. This equals 25.000 10MW turbines. With the present installation rate of 2.5 GW/year, the European countries involved in building offshore wind parks have to speed up the process to 7.5 GW/year at least,

which are 750 10MW turbines per year. This accounts for a linear increase in capacity, it is plausible that the maximum rate of capacity increase will be higher.

1.2. Offshore wind turbine foundations

According (Moné et al., 2015, [37]) the installation and assembly cost of an offshore wind turbine is in order of 20 % of the total cost. This is a significant higher value compared to 6% for land wind turbines. To speed up the energy transition and to compete with other sustainable and non-sustainable energy sources, it is necessary to decrease the installation and assembly costs.

It is necessary to cut costs in every cost component but this thesis focus on the decrease in installation costs of the turbine foundation. The different types of foundation can be split up in two main categories: floating and bottom fixed foundation. Floating foundations are from financial point of view more feasible at location with a water depth of more than 100 m. Bottom fixed foundations are used in shallow water. Bottom fixed foundation is a proven concept in contrast to floating foundation which is still in the experimental phase.

Figure 1.3 shows an overview of widely used bottom fixed offshore wind turbine foundations.

Several types of bottom fixed OWT foundations are developed. Circumstances influencing the choice of a foundation type are:

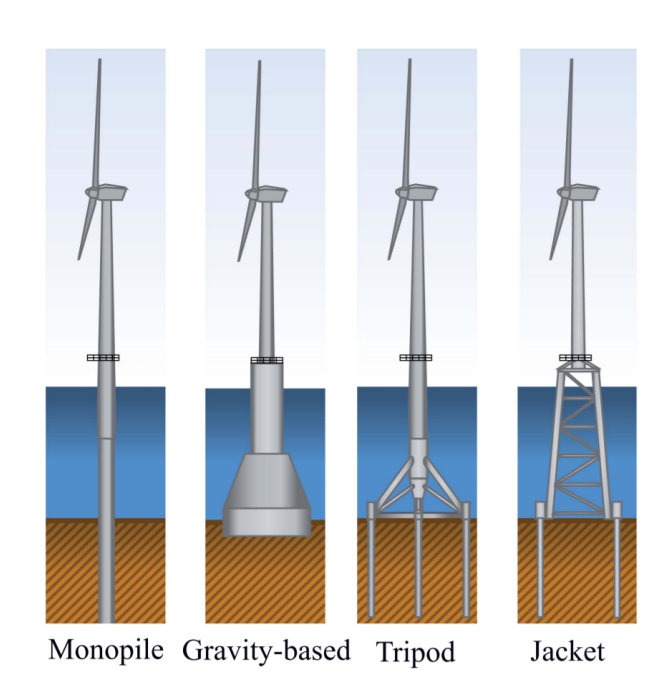


Figure 1.3: Various OWT foundations, [Wiser et al., 2011, [44]]

- Water depth
- Soil properties

Foundation Type	Total installed till 2014	Annually installed 2013	Annually installed 2014
Mono-pile	78.8%	79%	91%
Gravity-based	10.4%	0.2%	0 %
Jacket	4.70%	14 %	8.10%
Tripod	4.10%	6%	0.90%

Table 1.1: Distribution of foundation types, [EWEA, 2014-2015]

A monopile foundation is widely used foundation method for the sake of simplicity with respect to fabrication compare to other foundation methods [30]. A monopile consists of several rolled plates welded together into one solid, massive pile. By increasing the diameter and wall thickness of the monopile, this solution is still feasible for future wind turbines which are expected to be larger in size. According table 1.1, monopile are taking the major part of the applied foundations and therefore the subject of the research. This thesis will investigate the possibility of a new, possible less time consuming, monopile installation method in order to decrease installation costs.

4 1. Introduction

1.3. Monopile installation

This section gives a brief introduction in the systems involved in monopile installation, nowadays installation methods and the installation sequence.

1.3.1. Current monopile installation methods

Several equipment is necessary for the installation of a monopile. The three major components are a crane, a vessel and a monopile gripper frame. The crane mounted on a vessel is used to upend the monopile and and placed it on the seabed. The monopile is lifted into a gripper frame which maintain the upright position of the monopile. An analogy can be made with driving a nail into the wood. The gripper frame have the same functionally as the fingers which is holding the nail.

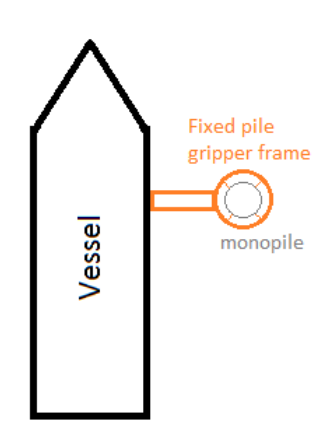


Real	Analogy
Vessel	Human body
Gripper frame	Fingers
Monopile	Nail
Hydro hammer	Hammer
Crane	-

Figure 1.4: Driving a nail

Table 1.2: Comparison

As seen in past projects, two types of installation vessels are used: a **jack-up vessel** and a **moored**, **floating vessels**. Two types of gripper frame concepts are used: a **fixed pile gripper** frame or a **dynamic/vessel motion compensated pile gripper frame** is used. Both gripper frame concepts are visualized in figure ?? and ??.



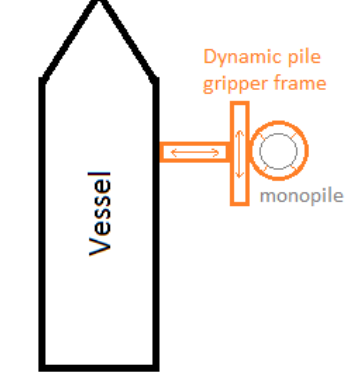


Figure 1.5: Fixed pile gripper frame

Figure 1.6: Motion compensated pile gripper frame

The position of the pile, in case of a fixed pile gripper frame, is fixed with respect to the vessel. The position of the monopile relative to the vessel can be controlled in case of a vessel motion compensated gripper frame. This implies, the other way around, that the dynamic part of the gripper frame is able to maintain a fixed position relative to an earth fixed point while connected to a moving vessel. The following combinations of vessels and gripper frames are used in the past.

Vessel	Pile gripper frame
Jack-up	Fixed frame
Moored	Fixed frame
Moored	Motion compensated gripper frame

Table 1.3: Vessel - pile gripper frame combinations in use

Reference projects with the three installation methods are listed below.

Jack-up vessel

A jack-up vessel uses legs settling down on the seabed to guarantee a fixed position relative to an earth fixed position. A monopile is lifted in a **fixed pile gripper frame**, lowered to the seabed and driven into the soil with a hydro hammer. The use of a jack-up vessel has proven to be successful in projects in the past because minor vessel motions are induced due to the environmental load. However, the jack-up method comes with a major drawback. Jacking a vessel is a time consuming operation. The time used for pile driving is in the same order as jacking-up the installation vessel [11]. Questions raised about the costs effectiveness of using jack-up vessel in the case of relative short offshore operations such as monopile installation.

SeaJacks Scylla, with a fixed pile gripper frame used by the consortium Boskalis and SeaJacks to install the 1300 mT mono-pile foundations for the Veja Mate wind farm, see figure 1.7. SeaJacks Scylla have a length of 140 meters, a width of 50 meters and a draft of 7.5 meters. With her 105 meter long legs, she can install monopile in a water depth up to 65 meters.



Figure 1.7: Mono-pile installation with the Scylla, [Boskalis, 2016]

Moored vessel

As already mentioned, moored, floating vessels are also used for monopile installation. Mooring lines keep the vessel stationary relative to the earth fixed location close to the position where the monopile is driven into the seabed. A catenary system or a taut leg system can be used. In a catenary system, the restoring force is generated by the weight of the mooring line. In a taut leg system by the elasticity of the mooring line. In both cases the vessel will have a footprint relative to the seabed. The footprint depend on the number of mooring lines, pretension in the mooring lines, mass of the mooring lines and the environmental conditions. A moored vessel is a passive motion compensated system. The mooring force is proportional to the vessel offset.

Both fixed or vessel motion compensated gripper frames are used to guarantee an upright position of the monopile during driving into the seabed. In case of a fixed gripper frame, the motions of the vessel are more limiting the operation because due to the rigid connection between vessel and monopile, the motion of the vessel are directly translated into motion of the monopile. For that reason, the weather window in which the operation can carried out is relative small [11]. A vessel motion compensated frame could be used to increase the weather window. In that case, the induced motions of the vessel can be compensated by the motion compensated gripper frame. This reduce the interaction force between vessel and

6 1. Introduction

monopile and the induced motions of the monopile due to the motions of the vessel. Larger vessel motions are allowed which implies an increase in weather window. Mooring is time consuming, 40% of the installation duration is used for mooring the vessel [38]. Next to that, extra anchor handling vessel are required.

HLV Svanen, with a **fixed pile gripper frame** used by Van Oord to install monopile foundations for the Arkona wind farm completed in 2017. The monopiles used for the project weighing up to 1200 mT, see figure 1.8

Oleg Strashnov, with a **motion compensated gripper frame** used by Seaway Heavy Lifting (SHL) to install 800-1200 mT mono-pile foundations. The induced vessel footprint by environmental forces on the vessel is passively compensated by the mooring lines. The inevitable motions of the vessel in the horizontal plane and rotation are compensated by the gripper frame to reduce the induced motions of the monopile and the interaction forces between vessel and monopile. This increases the operational weather window [11].





Figure 1.8: Mono-pile installation with the Svanen, [Van Oord, 2017]

Figure 1.9: Mono-pile installation with the Oleg Strashnov, [heavyliftnews, 2016]

As a conclusion, all the three installation methods come with at least one major drawback, namely time. By increasing the number of monopiles installed per day, the installation cost will decrease. Furthermore, a moored vessel or a jack-up can not change the heading during operation which can lead to more unfavorable vessel motions and a smaller operational weather window. Weathervaning can reduce this effect.

1.3.2. Monopile installation sequence

Six steps can be distinguished in the installation procedure of monopiles.

Phase 1 First of all, the monopile is transported from the production facility to the installation site. This can be done in several ways. With end caps, the monopile can be made floating and towed by a tug to the side. Or the monopile can be placed on a barge or on the deck of the installation vessel.

Phase 2 The monopile is transported horizontally, so it is necessary to up-end the monopile before installation. Up-ending is done with a crane mounted on the installation vessel. During up-ending, horizontal and vertical loads act on the crane (and vessel).

Phase 3 After up-ending the monopile, the monopile is hanging vertically in the crane. The monopile is lowered, through the splash zone, and set down on the sea bed. The first order wave forces on the monopile while lowering through the splash zone and the motions of the vessel (roll and pitch motions introduces relative large crane tip motions) induces monopile motions.

Phase 4 The monopile set down on the sea bed. The earth fixed location of the monopile bottom end is determined. The monopile roughly self penetrates the sea bed half the pile diameter due to its own weight [30]. This depends upon the soil properties. The crane wire is still attached to the monopile so crane tip motions and wave forces applies forces on the monopile. These forces are counteracted by the interaction between soil and monopile. The gripper frame is attached to the monopile.

Phase 5 The ILT connected to the crane is disconnected from the monopile and a hydro hammer is picked up from the vessel deck and placed on top of the monopile to hammer the monopile into the soil. The monopile acts as an inverted pendulum due to the limited

monopile soil interaction [30]. This means unstable behavior of the monopile without maintaining the upright position of the monopile by the pile gripper frame. During this installation phase, the monopile is hammered into the soil to a penetration depth for which the monopile can maintain upright position under monopile soil interaction. The gripper frame disconnects from the monopile, the inclination is measured and corrected to the installation requirement with respect and the monopile is hammered into the soil to its final penetration depth.

Phase 6 The monopile reach its final penetration depth. The gripper frame has already released the monopile. The hydro hammer will be recovered back on the vessel deck.

Finish The monopile is installed. The offshore operation can be extended by installing the transition piece. After finishing the operation, the installation vessel sails away to the next installation site.

The operation sequence is visualized in figure 1.10.

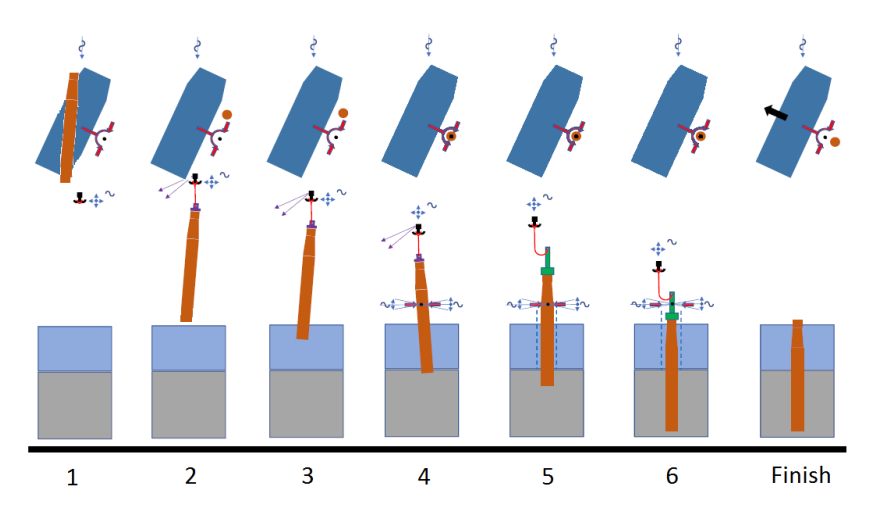


Figure 1.10: Operational sequence mono-pile installation, respectively top view and side view

1.3.3. Proposed monopile installation method

In the early 60s, another method has been developed to achieve station keeping under environmental load, namely Dynamic Positioning (DP). A DP system makes use of own vessel propulsion to counteract for environmental forces. Compared to a jack-up or a moored vessel, achieving the station keeping situation is less time consuming for a DP vessel. A DP vessel will have a certain footprint around its set position due to the time-varying environmental forces acting on the vessel. The magnitude of this offset is depended on environmental conditions, vessel size, installed power, thruster dynamics, DP controller design, etc. To counteract for those vessel motions, to keep the interaction force between monopile and vessel as low as possible and to increase the operational weather window, a vessel motion compensated gripper frame is required to compensate for vessel motion and to maintain upright position of the monopile.

The use of a DP vessel instead of a jack-up or moored vessel is preferable mainly for the foreseen cut in installation time. Beside that, a DP vessel can apply weathervaning to reduce the environment load on the vessel which increase the operational weather window. Question raise about the cost effectiveness of using a jack-up vessel instead of a floating vessel because of the relative large total installation time compare to the time used for pile hammering. The reason to do research on this topic are the possible problems in vessel station keeping which can occur when using a DP vessel in a monopile installation operation. Furthermore, the operation is never carried out. Research is necessary to minimize the risks and to have a more clear view into the system behavior. More about the problem description can be found in section 1.4.

8 1. Introduction

1.4. Problem description

Environmental forces are acting on the vessel in a normal DP operation. In the past, DP control systems are designed to compensate for these forces with the thrusters. However, when extra forces are acting on the vessel, the DP behavior of the vessel could change. In this particular offshore operation, depended on the installation phase, these forces are composed of crane forces, environmental forces on the monopile, forces from the gripper frame to counteract the instable tendency of the monopile and mooring forces from the monopile when the monopile have a reasonable penetration depth. Adding the gripper frame and monopile to the vessel is an off-design condition for the DP vessel. Because of the unknown behavior of the system i.e. the influence on the vessel due to the forces applied by the motion compensate gripper frame on the vessel, it is valuable to do research on the topic; the operation is new so no operational data of the combined operation is available. This thesis should be read as a feasibility study. DP performance issues occur in the past with a DP vessel carrying out a heavy lift operation, see figure 1.11.

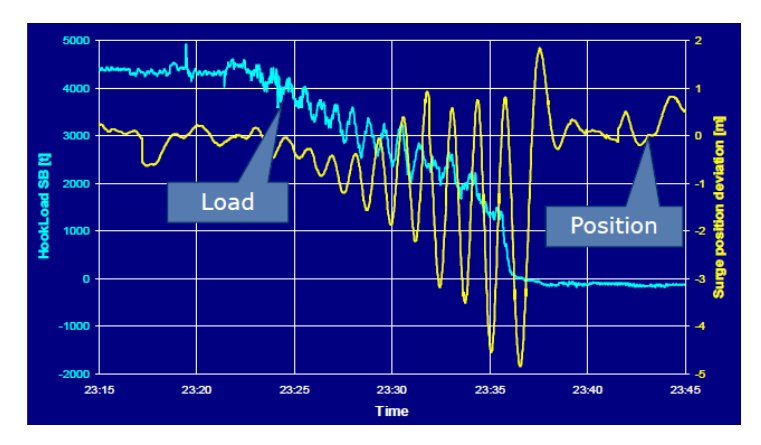




Figure 1.11: Incident during a DP heavy lift operation [43]

Figure 1.12: Crane operation (HMC)

While the topside was placed on a jacket, the load was transfered from the crane wires to the jacket, the vessel starts to oscillate around its set point with an increasing amplitude (yellow line, figure 1.11). The horizontal force in the crane wire (blue line, figure 1.11) acts as a mooring stiffness on the DP vessel. The magnitude of the mooring force is depended on the offset of the vessel from its set point. A more detailed description of the problem can be found in [8]. The disturb in performance of a DP vessel in case of large, irregular and intermittent loads acting on the vessel is also mentioned by [23]. Relative stationary forces on the vessel, unknown by the DP control system may lead to a drift of the vessel [13]. The conclusion can be made that large force acting on the vessel, which are unknown for the DP control system, can influence the DP performance of the vessel significantly. Two issues can be distinguished: **DP stability issues** and **enlarged footprint issues**

The footprint of the vessel is directly related to the envelope of the gripper frame. The larger the vessel footprint, the larger the required envelope of the gripper frame. The gripper frame will be designed for a vessel with a stable DP behavior so unstable DP behavior have to be prevented anyhow. Furthermore, the magnitude of the vessel footprint is limited because of the limited envelope of the gripper frame. A small required envelope of the gripper frame is preferable. This increases the cost effectiveness of the operation.

Next to the mentioned problem, the overall system consists of two dynamic systems, namely: the DP vessel and the monopile/gripper frame combination. The gripper frame needs to be able to compensate for the induced motions of the vessel without destabilizing the monopile. A destabilized monopile could also destabilize the vessel which could possible lead to a loss of the monopile or a dangerous situation for on board personnel.

1.5. Objectives and methodology

The objective of this research is to investigate how the forces from the gripper frame on the vessel will influence the DP behavior of the vessel and furthermore investigate what the influence is of specific system parameters on the overall performance of the system. The overall performance of the system can be defined as the ability of the systems to guarantee stable vessel behavior, respect acceptable geometrical limits of the gripper frame and maintain upright position of the monopile. The main objective is formulated below:

"Investigate the influence of the installation force, applied by the motion compensate pile gripper frame, on the DP performance of the vessel and investigate the feasibility of the operation in terms of gripper frame requirements"

The following methodology is used to obtain the main objective:

- 1. Literature review
 - Literature review on monopiles, environmental forces, DP control system, motion compensated systems, hydraulic system components and ship motions frames
 - Stability of a dual dynamic system
- 2. Setup simulation model
 - Verify and implement the, from the industry available, DP control system and 5 DOF vessel simulator in Matlab/Simulink
 - Build a mathematic model of a monopile which represent realistic behavior under influence of environmental forces, monopile soil interaction and external forces applied by the gripper frame
 - Develop gripper frame model including monopile inclination controller and a induced vessel motion compensation controller based on typical characteristics of a hydraulic system
 - Calculation of the motions of the fixed part of the gripper frame due to the 5DOF vessel motions to calculate the required motion compensation by the dynamic part of the gripper frame in vessel surge and sway direction
 - \bullet Combine these separate models into an overall system
- 3. Analysis of system dynamics
 - Investigate the nature of the installation forces acting on the vessel, and determine if stability problems are an issue
 - Investigate if the proposed interaction (kalman filter feed forward) between controllers is sufficient to maintain stable behavior of the vessel
 - Determine, based on governing test cases, the feasibility of the operation is terms of requirements on the motion compensated pile gripper frame

10 1. Introduction

1.6. Thesis scope

The DP vessel simulator of the company RH Marine is used as a starting point. The Dynamic Positioned vessel model consists of two blocks. The DP controller and a model of the vessel. Both a provided by the company RH Marine. The DP controller is industry used and therefore, realistic behavior of the DP controller is assumed. The vessel model is a model of the Bokalift1 from the company Boskalis and consist of a hydrodynamic model of the vessel, thrusters and sensors. The modeled vessel is comparable in dimension with other construction vessels and therefore fixed in this research. The DP controller is a black box.

The early hammering phase (start of installation phase 5) of the monopile is analyzed. The monopile have limited soil interaction and therefore the monopile acts as an inverted pendulum. The hydro hammer placed on top of the monopile contributes to the unstable behavior of the monopile. Installation phase 5 is governing in terms of risk. The installation procedure can be stopped in the other installation phases when something goes wrong or weather circumstance deteriorate beyond acceptable limits. The monopile can be lifted back on deck during the crane operation or the gripper can be released in the case when the monopile have sufficient penetration depth. However, during the early hammering phase in installation phase 5, the installation have to be continued. The crane is not connected to the monopile anymore. Releasing the monopile from the gripper frame means a loss of the monopile and potential danger for on board personnel. The monopile in clamped in the gripper frame. Losing position of the vessel may damage the gripper frame and/or monopile.

The monopile and vessel are subject to environmental forces from wind, waves and current.

The motion compensated pile gripper frame is based on a hydraulic system model. This is a proven concept used for monopile installation in the past and other offshore vessel motion compensation application in the past.

The feasibility study is done two sizes of monopile and for governing environmental conditions to investigate the sensitivity of this parameters on the performance of the overall system.

1.7. Thesis outline

Chapter one: Introduction Chapter two: Literature review

Chapter three: Simulation setup and verification

Chapter four: System analysis

Chapter two: Conclusions, recommendations and limitations

 \sum

Literature review

A literature review is performed in order to get an insight view on the subjects involved in this research. Four domains can be distinguished and are summarized below in one sentence:

'Offshore Wind Turbine monopile installation with a **Dynamic Positioned vessel** and a controlled hydraulic monopile gripper frame to compensate for induced vessel motions'

All these subjects come along in separate sections. The section 'monopile' discusses the dynamic behavior of the monopile under environmental load, external load and interaction with the soil. The literature review on 'DP vessels' contains theoretical information on the working principle of a DP system in general especially with a focus on the DP control system. The next paragraph is devoted to the working principles of hydraulic systems. And last but not least, this part of the chapter describes the reference frames, give the definition of the vessel state in the inertial and body-fixed frame and describe rotation and transformation matrices to switch between frames. Beside the mentioned subjects, research is done on the stability of two interacting dynamic systems. The information, collected in this literature review will be the fundamentals of the simulation carried out and discussed in chapter 3.

2.1. Monopile

2.1.1. Monopile dimensions

A monopile is used to fix the tower with a nacelle of an offshore wind turbine to the earth. In most cases, the tower is connected to the monopile via a transition piece.

12 2. Literature review

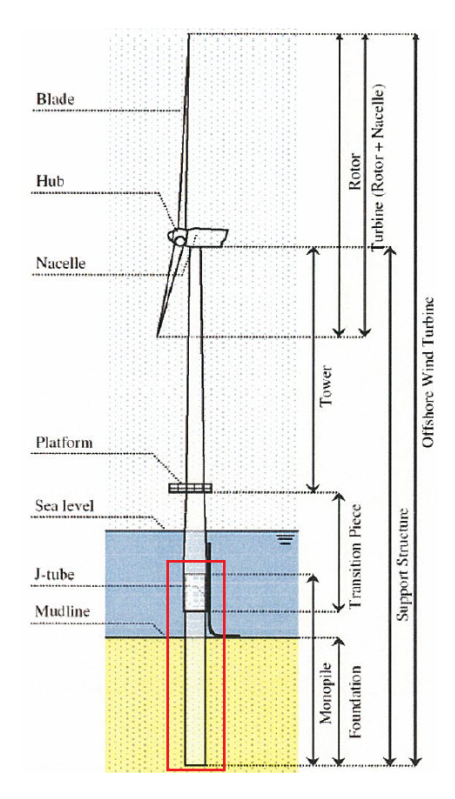


Figure 2.1: Overview Offshore Wind Turbine components

Figure 2.1 shows all the relevant parts of an offshore wind turbine. The monopile is the steel tube half under and half above the mud line. The interaction between monopile and soil provide the construction the strength to withstand environmental forces.

As mentioned before, the monopile is still a widely used foundation method for offshore wind turbines. In 2014, more than 90% of the offshore wind turbines are founded on monopiles. For the reason of decreasing the cost of offshore energy, the turbine sizes are scaling up. Till 2015, most of the installed turbines were in the range of 3-5 MW capacity. Nowaday installed wind turbines are in top of the 5-10 MW range. The consequences for the mass and size of the monopile foundation are stated in [18] and shown in table 2.1 and 2.2.

3.3 MW TURBINE							
Water depth [m]	Embedded length [m]	Total length [m]	Diameter (in soil) [m]	Thickness (in soil) [mm]	Weight [mT]		
15	20.4	35.4	7.0	90	488.1		
20	22.4	42.4	7.0	90	577.1		
25	23.2	48.2	7.0	90	647.8		
30	27	57.0	7.0	90	764.5		
35	33	68.0	7.0	95	942.6		
40	38	78.0	7.0	110	1252.2		

Table 2.1: 3.3 MW Turbine MP dimensions

8.0 MW TURBINE						
Water depth [m]	Embedded length [m]	Total length [m]	Diameter (in soil) [m]	Thickness (in soil) [mm]	Weight [mT]	
15	25	40.0	9.0	100	841.0	
20	27	47.0	9.0	105	1011.5	
25	29	54.0	9.0	110	1186.4	
30	30	60.0	9.0	110	1308.0	
35	33	68.0	9.0	110	1477.7	
40	39	79.0	9.0	110	1719.8	
45	42	87.0	9.0	125	2155.4	
50	50	100.0	9.0	140	2743.3	

Table 2.2: 8.0 MW Turbine MP dimensions

2.1. Monopile 13

In the near future, turbine sizes and water depth of installation sites will be increased. The monopiles to be installed in the future are in the range of 900 - 2800 mT.

For this thesis, it is relevant to study the dynamic behavior of a monopile, placed in the sea bed soil, under environmental load and beside that, the force from the dynamic gripper frame acting on the monopile. Two areas of research can be distinguished. The interaction between monopile and soil and the forces on the monopile due to the environmental load from, waves, wind and current force.

2.1.2. Monopile soil interaction

Soil resistance standards in lateral direction used by Germianischer Lloyd (GL) [5], American Petroleum Institute (API, 1993) [42] and Det Norske Veritas are based on the p-y curve method. The non-linear relation between soil resistance (p) and pile deflection (y) is described by this curve. The development of p-y curve is based on the following (empirical) research [10]:

- A serie of linear-elastic uncoupled springs which represents the soil, introduced by Winkler (1867)
- Reese and Matlock (1956) propose the basis principles of the nowaday widely used p-y curve
- Full scale test at Mustang Island in 1966 and the results are processed by Cox et al. (1970)
- Semi-emperical p-y curve expression based on the Mustang Island test by Reese et al. (1974)
- The p-y curve proposed by Reese et al. are compared by Murchison and O'Neill (1984) to a database of lateral pile load tests

The soil resistance is depended on the type of soil and typical parameter such as angle of internal friction and density. The force on a certain point on the monopile and the resistance force from the soil is schematically visualized by figure 2.2.

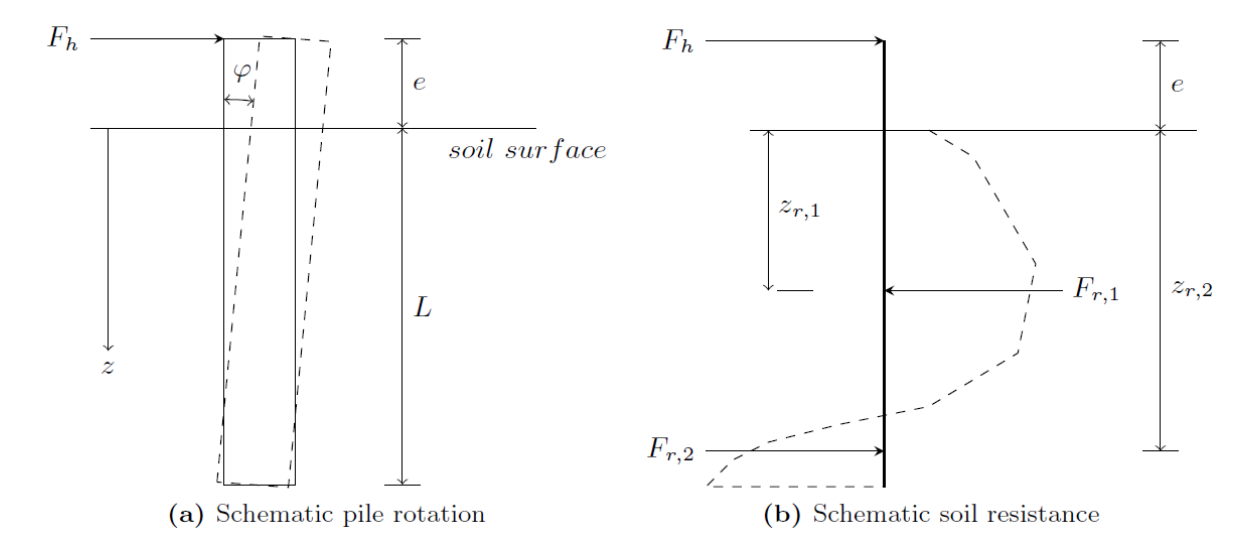


Figure 2.2: Pile rotation and corresponding soil resistance [3]

14 2. Literature review

A increasing soil stiffness is observed with increasing depth. The monopile rotates approximately around 0.8 time the penetrated pile length [24]. The soil resistance is depended on the depth. The lateral force from the soil composed from the p-y curve is given by 2.1. The spring stiffness is determined from the p-y curve.

$$P(z) = E_{py} * y(z) \tag{2.1}$$

As mentioned before, the p-y curve represents a non-linear relation between displacement and force. However, the first part of the p-y curve shows a linear relation between the resistance force and the pile displacement. This is valid for small pile displacement.

P-y curve construction according API The regulation code (API and DNV) propose a formulation for the ultimate soil resistance p_u is given by the minimum value of equations 2.2 and 2.3.

$$p_{us} = (C_1 * z + C_2 * D) * \gamma * z$$
 (2.2)

And:

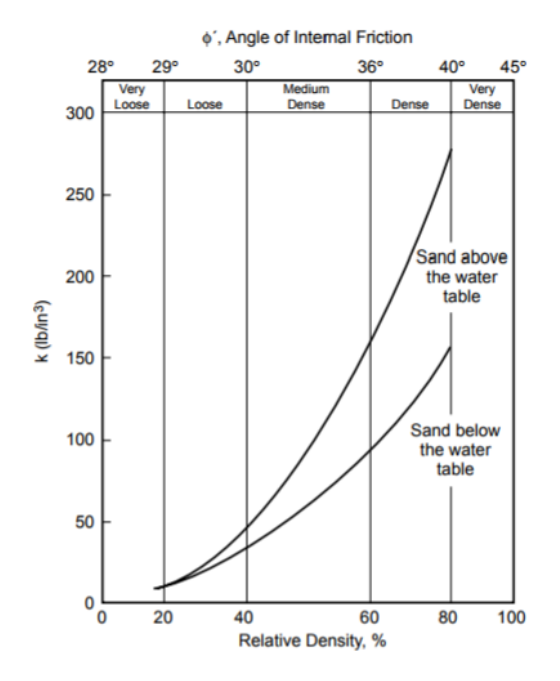
$$p_{ud} = C_3 * D * \gamma * z \tag{2.3}$$

With:

- p_{ij} is the ultimate soil resistance (s = shallow, d = deep) in (kN/m)
- Y is the effective soil weight in (kN/m^3)
- z is soil depth (m)
- D is average pile diameter (m)
- \bullet $\text{C}_1\text{, }\text{C}_2$ and C_3 are dimensionless parameters

 C_1 , C_2 and C_3 are function of angle of internal friction according the figure 2.4. These parameter were empirically determined in scale tests. The angle of internal friction is a shear strength parameter of soils. Its definition is derived from the Mohr-Coulomb failure criterion and it is used to describe the friction shear resistance of soils together with the normal effective stress.

2.1. Monopile 15



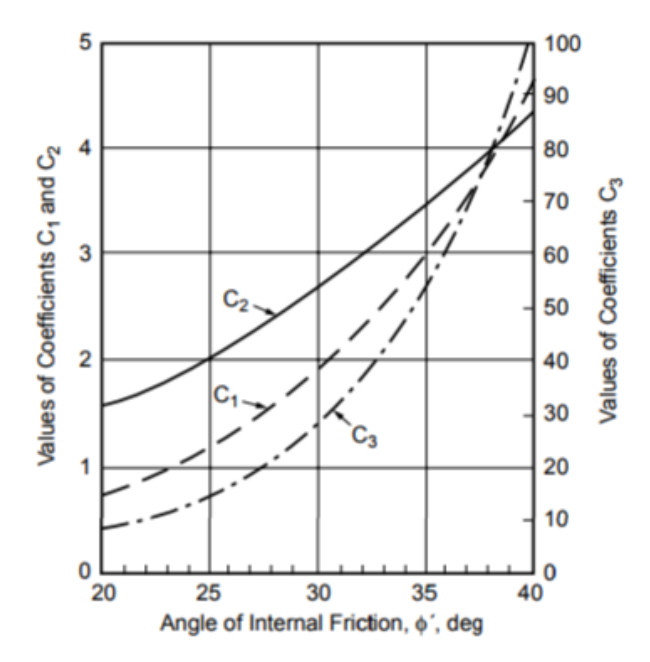


Figure 2.3: Initial modulus of subgrade 'k' as function of the angle of internal friction

Figure 2.4: Dimensionless parameters C1, C2 and C3 as function of the angle of internal friction

The lateral soil resistance-deflection relationships for sand may be approximated at any specific depth by the following expression:

$$P = A * p_u * tanh(\frac{k * z}{A * p_u} * y)$$
(2.4)

With:

- \bullet P is the soil resistance as function of the depth (kN/m)
- A is factor to account for cyclic or static loading condition (-)
- y is the lateral deflection (m)
- k is the initial modulus of sub-grade reaction (kN/m^3)

For cyclic loading:

$$A = 0.9 \tag{2.5}$$

For static loading:

$$A = (3.0 - 0.8 \frac{z}{D}) \ge 0.9 \tag{2.6}$$

The initial modulus of subgrade reaction is determined as function of the friction angle according figure 2.3

A p-y curve can be construct for a number of soil layers. The Winkler approach can be used to combine these separate uncoupled springs acting on specific location on the monopile. This approach is shown in figure 2.5.

16 2. Literature review

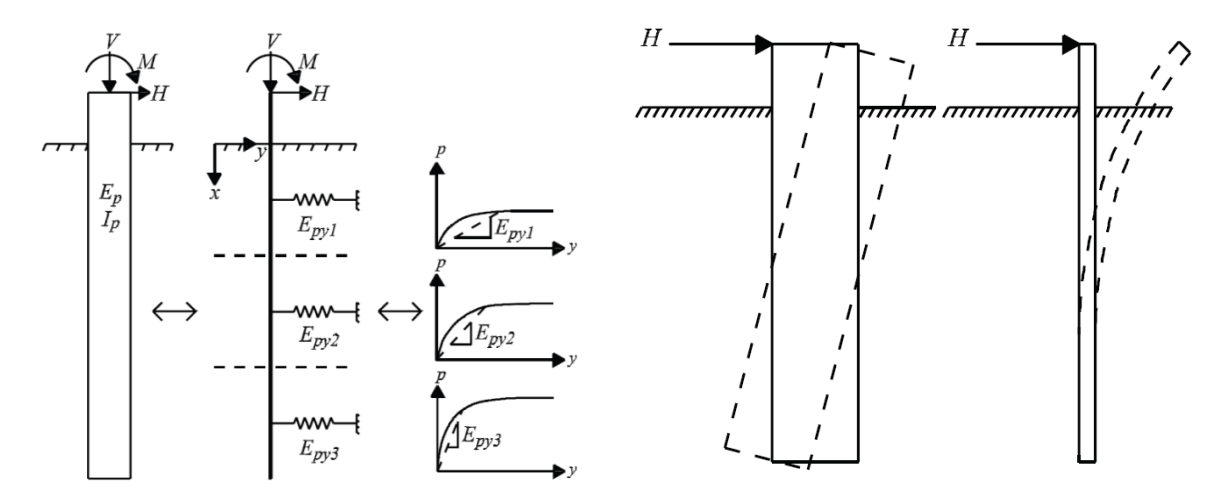


Figure 2.5: Winkler approach with non-linear uncoupled springs

Figure 2.6: Difference in behavior between rigid and flexible piles under horizontal load

Limitations API formulation The p-y curve formulation are based on full scale tests with pile diameters much smaller than 10 m diameter which are nowadays normal pile diameters for large size Offshore Wind Turbines. The piles tested at Mustang Island had a slenderness ratio of $L_{\rm em}/D=34.4$. $L_{\rm em}$ is the embedded length. Monopiles with a diameter of 10 meter and an embedded length in order of 40 meter have a slenderness ratio in order of 4. During the early hammering phase, i.e. when the monopile have a limited penetration depth in order of 40% of the pile diameter [30], the slenderness ratio is even lower. The difference in behavior of rigid and flexible piles is visualized in figure 2.6.

Poulus and Hull (1989) [22] formulates a definition for rigid or flexible behavior of a monopile. Rigid behavior when:

$$L_{em} < 1.48 \left(\frac{E_p I_p}{E_s}\right)^{0.25} \tag{2.7}$$

And flexible when:

$$L_{em} > 4.44 \left(\frac{E_p I_p}{E_s}\right)^{0.25} \tag{2.8}$$

With:

- E_p is young modulus of steel (N/m²)
- I_p is the area moment of inertia of the monopile (m^4)
- E_s is young modulus of soil (N/m²)

D (m)	t _w (cm)	Rigid when L _{em} (m) < than:	Flexible when L _{em} (m) > than:
5	5	9.2	27.6
10	10	18.4	55.2

Table 2.3: Rigid/flexible calculation

Rigid behavior of the monopile is assumed during the early hammering phase, so the structural stiffness need not to be incorporated in the monopile soil stiffness calculation.

Alderlieste (2011) [3] investigate the effect of an increase in diameter on the accuracy of the p-y curve with experiments. Both 2.2 m and 4.4 m diameter mono-piles are investigated

2.1. Monopile 17

respectively with an embedded length of 11 m and 22 m. Figure 2.7 shows the overestimation of the ultimate soil strength by the API approach when certain soil parameters are wrongly chosen.

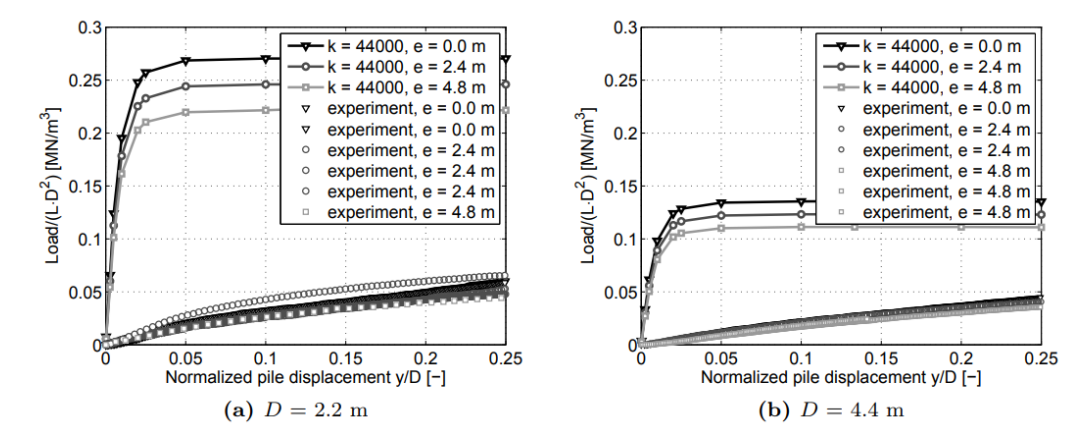


Figure 2.7: Comparison of experimental results with standard p-y curve

The initial modulus of subgrade 'k' is a function of the angle of internal friction, according figure 2.3. Alderlieste stated that with an adapted initial modulus of 'k(z)', a better fit can be made between the API approach and the experimental results.

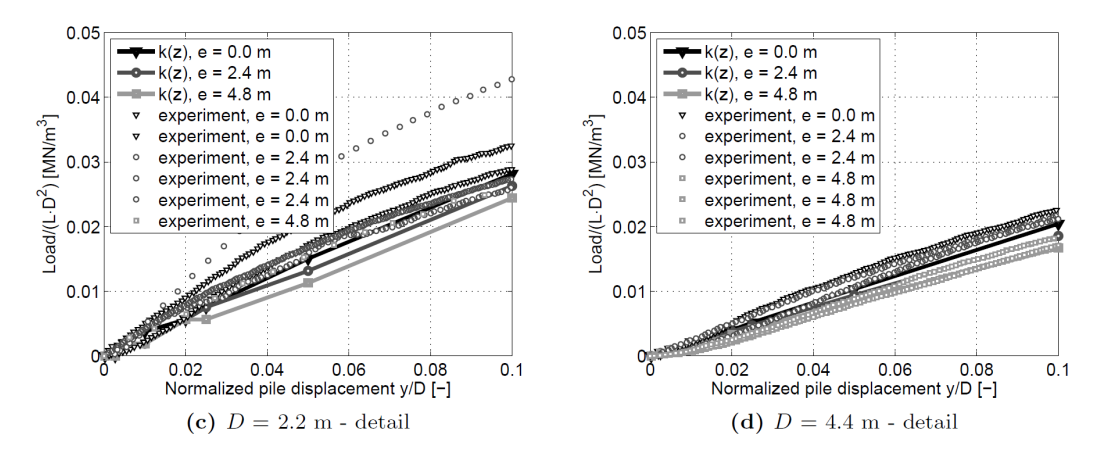


Figure 2.8: Comparison test results with modified p-y curve

$$k(z) = k_{500kPa} * \left(\frac{z * \gamma}{500kPa}\right)^n$$
 (2.9)

The adapted soil stiffness is used in the next chapter which describes the specific simulation details. The p-y curves are given in appendix A.

2.1.3. Environmental load

The environmental load on the monopile consists of wind, current and wave loads.

Wind load The wind load is depended on the wind velocity. At sea, the variation in the mean wind velocity is small compared to the wave period. The fluctuations around the mean wind speed will impose dynamic forces on an offshore structure, but in general these aerodynamic forces may be neglected in comparison with the hydrodynamic forces, when considering the structures dynamic behavior. The wind will be considered as steady, both in magnitude and

18 2. Literature review

direction, resulting in constant forces and a constant moment on a fixed floating or a sailing body [26].

Unless data indicate otherwise, the following expression can be used for calculation of the mean wind speed U with averaging period T at height z above sea level as [1]:

$$U(T,z) = U_{10} * \left(1 + 0.137 ln\left(\frac{z}{H}\right) - 0.047 ln\left(\frac{T}{T_{10}}\right)\right)$$
 (2.10)

With:

- \bullet $\rm U_{10}$ is wind velocity at 10m reference height (m/s)
- H is reference height -> 10m
- z is height above sea level (m), z0 is at sea level
- T_{10} is time period for reference mean wind velocity -> 10 min
- T is time period for calculated mean wind speed (s) -> 1 min

The force which the wind exerts on a length dz of the structure, can be computed by [26]:

$$F_{w} = 0.5 * \rho_{air} * C_{D} * D * dz * U(T, z)^{2}$$
(2.11)

Current load The current load is depended on the current velocity. When detailed field measurements are not available, the variation in current velocity with depth may be taken as [1]:

$$v_{tide}(z) = v_{tide,0} * \left(\frac{h+z}{h}\right)^{\alpha}$$
 (2.12)

With:

- $v_{\text{tide},0}$ is tide current velocity at still water level (m/s)
- h is depth to still water level (m), taken positive
- z is distance from still water level (m), positive upwards
- α , exponent typically 1/7

The force which the current exerts on a length dz of the structure, can therefore be computed by [26]:

$$F_c = 0.5 * \rho_{seawater} * C_D * D * dz * v_{tide}(z)^2$$
 (2.13)

Wave load According DNV (2014) [1], wave forces on a slender structure with a diameter to wavelength ratio of less than 1/5, can be calculated by the Morison equation. The Morison equation consists of a drag force and an inertia force. By this equation, the horizontal force on a vertical element dz of the structure at level z is expressed as:

$$F_{Morison} = F_{drag} + F_{inertia} (2.14)$$

$$F_{Morison} = 0.5\rho_{seawater}C_DDdzu|u| + \rho_{seawater}(C_m + 1)Ddz\dot{u}$$
 (2.15)

With:

2.1. Monopile 19

- F is the force per unit length 'dz' (N)
- ullet u is wave induced particle velocity (m/s)
- \dot{u} is wave induced particle acceleration (m/s²)
- D is cylinder diameter (m)
- \bullet $C_{\rm m}$ is hydrodynamic mass coefficient (-)
- \bullet C_{D} is drag coefficient (-)
- ρ is fluid density (kg/m^3)

The load on a structure is depends on the wave spectrum, which determine the particle kinematics, and the structure properties on which the wave is acting.

The following procedure is proposed to calculate wave forces on structures:

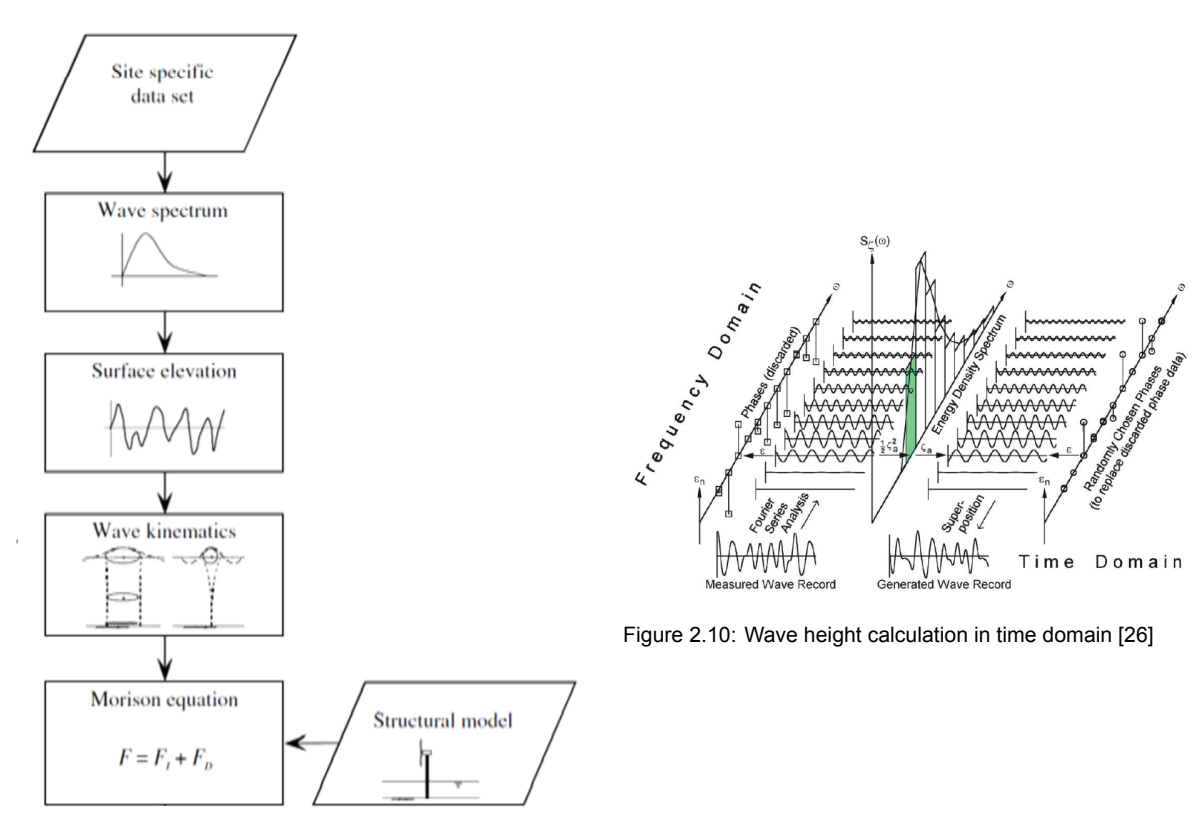


Figure 2.9: Flow chart for wave force calculation [41]

A measured wave record is translate into a serie of regular wave which are recalculated into an wave spectrum which describes the energy density as function of the wave frequency. The widely used JONSWAP wave spectrum is given by:

$$S_{\zeta}(\omega) = \frac{320H_{1/3}^2}{T_p^4} \omega^{-5} exp\left(\frac{-1950}{T_p^4}\omega^{-4}\right) \gamma^A$$
 (2.16)

With:

20 2. Literature review

$$A = exp\left(-\left(\frac{\frac{\omega}{\omega_p} - 1}{\sigma\sqrt{2}}\right)^2\right) \tag{2.17}$$

$$H_{1/3}$$
 = Significant wave height (2.18)

$$T_P$$
 = Wave period with the height energy (2.19)

With inverse FFT, the wave spectrum can be translated into a serie of sinusoidal regular waves. By superposition of these serie of regular waves, a wave elevation plot can be constructed in the time domain according figure 2.10.

The corresponding wave kinematics (water particle velocity and acceleration), depended on actual wave height, other wave parameters, the ratio between wave length and water depth etc. can be calculated according [26].

2.2. DP system

According the definition of MARIN (Maritime Research Institute Netherlands) dynamic positioning can be defined as [34]: 'Dynamic Positioning (DP) and Dynamic Tracking (DT) are methodologies to keep a vessel at a certain position (DP) or track (DT) using thrusters instead of mooring lines. By measuring its position (and heading) and comparing it to the required position, the DP system on board can determine its position error. The control system reacts on that by determining what thruster action is needed to bring the vessel as close as possible to the required position. DP systems can nowadays be found on many types of vessels: drilling vessels, installation vessels, heavy lift vessels, cable and pipe laying vessels and FPSOs.' Dynamic positioning is available for commercial maritime operation since the 1960s. In the next 55 years, continuous improvements are made in order to outperform the previous launched DP systems. In the early years, DP controllers were simple PID controllers with low pass and/or notch filters to filter sensor noise. More optimal control techniques, for example a Kalman estimator, has developed and proposed and replaced the simple approach. It is not desirable to counteract the relative high frequency, mean zero, first order wave force by the thruster because of the limited dynamic possibilities of a thruster and the mean zero characteristic of the force. Only low frequency environmental forces due to current, wind and the mean value of second-order wave force needs to be counteract by the thrusters. Pros and cons of the use of dynamic positioning relative to moored station keeping are as following:

Dynamic Positioning					
Pros	Cons				
Applicable in shallow and deep water	High CAPEX				
Costs and performance independent on water depth	Fuel consumption				
Quick 'mooring' and 'disconnection'	Maintenance costs				
No tugs required -> lower OPEX					
Possibility of weathervaning					

Table 2.4: Dynamic Positioning Pros and Cons relative to Mooring

The flexibility and the the possibility of quick application is highlighted in the pros. The high CAPEX can possible be canceled by the lower OPEX. The ratio between those costs have to be investigated in the future to determine in detail the possible advantage in increase in cost effectiveness.

Like every object in space, a vessel has 6 degrees of freedom in space, 3 translation and 3 rotational degrees of freedom, illustrated in figure 2.11.

2.2. DP system 21

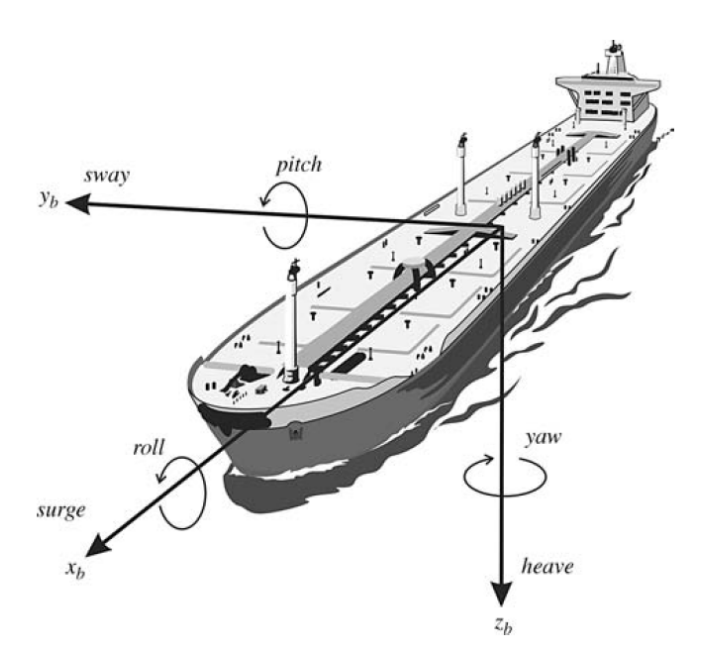


Figure 2.11: Motion in 6 DOF [20]

The Dynamic Positioning system controls the position and orientation in the horizontal plane. In other words, it controls surge, sway and yaw by applying a certain amount of thrust to counteract the environmental forces of current, wind and waves. Beside the control of horizontal plane motions, application are developed to reduce the roll motion of the vessel with the thrusters. However, this is outside the scope of this research.

2.2.1. DP system overview

A DP system consists of several sub-systems according figure 2.12. Beside the physical model of the vessel, the DP system and the DP control system can be recognized in the figure. The DP controller is the software part of the DP system which determine thruster set point based on sensor measurement. The DP systems consist of the DP controller, power management system, the thrusters and the sensors.

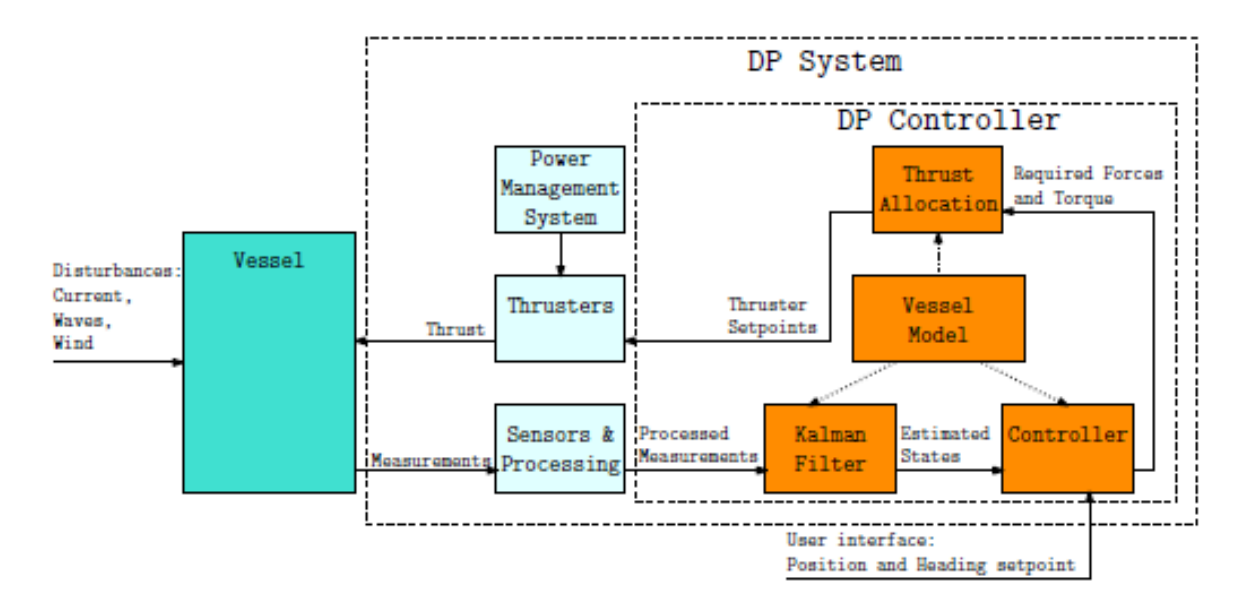


Figure 2.12: Overview DP system [16]

22 2. Literature review

The **Power Management System** involves the power generation including prime mover and generators, distribution of the generated power (switchboards), transformers, variable speed drives, motors and uninterrupted power supply (UPS) of sensitive equipment and automation systems.

The **Thrusters** uses the generated power to apply a force on the vessel. Most often, the thrusters are azimuth thrusters which can apply thrust in all the necessary directions on the vessel by rotating the thruster. Also the bow thrusters are involved. The rotational motion is transformed into thrust by the propeller. Thrusters have a certain ramp up and down rate because of the delay in power generation and the inertia of heavy mechanical components. In other words, it might be possible that is take some time before the required thrust from the controller is produced by the thruster.

Several types of **Sensors** are involved to measure the motions of the vessel, the position of the vessel and the amount of environmental force on the vessel. Gyros and motion reference units provide information about the acceleration of the vessel. Position reference systems like Global Navigation Satellite Systems (GNSS), hydro-acoustic systems, taut wires, micro wave systems, laser systems etc. Hardware, software and sensors to supply information and/or corrections necessary to give accurate position and heading references. Furthermore, wind sensors measures the wind speed and direction. In some cases, the output of these sensors are noisy.

The model based **DP controller** consists of three blocks: Kalman filter, the PID controller and a thrust allocator.

Kalman Filter is a state estimator and observer used to estimate the velocity state of the vessel because this is not available from sensors. Beside that, it compute a smooth position and heading states to avoid the noisy input from the sensors due to wind, waves and vessel roll and pitch. The Kalman filter is also able to estimate the slow varying forces on the vessel from current and second order wave forces with the current build up model. 2.13. The wind forces on the vessel are measured and feed forward in the DP controller. The current and slow varying second order wave forces are not measured. However, they influence the behavior of the vessel and they need to be counteracted.

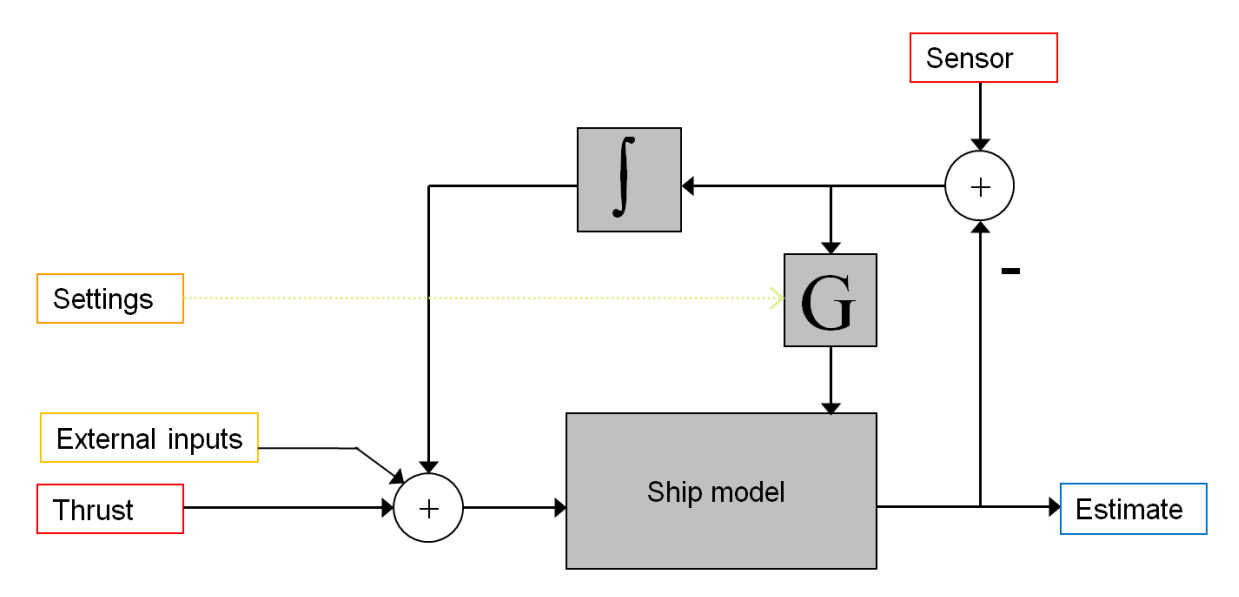


Figure 2.13: Working principle Kalman filter [16]

A mathematic model of the vessel is incorporated in the Kalman filter. The derivative of the estimated state vector is given by:

$$\dot{\hat{x}} = A\hat{x} + Bu + G(y - \hat{y}) \tag{2.20}$$

'A' consists of a mathematical model of the vessel. 'B' is the input matrix. 'u' is the input vector which are the external inputs and the feedback thrust. 'G' is the Kalman gain which

2.2. DP system 23

can be chosen manually to give more emphasis on the sensor output vector 'y' or on the estimated output values \hat{y} .

The estimated output vector \hat{y} is given by:

$$\hat{y} = C\hat{x} \tag{2.21}$$

The estimated output vector \hat{y} is calculated with the output matrix 'C' and the estimated state vector \hat{x}

When there is a stationary difference between the estimated output vector and the state vector from the sensors, an integral action is built up to account for the difference. This estimated force is included in the input vector 'u'. This is called the current built up model. Ideally, the estimated position and velocity is a smooth low frequency signal on which the thruster can react. The possible high frequency sensor signals are filtered. The estimated output vector is fed to the PID controller.

Controller. Several types of controllers are used. A widely used controller is the classic PID controller. The classic PID controller is described by linear differential equations in time domain. A schematic overview of a classic PID controller is given in figure 2.14.

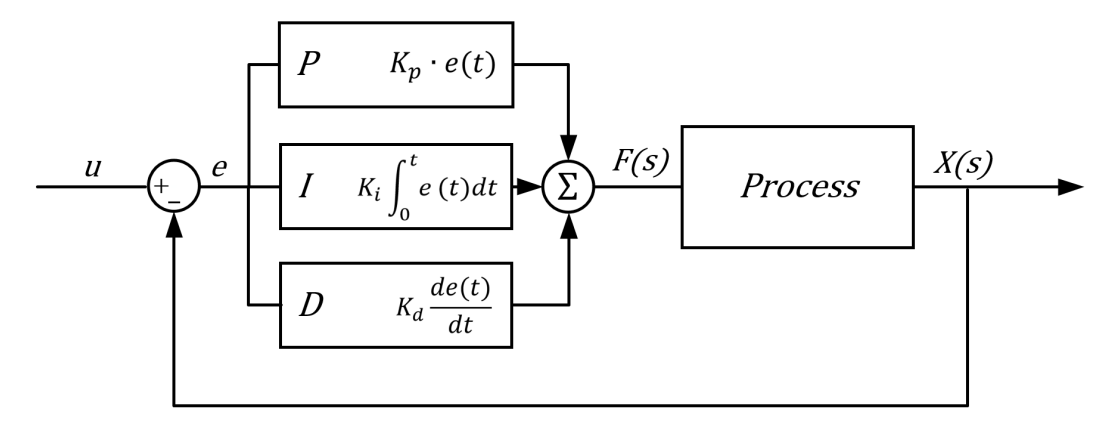


Figure 2.14: PID control scheme

Where P represents the proportional gain, I the integral gain and D the derivative gain. All based on the error signal e(t). The error signal is the set point state of the system minus the actual state of the system. The actual state is fed back which results in a closed control loop. The proportional term reacts on the position error, the derivative term on the velocity error and the integral term on a historic cumulative value of the error. A PID controller can be used for each degree of freedom. Several control algorithms are developed in the past to achieve more accurate positioning and recovery, faster response, less rapid variation in thruster commands and better handling of thruster limitations. The global required surge and sway force and yaw moment are the output of the controller. This global required control force is fed into the allocation algorithm.

Allocation algorithm. A thrust allocation algorithm is developed to allocate the global required thrust from the controller into several local forces on the geometric location of main propulsion, azimuth thrusters, bow thrusters, tunnel thrusters and rudders. The algorithm is based on minimize the cost function by minimizing the total squared thrust. The Lagrange multiplier method is used to find the optimal solution. Penalties are included in the formulation when thrusters saturates.

2.2.2. DP capability

A DP capability plot according DNVGL (2015) [14]: 'A capability plot is an analytical presentation of the vessel's performance during station keeping operations while exposed to external forces - environmental forces such as wind, current, and waves - as well as external force generated by industrial mission of the vessel. Capability plots do not indicate the excursions of the vessel. They represent analysis of the equilibrium of the steady-state forces and moments

of the vessel and establish the static holding capabilities. A dynamic time-domain simulation is not required by the classification societies.'

Figure 2.15 visualize a typical DP capability plot.

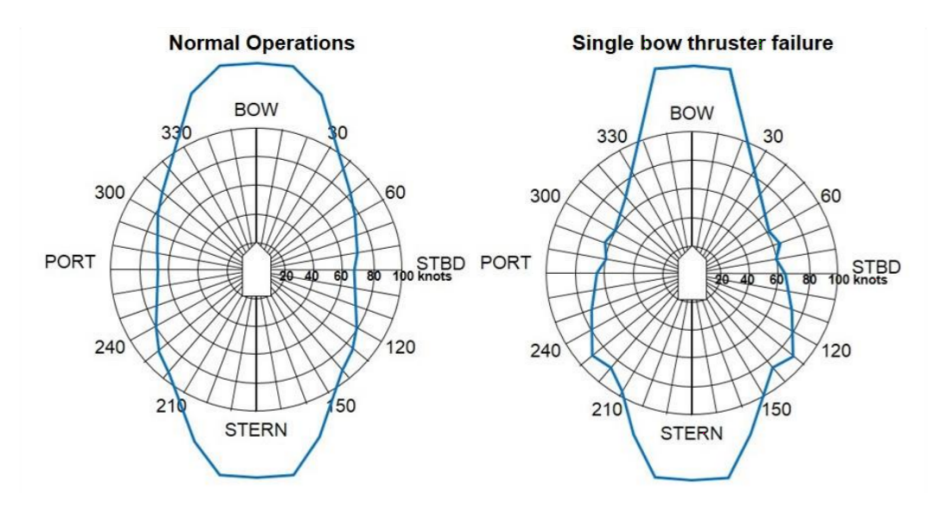


Figure 2.15: Typical DP capability plot

The blue line represents the maximum magnitude of the wind velocity in knots acting on the vessel for which the vessel is still able to maintain it position. Stated in the plot is the larger operational weather window in case of wind force acting from the bow or the stern on the vessel. This is due to the smaller frontal area. For that reason is weathervaning interesting.

2.3. Hydraulic frame

Hydraulic cylinders are applied in many motion controlled systems. A hydraulic cylinder is able to apply a force on a system in order to introduce motions of the system which is coupled to the hydraulic cylinder. Electric actuators are also used for motion control but in heavy marine operation, most often, more robust and stronger hydraulic actuators are used. This chapter provides an overview of other offshore ship motion compensated equipment including similarities and differences and a list of hydraulic system components.

2.3.1. Ship motion compensated platforms

Several ship motion compensated platform have entered the commercial market the last years. The main reasons for the development of these products is the need for an increased operational weather window and the focus on safety in offshore operations.

People and small equipment transfer To support safe offshore transfers of people from a vessel to a fixed offshore structure the Dutch company Ampelmann designed a so called six degree of freedom Stewart platform for offshore application. Six hydraulic cylinders, on both side connected to universal joints, are able to vary the leg length. An Ampelmann platform can be seen as an inverted flight simulator. A flight simulator induces the required motions and an Ampelmann compensates for the vessel induced motions.

2.3. Hydraulic frame 25



Figure 2.16: People transfer with an Ampelmann platform, [www.ampelmann.nl, 2018]

The Ampelmann platform is meant for relatively light applications, the mass of the platform is major relative to the mass of the people using the platform. In other words, the variation of system mass is low and therefore the mass of the system is highly predictable. On the other hand, the mass of the platform is negligible relative to the vessel mass. The assumption can be made that the control forces will not influence the motions of the vessel.

Heavy payload applications Barge Master delivers a multipurpose motion compensated platform. The platform is a carrying frame for heavy duty applications. Three degrees of freedom load compensation is applied by three vertical hydraulic cylinders on both sides connected to spherical joints. Vessel roll, pitch and heave motions are compensated and horizontal planar motions (surge, sway and yaw) are constrained by the construction.



Figure 2.17: Heavy payload vessel motion compensated platform, [www.barge-master.com, 2018]

The Barge Master T700 can carry a payloads of 700mT. This load can be significant relative to the vessel mass. In contrast to the Ampelmann system, in case of the Barge Master system the assumption can be made that platform control forces will influence the vessel motions. In other words, the platform also has to compensate for vessel motions induced by the platform. The Barge Master T700 is put on the market as a multipurpose motion compensated platform. Several types of equipment are allowed to be placed on the platform and various offshore operations can be carried out from the platform basis. Beside the control forces applied on the platform to compensate for vessel motions, the controller also need to apply control forces to compensate for unknown installation forces and for a range of possible equipment mass

placed on the platform. In other words, the controller needs to be robust because of the large variation in system dynamics.

Motion compensated offshore crane Vessel motion can be a risk or a limitation for offshore loading and unloading operations. To prevent extensive motions of the load and difficulties with placing a load on a desired position, motion compensated cranes are widely used to reduce safety risks and increase the operational window. The Finnish company MacGregor designs and constructs offshore cranes with a motion compensation mode.



Figure 2.18: Motion compensated offshore crane, [www.youtube.com/Cargotec, 2018]

To achieve a relative fixed position of the load, MacGregor uses three compensation axes to compensate for the induced linear motions of the load due to the vessel motions. A telescoping jib and a rotation crane to compensate for the induced horizontal linear motions and a winch to compensate for the induced heave motions.

Comparison to motion compensated pile gripper frame In the sections above, different types of offshore motion compensated equipment are summarized. They all have different applications. Compare to the motion compensated pile gripper frame there are similarities and differences between the systems. One of the main similarities is the way of applying control forces on the system: hydraulic actuators are used in all equipment. For that reason this is assumed to be feasible to design a motion compensated pile gripper frame based on hydraulic actuators. Furthermore, the assumption is made that the control forces to maintain pile position are relative large compared to the vessels mass. The control forces will have influence on the motions of the vessel, which is also the case in the Barge Master multipurpose platform. On that point, the monopile gripper frame system differs from the Ampelmann platform. Another important difference to highlight is the degrees of freedom which are compensated by the system. In case of the pile gripper frame, only the induced linear motions in the horizontal xy-plane, originate from roll, pitch, yaw and linear vessel motions, are compensated. In all mentioned systems, also the vertical induced motion is compensated. For that reason, gravity plays a major role in the mentioned systems and a minor role in the pile gripper system. On the other hand, environmental forces on the monopile requires compensation from the gripper frame. Due to the fact that the monopile is a submerged body, this 2.3. Hydraulic frame 27

forces are assumed to be much larger compare to the wind forces acting on the systems from Ampelmann, Barge-master and MacGregor.

2.3.2. Hydraulic system components

An overview is given of the components involved in a hydraulic actuator system. The hydraulic cylinder consists of two chambers separated by a piston. The pressure difference between chamber one and chamber two apply, depended on the area of the piston, a force on the load. To move the load, fluid has to enter a certain chamber and leave the other chamber. Depended on the compressibility of the hydraulic fluid, the pressure will increase of decrease when a certain amount of hydraulic fluid will enter of leave the chamber.

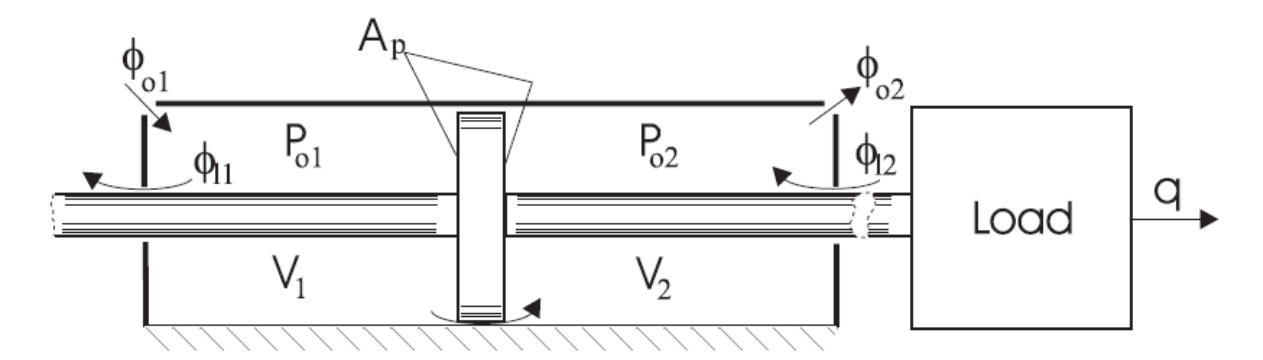


Figure 2.19: Schematic overview hydraulic cylinder

To provide a certain flow of pressurized hydraulic fluid, a pump is used. Mechanical energy in the form of torque and rotational velocity is converted into hydraulic energy in a form of fluid pressure and a certain volume flow of the fluid. Simple gear pump, screw pumps, axial or radial piston pumps are used for this task.

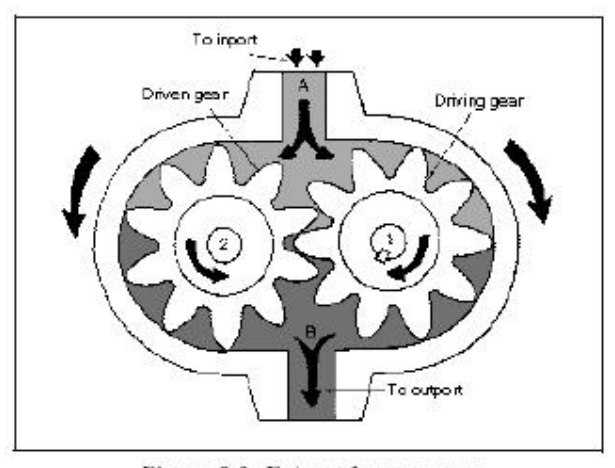


Figure 3-6. External gear pump

Figure 2.20: Rotational geared pump

For the sake of simplicity, a constant pressure pump is used. The supply pressure is constant and the load flow is depended on the load pressure. The flow which is not be used to move the cylinder is directed to the reservoir. So, the rotational speed of the pump is constant. By changing the drive torque, the pressurization of the fluid can be controlled.

To distribute the hydraulic fluid from and to a certain chamber of the cylinder and from and back to the reservoir, a valve is used. The valve provides the ability to distribute the fluid in several directions by moving a spool in axial direction.

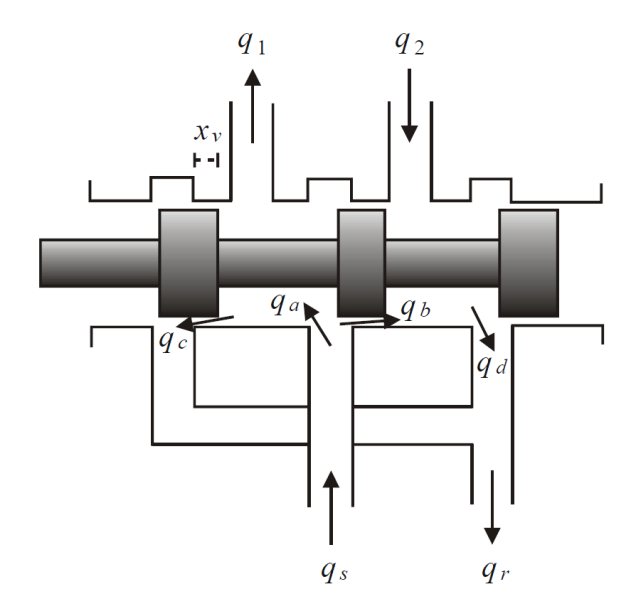


Figure 2.21: Cross section of a matched and symmetric four way valve, [Olav Egeland and Jan Tommy Gravdahl, 2002]

A overview of a four way hydraulic valve is visualized in figure 2.21. Flow from the pump (q_s) , to the reservoir (q_r) , to cylinder chamber 1 (q_1) and from cylinder chamber 2 (q_2) .

The next chapter will provide a more in-depth and mathematical description on modeling a hydraulic system.

2.4. Kinematics

The definition of the ship motions and the different frames, in which the motions can be defined, is described in this section and according [20]. In general, objects have 6 degrees of freedom. In ship motion term this are the three linear degrees of freedom, surge, sway and heave in forward, lateral and downward direction respectively (x, y, z) and roll, pitch and yaw (ϕ, θ, ψ) around the listed axes.

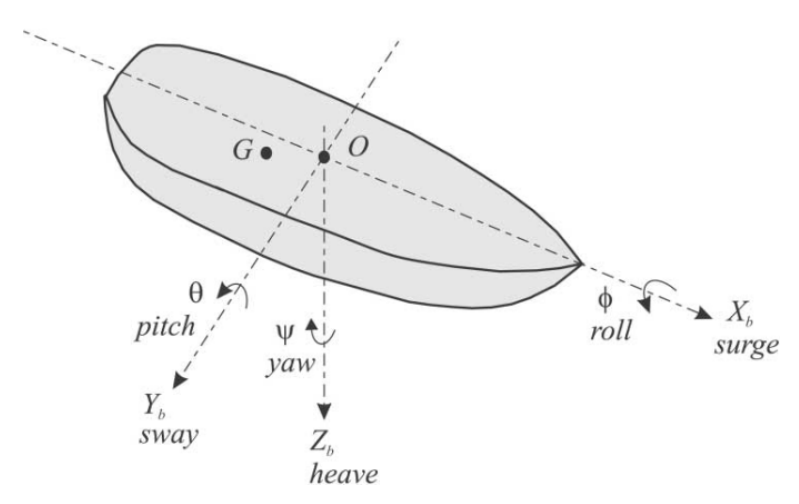


Figure 2.22: 6 Degrees of Freedom of a vessel [26]

2.4.1. Reference frames

According Fossen (2011) [20] four reference frames can be distinguished to describe the relative location and orientation of an object.

2.4. Kinematics 29

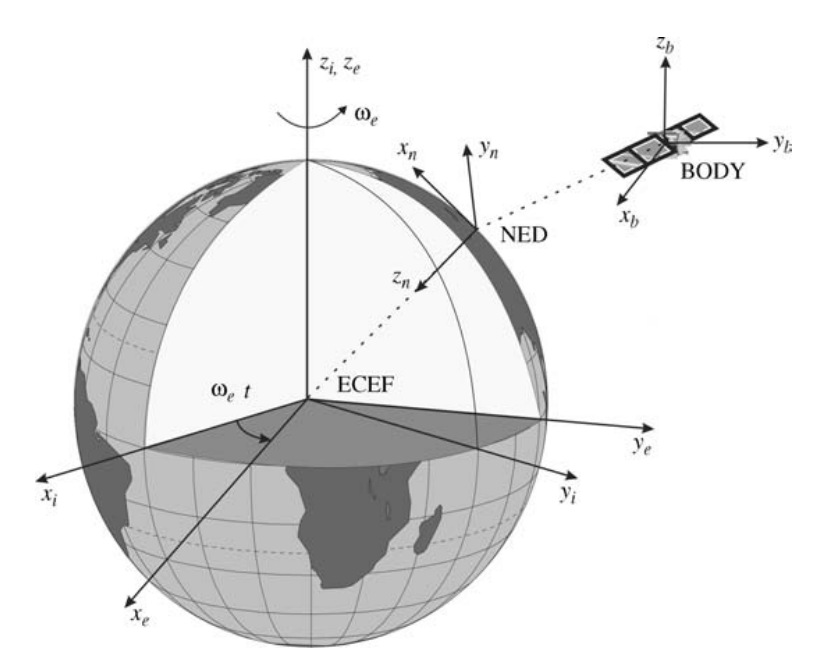


Figure 2.23: 6 Degrees of Freedom of a vessel

ECI: Earth-Center-Inertial frame (i) = non-accelerating inertial frame in which Newton's law of motion can be applied. Center of the frame is in the earth center.

ECEF: Earth-Center-Earth-Fixed frame (e) = an earth fixed reference frame which rotate relative to the ECI frame with the angular rate of rotation of the earth. Used for guidance, navigation and control in transit operation.

NED: North-East-Down coordinate system (n) = a reference frame with its origin is on the earth surface. The x-axis is towards the true North, the y-axis is towards the East and the z-axis is pointing downwards normal to the earth surface. The location of (n) relative to (e) can be calculated with the LON and LAT values.

BODY: Body-fixed reference frame (b) = a reference frame with its origin is fixed to a moving object. The axes are usually defined as: x-axis – longitudinal axis, y-axis – transversal axis and z-axis – normal axis. The position and orientation of a craft are described relative to an inertial frame ((e) or (n))

In the next sections, the kinematic equations relating the BODY, NED and ECEF reference frames to each other will be presented.

2.4.2. Transformation matrices

Pose vectors The location and orientation of a vessel relative to the, inertial, North-East-Down frame is given by three translations and three rotations in the pose vector η :

$$\eta = \begin{vmatrix} N \\ E \\ D \\ \phi \\ \theta \\ \psi \end{vmatrix}$$
(2.22)

With:

- N position in north direction (m)
- E position in east direction (m)
- D position in down direction (m)

- ullet ϕ is the Euler angle roll (rad)
- ullet heta is the Euler angle pitch (rad)
- ullet ψ is the Euler angle yaw (rad)

The generalized velocity vector in $\mbox{\ensuremath{\mbox{S}}}$ frame (body-fixed) is given by the vector $\mbox{\ensuremath{\mbox{v}}}$:

$$v = \begin{vmatrix} u \\ v \\ p \\ q \\ r \end{vmatrix}$$
 (2.23)

With:

- ullet u is the body fixed surge velocity (m/s)
- v is the body fixed sway velocity (m/s)
- w is the body fixed heave velocity (m/s)
- \bullet p is the body fixed rotational velocity around the x axis (rad/s)
- q is the body fixed rotational velocity around the y axis (rad/s)
- r is the body fixed rotational velocity around the z axis (rad/s)

From NED to body-fixed linear velocity transformation Figure 2.24 visualize the difference between the earth-fixed frame (n) and the body-fixed frame (b). A rigid body of the vessel is assumed.

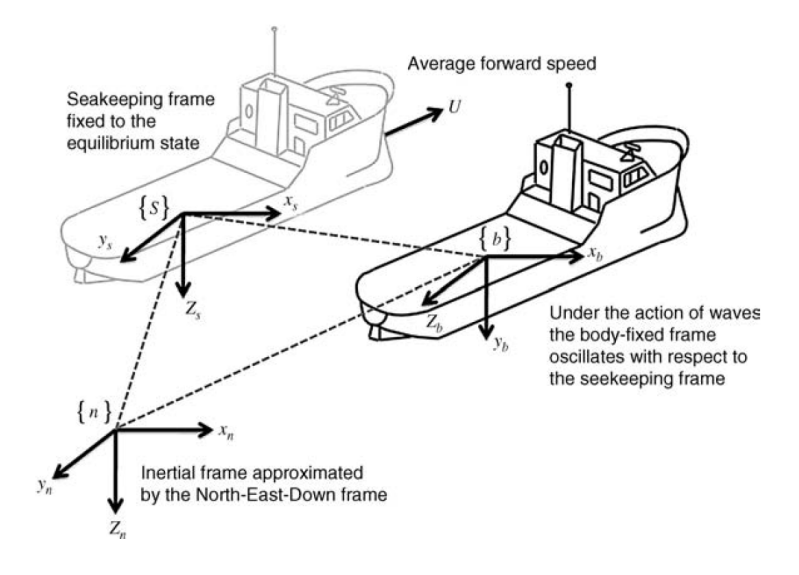


Figure 2.24: Coordinate systems, Fossen (2011) [20]

2.4. Kinematics 31

The principle rotation matrices can be used to switch from the NED coordinate system to the body-fixed reference frame or vice versa. The following rotation matrices are respectively used for the x, y and z axes.

$$R_{x,\phi} = \begin{vmatrix} 1 & 0 & 0 \\ 0 & \cos\phi & -\sin\phi \\ 0 & \sin\phi & \cos\phi \end{vmatrix}$$
 (2.24)

$$R_{y,\theta} = \begin{vmatrix} \cos\theta & 0 & \sin\theta \\ 0 & 1 & 0 \\ -\sin\theta & 0 & \cos\theta \end{vmatrix}$$
 (2.25)

$$R_{x,\psi} = \begin{vmatrix} \cos\psi & -\sin\psi & 0\\ \sin\psi & \cos\psi & 0\\ 0 & 0 & 1 \end{vmatrix}$$
 (2.26)

Euler angles in matrix form:

$$\Theta_{nb} = \begin{vmatrix} \phi \\ \theta \\ \psi \end{vmatrix} \tag{2.27}$$

The transformation to transform a vector from the body-fixed (b) frame to the earth-fixed (NED) frame is equivalent to:

$$R_n^b(\Theta_{nb}) = R_{z,\psi} R_{\gamma,\theta} R_{x,\phi} \tag{2.28}$$

The inverse transformation is written as:

$$R_n^b(\Theta_{nb})^{-1} = R_b^n(\Theta_{nb}) = R_{z,\psi}^T R_{y,\theta}^T R_{x,\phi}^T$$
 (2.29)

Expanding equation 2.28:

$$R_{n}^{b}(\Theta_{nb}) = \begin{vmatrix} cos\psi cos\theta & -sin\psi cos\phi + cos\psi sin\theta sin\phi & sin\psi sin\phi + cos\psi cos\phi sin\theta \\ sin\psi cos\theta & cos\psi cos\phi + sin\phi sin\theta sin\psi & -cos\psi sin\phi + sin\theta sin\psi cos\phi \\ -sin\theta & cos\theta sin\psi & cos\theta cos\phi \end{vmatrix}$$
(2.30)

The body-fixed velocity vector $v_{b/n}^{n}$ can be expressed in (NED) as:

$$\dot{p}_{b/n}^{n} = R_b^n(\Theta_{nb}) \nu_{b/n}^b \tag{2.31}$$

With:

$$\dot{p}_{b/n}^n = \text{NED linear velocity vector}$$
 (2.32)

From NED to body-fixed angular velocity transformation The Euler rate vector can be written as function of the body-fixed angular velocity vector and vice versa via a transformation matrix.

The Euler rate vector is defined as:

$$\dot{\Theta}_{nb} = \begin{vmatrix} \dot{\phi} \\ \dot{\theta} \\ \dot{\eta} \end{vmatrix} \tag{2.33}$$

And the body-fixed angular velocity vector as:

$$\omega_{b/n}^b = \begin{vmatrix} p \\ q \\ r \end{vmatrix} \tag{2.34}$$

The body-fixed angular velocity vector can be written as function of the Euler rate vector:

$$\omega_{b/n}^b = T_{\Theta}^{-1}(\Theta_{nb})\dot{\Theta}_{nb} \tag{2.35}$$

With the inverse transformation defined as:

$$\omega_{b/n}^{b} = \begin{vmatrix} \dot{\phi} \\ 0 \\ 0 \end{vmatrix} + R_{x,\phi}^{T} \begin{vmatrix} 0 \\ \dot{\theta} \\ 0 \end{vmatrix} + R_{x,\phi}^{T} R_{y,\theta}^{T} \begin{vmatrix} 0 \\ 0 \\ \dot{\psi} \end{vmatrix} = T_{\Theta}^{-1}(\Theta_{nb})\dot{\Theta}_{nb}$$
 (2.36)

Expanding equation 2.36:

$$T_{\Theta}^{-1}(\Theta_{nb}) = \begin{vmatrix} 1 & 0 & -\sin\theta \\ 0 & \cos\phi & \cos\theta\sin\phi \\ 0 & -\sin\phi & \cos\theta\cos\phi \end{vmatrix}$$
 (2.37)

6 DoF Kinematic equations Combining the transformation and rotation matrices, the following vector form is obtained:

$$\dot{\eta} = I_{\Theta}(\eta) * \nu \tag{2.38}$$

$$\begin{vmatrix} \dot{p}_{b/n}^n \\ \dot{\Theta}_{nb} \end{vmatrix} = \begin{vmatrix} R_b^n(\Theta_{nb}) & 0_{3x3} \\ 0_{3x3} & T_{\Theta}(\Theta_{nb}) \end{vmatrix} \begin{vmatrix} v_{b/n}^b \\ \omega_{b/n}^b \end{vmatrix}$$
(2.39)

Transformation LAT/LON to North East position The latitude (μ) and longitude (μ) and altitude (μ) relative to a reference latitude (μ), longitude (μ) and height (μ).

The small change in longitude and latitude is given by:

$$d\mu = \mu - \mu_0 \tag{2.40}$$

And:

$$dl = l - l_0 \tag{2.41}$$

To convert geodetic latitude and longitude to the North and East coordinates, the estimation uses the radius of curvature in the prime vertical (R_N) and the radius of curvature in the meridian (R_M) . (R_N) and (R_M) are defined by the following relationships:

$$R_N = \frac{R}{\sqrt{1 - (2f - f^2)\sin^2 \mu_0}} \tag{2.42}$$

And:

$$R_M = R_N \frac{1 - (2f - f^2)}{1 - (2f - f^2)\sin^2 \mu_0}$$
 (2.43)

With:

- R is the equatorial radius of the planet (m)
- f is the flattening of the planet (-)

Small changes in NED North (dN) and East (dE) positions due to small changes in latitude and/or longitude:

$$dN = \frac{d\mu}{atan(\frac{1}{R_M})} \tag{2.44}$$

And:

$$dE = \frac{dl}{atan(\frac{1}{R_N cos\mu_0})}$$
 (2.45)

2.5. Stability of a dynamic system

The stability of a dynamic system is a point of interest. When a system return to its rest position, the conclusion can be made that the system is asymptotically stable. This can be done by simulating many initial condition to prove if this is true for any initial condition. However, it is valuable to prove if this is the case for any initial condition.

2.5.1. Stability criteria

The Russian mathematician Lyapunov propose in its Doctoral dissertation a method to prove the stability of a dynamic system [31]. The so-called second method, also known as the Lyapunov stability criterion, uses the Lyapunov function V(x). In a mechanical system, this Lyapunov function has an analogy with the energy function the system. Consider a function:

$$V(x): \mathbb{R}^n \to \mathbb{R} \tag{2.46}$$

Requirements:

$$V(x) = 0 \text{ if and only if } x = 0$$
 (2.47)

$$V(x) > 0$$
 if and only if $x \neq 0$ (2.48)

$$\dot{V}(x) = \frac{d}{dt}V(x) = \frac{dV}{dx}\frac{dx}{dt} \le 0$$
 (2.49)

In case of a physical system, the total energy of the system can be used as a Lyapunov function. The total energy consists of potential and kinetic energy. The derivative of the Lyapunov function is the energy which is subtracted or added to the system. If case that energy is subtracted from the system for all states, the system is asymptotic stable.

2.5.2. Mass spring damper example

First of all, the concept is proven with a simple mass spring damper system.

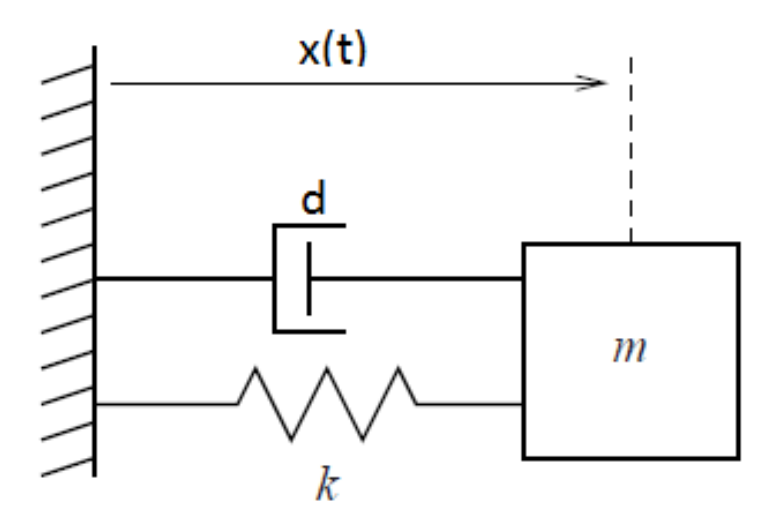


Figure 2.25: Mass spring damper [7]

The equation of motions is given by:

$$m\ddot{x} + d\dot{x} + kx = 0 \tag{2.50}$$

$$m\ddot{x} = -d\dot{x} - kx \tag{2.51}$$

$$d\dot{x} = -m\ddot{x} - kx \tag{2.52}$$

$$kx = -m\ddot{x} - d\dot{x} \tag{2.53}$$

Suppose the following Lyapunov function:

$$V(x) = \frac{1}{2}kx^2 + \frac{1}{2}m\dot{x}^2 \tag{2.54}$$

This function fulfill the requirements for the Lyapunov function for all system states. The time derivative of the propose Lyapunov function is given by:

$$\dot{V}(x) = kx\dot{x} + m\ddot{x}\dot{x} \tag{2.55}$$

$$\dot{V}(x) = (-m\ddot{x} - d\dot{x})\dot{x} + (-d\dot{x} - kx)\dot{x}$$
 (2.56)

$$\dot{V}(x) = -d\dot{x}^2 \tag{2.57}$$

The time derivative of the Lyapunov function is negative for all system states (energy is dissipating from the system), so the system is asymptotic stable. The system always converge to its equilibrium state.

2.5.3. Stability simplified Vessel-Gripper frame-Monopile model

In this section, the stability criteria of Lyapunov is used to prove the stability of a two mass spring damper system which represents the vessel and monopile. The system is drawn in a schematic overview and presented in figure 2.26.

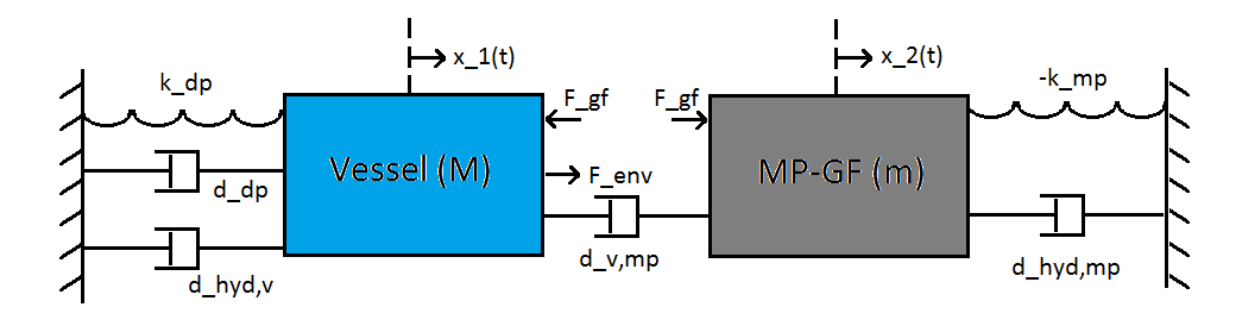


Figure 2.26: Simplified representation vessel-gripper-monopile model

Designation	Symbol
Proportional term DP system	k_dp
Damping term DP system	d_dp
Hydrodynamic damping vessel	d_hyd,v
Viscous damping vessel-MP	d_v,mp
Hydrodynamic damping monopile	d_hyd,mp
Negative hydrostatic stiffness monopile	-k_mp
Force gripper frame	F_gf

Table 2.5: Specification vessel-gripper-monopile model

The control law of the gripper frame controller is based on the state of the monopile and given by:

$$F_{GF} = -k_{GF}x_2 - d_{GF}\dot{x}_2 \tag{2.58}$$

Designation	Symbol
Proportional term gripper frame	k_GF
Damping term DP gripper frame	d_GF

Table 2.6: Specification control law gripper frame

Equations of motion:

$$M\ddot{x}_1 + (d_{dp} + d_{hyd,v})\dot{x}_1 + d_{v,mp}(\dot{x}_1 - \dot{x}_2) + k_{dp}x_1 = F_{env} - F_{GF}$$
(2.59)

$$m\ddot{x}_2 + d_{hvd\,mn}\dot{x}_2 + d_{v\,mn}(\dot{x}_2 - \dot{x}_1) - k_{mn}x_2 = F_{GF}$$
 (2.60)

In state space:

$$\begin{bmatrix} \dot{x}_1 \\ \dot{x}_2 \\ \ddot{x}_1 \\ \ddot{x}_2 \end{bmatrix} = \begin{bmatrix} 0 & 0 & 1 & 0 \\ 0 & 0 & 0 & 1 \\ -\frac{k_{dp}}{M} & \frac{k_{GF}}{M} & -\frac{d_{dp}+d_{hyd,v}+d_{v,mp}}{M} & \frac{d_{v,mp}+d_{GF}}{M} \\ 0 & -\frac{k_{GF}-k_{mp}}{M} & -\frac{d_{GF}+d_{hyd,mp}+d_{v,mp}}{M} & \frac{d_{v,mp}}{M} & \frac{d_{v,mp}}{M} \\ \end{bmatrix} \begin{bmatrix} x_1 \\ x_2 \\ \dot{x}_1 \\ \dot{x}_2 \end{bmatrix} + \begin{bmatrix} 0 & 0 \\ 0 & 0 \\ 1/M & 0 \\ 0 & 1/m \end{bmatrix} \begin{bmatrix} F_{env} \\ 0 \end{bmatrix}$$

$$[y] = \begin{bmatrix} 1 & 0 & 0 & 0 \\ 0 & 1 & 0 & 0 \end{bmatrix} \begin{bmatrix} x_1 \\ x_2 \\ \dot{x}_1 \\ \dot{x}_2 \end{bmatrix}$$

Lets define the total energy function of the system as:

$$V(x) = \frac{1}{2}k_{dp}x_1^2 - \frac{1}{2}k_{GF}x_2^2 + \frac{1}{2}M\dot{x}_1^2 - \frac{1}{2}k_{mp}x_2^2 + \frac{1}{2}k_{GF}x_2^2 + \frac{1}{2}m\dot{x}_2^2$$
 (2.61)

The function V(x) needs to be positive defined for all states.

The derivative of the total energy function V(x):

$$\dot{V}(x) = k_{dp}x_1\dot{x}_1 - k_{GF}x_2\dot{x}_2 + M\ddot{x}_1\dot{x}_1 - k_{mp}x_2\dot{x}_2 + k_{GF}x_2\dot{x}_2 + m\ddot{x}_1\dot{x}_1$$
 (2.62)

The total energy function is split into two energy functions. One for both subsystem. The energy function for the vessel reads:

$$V_1(x) = \frac{1}{2}k_{dp}x_1^2 - \frac{1}{2}k_{GF}x_2^2 + \frac{1}{2}M\dot{x}_1^2$$
 (2.63)

The energy function for the gripper frame/monopile combination reads:

$$V_2(x) = -\frac{1}{2}k_{mp}x_2^2 + \frac{1}{2}k_{GF}x_2^2 + \frac{1}{2}m\dot{x}_2^2$$
 (2.64)

Suppose:

$$x_1 = ax_2 \tag{2.65}$$

And:

$$\dot{x}_1 = b\dot{x}_2 \tag{2.66}$$

Vessel stability First investigate the stability of the vessel. Suppose:

$$V_1(x) = \frac{1}{2}(k_{dp} - \frac{1}{a}k_{GF})x_1^2 + \frac{1}{2}M\dot{x}_1^2$$
 (2.67)

Requirement 1: $V_1(x)$ is guaranteed positive for all states if:

$$k_{dp} \ge \frac{1}{a} k_{GF} \tag{2.68}$$

$$\dot{V}_1(x) = (k_{dp} - \frac{1}{a}k_{GF})x_1\dot{x}_1 + M\ddot{x}_1\dot{x}_1 \tag{2.69}$$

Combining equation 2.69 and 2.59:

$$\dot{V}_1(x) = -(d_{dp} + d_{hyd,v} + d_{v,mp})\dot{x}_1^2 + (d_{v,mp} + d_{GF})\dot{x}_2\dot{x}_1$$
(2.70)

Filling equation 2.65:

$$\dot{V}_1(x) = -(d_{dp} + d_{hyd,v} + (1 - \frac{1}{b})d_{v,mp} - \frac{1}{b}d_{GF})\dot{x}_1^2$$
(2.71)

Requirement 2: negative for all states if:

$$d_{dp} \ge \frac{1}{b} d_{GF} - d_{hyd,v} - (1 - \frac{1}{b}) d_{v,mp}$$
 (2.72)

Monopile stability Secondly, investigate the stability of the monopile:

$$V_2(x) = \frac{1}{2}(k_{GF} - k_{mp})x_2^2 + \frac{1}{2}m\dot{x}_2^2$$
 (2.73)

Requirement 3: $V_2(x)$ is guaranteed to be positive for all states if:

$$k_{GF} \ge k_{MP} \tag{2.74}$$

$$\dot{V}_2(x) = (k_{GF} - k_{mn})x_2\dot{x}_2 + m\ddot{x}_2\dot{x}_2 \tag{2.75}$$

Combining equation 2.75 and 2.60:

$$\dot{V}_2(x) = -(d_{GF} + d_{hyd,mp} + d_{v,mp})\dot{x}_2^2 + (d_{v,mp})\dot{x}_1\dot{x}_2$$
 (2.76)

$$\dot{V}_2(x) = -(d_{GF} + d_{hvd,mp} + (1-b)d_{v,mp})\dot{x}_2^2$$
(2.77)

Requirement 4: equation 2.77 is negative for all state if:

$$d_{GF} \ge -(1-b)d_{v,mp} - d_{hvd,mp} \tag{2.78}$$

The value 'a' in equation 2.65 represents the ratio between vessel motions and linear monopile motions at gripper frame level. The gripper frame apply motion compensation so the assumptions is made that the value of 'a' is larger than one. In other words, the motion amplitude of the vessel is larger than the motion amplitude of the monopile. The higher the ratio between vessel motions and monopile motions, or, the better the upright position of the monopile is maintained, the smaller the force from the monopile on the vessel. This reduce the required magnitude of the proportional term of the DP controller or give more margin when a proportional term is already determined.

The required proportional term for the gripper frame can be determined more straight forward. To maintain the upright position of the monopile, the proportional term needs to be at least larger than the negative stiffness of the monopile (due to the tipping over tendency). When the proportional term of the gripper frame is larger than the negative monopile spring stiffness, the total stiffness is positive. This total positive stiffness, pull the monopile back to it set point.

The required gripper frame damping is composed of the hydrodynamic damping of the monopile which is positive and the damping between vessel and monopile. The value 'b' in equation 2.66 represents the ratio between vessel velocity and linear monopile velocity at gripper frame level. When 'b' is larger than one and the phase shift between vessel and monopile motions is zero, the viscous damping between vessel and monopile add a negative damping force to the monopile. The hydrodynamic damping is adding a positive damping to the monopile. When the magnitude of the negative viscous damping is higher than the hydrodynamic damping of the monopile, the damping force added by the gripper frame on the monopile has to fill the gap. However, the damping of the monopile is likely larger than the friction force of the gripper frame. When that is the case, stability of the monopile can be maintained.

The required damping of the PD control system is derived in terms of the hydrodynamic damping of the vessel, friction in the gripper frame and damping force from the gripper frame controller. When 'b' is larger than one (which is likely the case because the gripper frame compensate for the vessel motions), the friction force between monopile and vessel add positive damping to the vessel. This lower the requirement on the damping of the DP system. Furthermore, the magnitude of the hydrodynamic damping of the vessel is inversely related to the required damping of the DP system. In other words, when the hydrodynamic damping is higher, the damping from the DP system can be smaller. The hydrodynamic damping in sway direction is larger compare to surge direction. A larger stability margin in sway direction is expected.

The simplified model describe the stability of the overall system. However, in the real world, the proportional and damping term is not directly related to the vessel state due to state estimation, thruster ramp up limitation and sensor error. This gives a phase shift of the proportional and damping term of the DP control system. The phase shift will decrease the stability margin and might cause instability. Furthermore, environmental forces acting on the vessel and monopile can reduce the stability margin. A richer simulation model is build to study the effect of the typical system specification on the overall performance of the DP system. This model is presented in chapter 3.

Simulation setup and verification

This chapter covers a description and verification of the simulation model which is built for the feasibility study. The simulation model can be split into two main components. The RH Marine Dynamic Positioning simulator and a Matlab/Simulink model with the other components necessary for a mono-pile installation. This chapter describes both models separately and provide the overall model which is a combination of both models. Furthermore, typical system parameters are given and this chapter ends with a model verification. The simulation model is based on the literature review of the chapter two.

3.1. Dynamic Positioning simulator

The DP simulator is an industry used system. Two parts of the system can be distinguished: DP control system and a simulated vessel. The DP control system is software and the simulated vessel represents the real world.

3.1.1. DP control system

The DP control system is model based and make use of a Kalman filter, PID controller and a Lagrange thruster allocation algorithm. This model is identical to the simulated vessel model.

3.1.2. Simulated vessel

A hydrodynamic model of the vessel is implemented in the simulator. This is a first principle model based on 5x5 mass and damping matrices. External force from wave, current and wind introduce motions of the vessel. In the past, research institute MARIN build and test a real world model to determine the elements of the mass and damping matrices. In this simulator, a simplified model of the extended model is used. Transfer functions between force and velocity (surge and sway) and between moment and rotational velocity (roll, pitch and yaw) are set up based on the simplified time delay function. No frequency depended added mass and damping is included in the vessel model. Because of the fact that a DP system is a low speed application [20], this is assume to be no problem for surge, sway and yaw motions.

Crucial for this research is realistic behavior of some components which are modeled in the simulator. The most important are:

- Maximum power build up rate of the thruster and main propulsion
- Maximum rotational rate of azimuth thrusters
- Sensor noise and delay
- Certain update frequency of GPS and MRU sensors

Modeling of this typical system behavior introduce extra delay corresponding with real world DP vessel behavior. A table with vessel size, installed power and thruster configuration is given in appendix B. Also station-keeping under different environmental conditions and a comparison of roll-pitch behavior under environmental load with the same vessel simulated in a different simulation environment can be found in appendix B

3.1.3. Output and input DP simulator

Table 3.1 gives the output and input variables to and from Matlab/Simulink. The input variables are external forces from the gripper frame on the vessel recalculated to induced vessel velocities. Note: the environmental forces on the vessel are an integrated part of the DP simulator and not mentioned as input in the table.

Output	Description	Unit
LAT	Latitude coordinate	deg.
LON	Longitude coordinate	deg.
u	body fixed surge velocity	m/s
V	body fixed sway velocity	m/s
ϕ	roll angle	rad
θ	pitch angle	rad
ψ	yaw angle	rad
р	roll rate	rad/s
q	pitch rate	rad/s
r	yaw rate	rad/s
Input	Description	Unit
F-x	Force in surge direction	kN
F-y	Force in sway direction	kN
M-roll	Induced roll moment	kNm
M-pitch	Induced pitch moment	kNm

Induced yaw moment

kNm

Table 3.1: Output and input DP simulator

3.2. Matlab/Simulink model

M-yaw

Matlab/Simulink is used to model a monopile, a PID controlled hydraulic gripper frame and for the computation of the velocity of the default position of the gripper frame due to vessel motions. All separate parts of the simulation are described below.

3.2.1. Monopile model

This subsection describe in a mathematical model the behavior of the monopile under influence of monopile soil interaction, own weight, reaction force applied by the gripper frame and environmental load. A one dimensional overview of the monopile and the forces in charge is given in figure 3.1. The parameters according figure 3.1 of two monopiles (FB24: 1653 mT and FB16: 870 mT) and there specific size based on data from Boskalis, are given in appendix E. These monopile sizes are based on a future market analysis performed by Boskalis. FB16 represents a shallow water pile and FB24 represents a deep water pile. Beside the monopile, a hydro hammer placed on top of the monopile, to drive the monopile into the soil, is taken into account into the mathematical model of the monopile. Dimensions of the hydro hammer are given in appendix E.

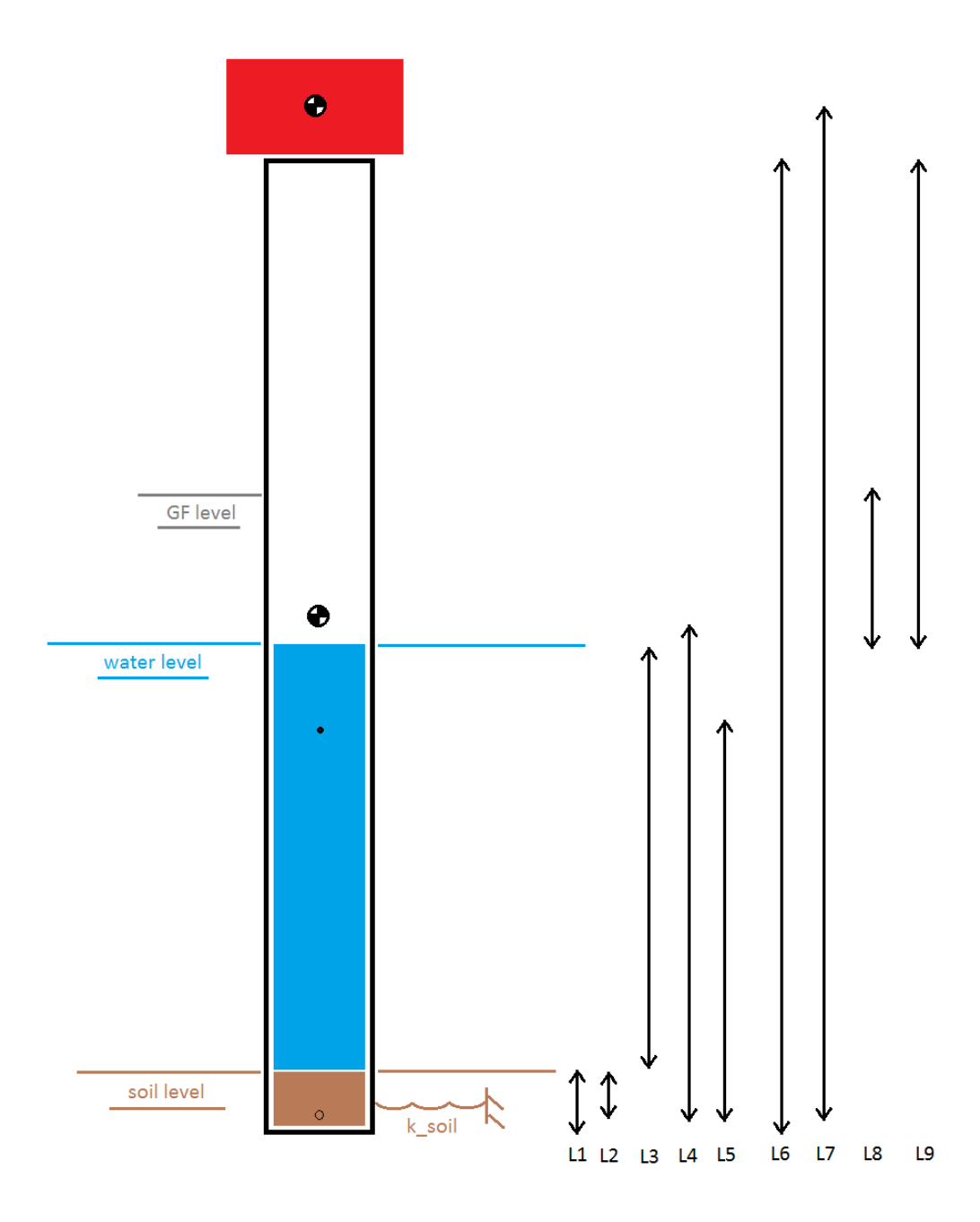


Figure 3.1: Functional overview mono-pile

- \mathtt{L}_1 is soil penetration depth,40% of pile diameter [30] (m)
- \bullet L $_2$ is 80% of soil penetration (m), soil level to point of rotation [24]
- L_3 is water depth (m)
- L_4 is CoG monopile to point of rotation (m)
- \bullet L_{5} is monopile radius of gyration to point of rotation (m)

- L_6 is total length monopile (m)
- L_7 is CoG hydro hammer to point of rotation (m)
- ullet L₈ is distance gripper frame above water level (m)
- L9 is distance monopile above water level (m)

The relevant and controllable linear vessel motion are in the horizontal x-y plane. The monopile model is a inverted pendulum with freedom of rotation around x and y axis in the pivot point. Rotation around the vertical z axis is not relevant in this research. The x-y position of the monopile at gripper frame level and the pile rotation is important in this research.

$$sin(\alpha) = \frac{x}{L_8} \tag{3.1}$$

Due to small angles, the goniometric relation can be approximated by a linear relation. The relative error between the linearized approximation and the non linearized value is 1% for an angle of 14 deg. An extreme angle of 14 deg will never be reached and the error is assumed to be acceptable so the linear approximation is assumed to be valid.

$$\alpha = \frac{x}{L_8} \tag{3.2}$$

A general formulation for an equation of motion of an inverted pendulum around a pivot point is given by:

$$I_{tot} * \ddot{\alpha} + d_{tot} * \dot{\alpha} + k_{tot} * \alpha = M \tag{3.3}$$

- \bullet I_{tot} is moment of inertia of monopile, hydro hammer and trapped water mass (kg.m2)
- d_{rot} is rotational damping composed by hydrodynamic and soil damping (Nm.s/rad)
- k_{tot} is rotational stiffness composed by soil stiffness and tipping over tendency of an inverted pendulums, negative when the monopile acts as an inverted pendulum (Nm/rad)
- M is a moment applied on the monopile around the pivot point by environmental forces (wave, current and wind) and control forces applied by the gripper frame (Nm)

The added mass of the water around the monopile is neglected, only the trapped water mass is taken into account. Furthermore, the assumption is made that the damping have a linear dependency on the rotational velocity of the monopile. The frequency depended added mass and wave making radiation damping is neglected in the dynamic model of the monopile.

Moment of inertia The monopile, hydro hammer and the trapped water contributes to the system moment of inertia. The moment of inertia is in terms of mass and distance of center of gravity to the pivot point and given by the following formulations:

$$I_{mp} = m_{mp} * L_5^2 (3.4)$$

$$I_{hh} = m_{hh} * L_7^2 (3.5)$$

$$I_{hh} = \frac{1}{3} * m_{tw} * L_3^2 \tag{3.6}$$

$$I_{tot} = I_{mp} + I_{tw} + I_{hh} (3.7)$$

- m_{mp} is mass mono-pile (kg)
- m_{tw} is mass trapped water (kg)
- \bullet m_{hh} is mass hydro hammer (kg)

Equivalent damping The linear rotational damping, composed of soil damping and hydro dynamic damping, is provided by Boskalis.

$$d_{tot} = d_{soil} + d_{hvdro} (3.8)$$

Total rotational stiffness The total rotational stiffness is given by:

$$k_{tot} = k_{rot,soil} - k_{to} (3.9)$$

Rotational spring stiffness by soil To calculate the equivalent spring stiffness, first a rotational stiffness of the monopile soil interaction around the pivot point is calculated. As stated in chapter 2, the stiffness of the springs are determined with a modified p-y curve to meet the large diameter monopile soil interaction. The p-y curves valid for every 1 meter of soil (i.e. 0->1 meter, 1->2 meter, 2->3 meter, etc), to a soil depth of 16 meter are given in appendix A. The first part of the p-y curve shows a linear increase in soil resistance (P) with increasing horizontal pile deflection (y). This first part can be modeled as a linear spring with a stiffness which is the same as the line gradient. The rotational stiffness for one spring is given by:

$$M_{soil} = k_{rot,soil} * \alpha \tag{3.10}$$

$$F * (L_2 - (i - 0.5)) = k_{rot,soil} * \frac{x}{(L_2 - (i - 0.5))}$$
(3.11)

$$k_{trans,soil}(i) * x * (L_2 - (i - 0.5)) = k_{rot,soil} * \frac{x}{(L_2 - (i - 0.5))}$$
 (3.12)

With:

• i is the ith soil spring

In summation form when taking all the springs in charge (depended on penetration depth) into account:

$$k_{rot,soil} = \sum_{n=1}^{L_1} k_{trans,soil}(i) * (L_2 - (i - 0.5))^2 \quad (Nm/rad)$$
(3.13)

The linear, or translation, soil stiffness are given in appendix A.

Tipping over moment The monopile acts as a inverted pendulum and the hydro hammer contributes to this tendency. The offset of the center of gravity from default (upright position) time the mass of monopile or hydro hammer causes a moment around the pivot point. General tipping over moment is given by:

$$M_{to} = \sin(\alpha) * L * m * g \tag{3.14}$$

- L is length center of gravity to pivot point (m)
- m is mass (kg)
- g is gravity constant (m/s^2)

Geometrical formulations are linearized according equation 3.1 and 3.2. The magnitude of the tipping over moment is depended on the angle. In the linearized case, the tipping over (to) tendency acts as a negative spring stiffness.

$$M_{to} = k_{to} * \alpha \tag{3.15}$$

With:

$$k_{to} = L * m * g \tag{3.16}$$

Equivalent negative spring stiffness for the monopile consists of two parts. The submerged part which takes advantage of the buoyancy effects and the part above water level. The submerged part:

$$k_{to,mp} = L_4 * m_{mp} * g (3.17)$$

And the hydro-hammer:

$$k_{to\,hh} = L_7 * m_{hh} * g \tag{3.18}$$

Total tipping over stiffness:

$$k_{to} = k_{to,mp} + k_{to,hh} (3.19)$$

Control moment Gripper Frame is depended on the height and force applied by the gripper frame:

$$M_{GF} = F_{GF} * (L_8 + L_3 + L_2) (3.20)$$

Overall transfer function A transfer function is the ratio of the output of a system to the input of a system in Laplace domain. The output is a rotation of the monopile from equilibrium and the input is a moment around the pivot point.

$$I_{tot} * \ddot{\alpha} + d_{rot} * \dot{\alpha} + (k_{rot,soil} - (k_{to,mp} + k_{to,hh})) * \alpha = M$$
(3.21)

$$M = M_{GF} + M_{CU} + M_W + M_{WF} (3.22)$$

Transfer function in Laplace domain:

$$H(s) = \frac{\alpha(s)}{M(s)} = \frac{1}{I_{tot} * s^2 + d_{rot} * s + (k_{rot,soil} - (k_{to,mp} + k_{to,hh}))}$$
(3.23)

This time continuous transfer function is convert to a time discrete transfer function and implemented in Matlab/Simulink.

Simulation parameters Table 3.2 gives typical moment of inertia, damping and stiffness parameters for two monopile sizes and related water depths. For clarification, the parameters are visualized in figure 3.2.

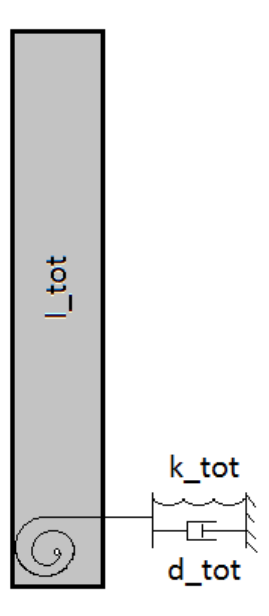


Figure 3.2: Overview specifications monopile

Monopile	I_tot (kg*m²)	d_tot (Nm*s/rad)	k_tot (Nm/rad)
FB16			
M-mp = 870mT			
M-hh = 850mT			
D = 7.6m			
L = 67m			
Water depth = 21m			
Penetration depth = 3m	5.62e9	1e9	-8.55e8
FB24 'scaled'			
M-mp = 1653mT			
M-hh = 850mT			
D = 10m			
L = 97m			
Water depth = 41m			
Penetration depth = 4m	1.28e10	3e9	-1.69e9

Table 3.2: Range of equivalent mono-pile parameters

The total system stiffness is negative which represents a inverted, instable pendulum.

Moment environmental force As mentioned before, current, wave and wind forces acting on the monopile. These forces are visualized in figure 3.3. The magnitude of these moments caused by this forces are calculated in this section. The formulas and sources are listed in chapter 2.

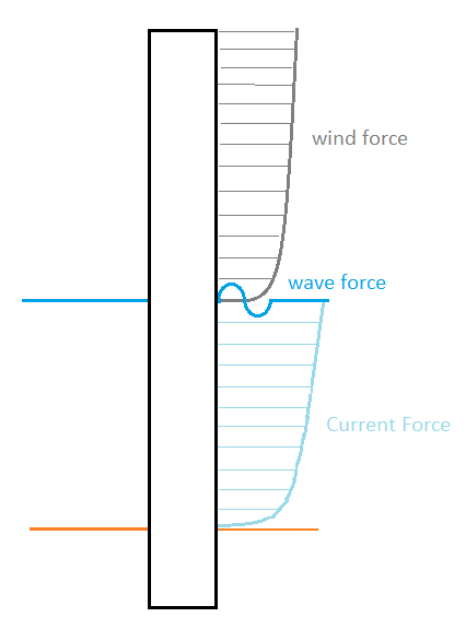


Figure 3.3: Overview environmental forces

Current moment Moment around the pivot point caused by current is given by:

$$M_{cu} = \frac{1}{2} * \rho * C_d * dz * D * \left(\sum_{i=1}^{L_3} v_{0,tide} \left(\frac{L_3 + (0.5 - i)}{L_3}\right)^{1/7}\right)^2 * \sum_{i=1}^{L_3} \left(L_2 + L_3 + (0.5 - i)\right)$$
(3.24)

- $v_{0,tide}$ is current velocity at still water level(m/s)
- dz is 1 meter step size
- C_d with relative low Reynolds number = 1.2
- $\rho = 1025 \text{ kg/m}3$

Water depth	D = 7.4m	D = 10m	Water depth	D = 7.4m	D = 10m
21m	0.44e3	0.62e3	21m	1.75e3	2.49e3
31m	0.90e3	1.27e3	31m	3.60e3	5.06e3
41m	1.53e3	2.13e3	41m	6.1e3	8.52e3
51m	2.32e3	3.22e3	51m	9.28e3	12.87e3

(a) current max = 1.0 kn, penetration depth = 3 or 4m (b) current max = 2.5kn, penetration depth = 3 or 4m

Table 3.3: Current moment depended on mono-pile diameter, water depth and current velocity (kN \cdot m)

The moment caused by current can be seen as stationary [1].

Wind moment During the earlier installation stage, when the monopile is lowered on the seabed, a large part of the monopile is above the water level. This wind forces applies a moment around the point of rotation of the monopile. The force is depended on the wind speed. The wind speed is depended on height. The relation between wind velocity, height and time period is given by [DNV offshore wind turbines] and can be found in chapter 2.

The moment is given by:

$$M_{cu} = \frac{1}{2} * \rho * C_d * dz * D * \left(\sum_{z=1}^{L_{11}} U(T, (z-0.5))^2 * (L_9 + L_2 + z - 0.5)\right)$$
(3.25)

Summarized for different wind velocities, different water depths (length of the arm is depended on water depth), monopile diameter and monopile length above water level (depended on the fixed, total length of the monopile according appendix E and the water depth):

Water depth	D = 7.4m	D = 10m	Water depth	D = 7.4m	D = 10m
21m	0.96e2	3.30e2	21m	0.38e3	1.32e3
31m	0.76e2	2.94e2	31m	0.30e3	1.18e3
41m	0.53e2	2.53e2	41m	0.21e3	1.01e3
51m	0.28e2	2.07e2	51m	0.11e3	0.83e3

(a) wind @ 10m = 2.5m/s, penetration depth = 3 or 4m (b) wind @ 10m = 5.0m/s, penetration depth = 3 or 4m

Table 3.4: Wind moment depended on mono-pile diameter, water depth and wind velocity (kN · m)

Water depth	D = 7.4m	D = 10m	Water depth	D = 7.4m	D = 10m
21m	0.86e3	2.97e3	21m	1.53e3	5.28e3
31m	0.68e3	2.65e3	31m	1.21e3	4.71e3
41m	0.47e3	2.28e3	41m	0.84e3	4.05e3
51m	0.25e3	1.86e3	51m	0.44e3	3.31e3

(a) wind @ 10m = 7.5m/s, penetration depth = 3 or 4m (b) wind @ 10m = 10.0m/s, penetration depth = 3 or 4m

Table 3.5: Wind moment depended on mono-pile diameter, water depth and wind velocity (kN · m)

Wave moment The first and second order wave forces acting on the monopile are calculated in Orcaflex according the flowchart mentioned in chapter 2. OrcaFlex is the world's leading package for the dynamic analysis of offshore marine systems used by over 260 clients. The wave forces are provided by the hydrodynamic department of Boskalis.

3.2.2. Induced vessel motions

In this section, the relative motion of the gripper frame to a NED set point of the mono-pile is calculated and recalculated to a vessel body fixed offset in which the gripper frame operates. Section 2.4 of the literature review is used as input. Figure 3.4 gives an overview of the calculation blocks.

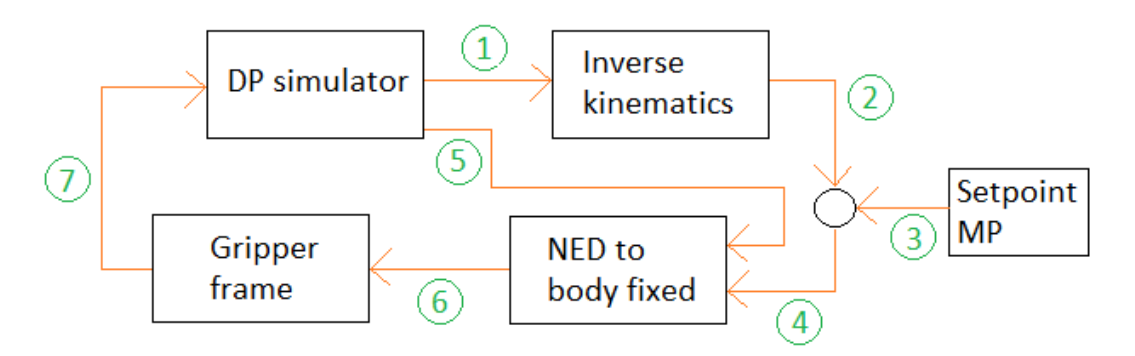


Figure 3.4: Overview inverse kinematics block

Table 3.7 summarize the outputs and inputs of the calculation blocks of figure 3.4:

Location	Variables	Description
1	LAT _{vessel-act}	Latitude coordinate vessel
	LON _{vessel-act}	Longitude coordinate vessel
	LAT _{vessel-set}	Latitude coordinate vessel set point
	LON _{vessel-set}	Longitude coordinate vessel set point
	U _{vessel-act,lin-BF}	Body fixed velocity vessel in surge direction
	V _{vessel-act,lin-BF}	Body fixed velocity vessel in sway direction
	ϕ_{vessel}	Euler angle roll
	θ_{vessel}	Euler angle pitch
	Ψ_{vessel}	Euler angle yaw
	$d\phi/dt_{vessel}$	Euler angle rate roll
	$d\theta/dt_{vessel}$	Euler angle rate pitch
	dψ/dt _{vessel}	Euler angle rate yaw
2	X _{GF-act-NED}	North direction position GF in NED
	y GF-act-NED	East direction position GF in NED
	u _{GF-act-NED}	North direction velocity GF in NED
	V _{GF-act-NED}	East direction velocity GF in NED
3	X _{MP-set-NED}	North direction position set point MP in NED
	y _{MP-set-NED}	East direction position set point MP in NED
	u _{MP-set-NED}	North direction velocity set point MP in NED
	V _{MP-set-NED}	East direction velocity set point MP in NED
4	X _{GF-offset-NED}	North direction position offset GF in NED
	y _{GF-offset-NED}	East direction position offset GF in NED
	U _{GF-offset-NED}	North direction velocity offset GF in NED
	V _{GF-offset-NED}	East direction velocity offset GF in NED
5	Ψ_{vessel}	Euler angle yaw
6	X _{GF-offset-BF}	North direction position offset GF vessel body fixed
	y GF-offset-BF	East direction position offset GF vessel body fixed
	U _{GF-offset-BF}	North direction velocity offset GF vessel body fixed
	V _{GF-offset-BF}	East direction velocity offset GF vessel body fixed
7	$F_{x,GF-vessel}$	vessel body fixed force from GF to vessel in surge direction
	$F_{y,GF-vessel}$	vessel body fixed force from GF to vessel in sway direction

Table 3.6: Block outputs

Inverse kinematics block Calculates the motions of the fixed part of the gripper frame in horizontal plane due to vessel motions. When knowing the induces motions of the fixed part of the gripper frame, inverse motions can be applied by the dynamic part of the gripper frame to achieve a fixed position in a earth fixed coordinate system (NED). For example, when the vessel have a surge offset of -1 meter from set point, the gripper need to have a +1 meter offset from it default position. In that case, the movable part of the gripper frame still have the same position in an earth fixed coordinate system.

Position A position change of the gripper frame in xy direction is caused by linear and rotational vessel motions. The 3x3 rotation matrix is given by matrix 2.30. State of the gripper frame due to vessel rotation with super positioned gripper to vessel NED frame origin set point is given by:

$$\begin{vmatrix} x_{GF-act,rot-b} \\ y_{GF-act,rot-b} \\ z_{GF-act,rot-b} \end{vmatrix} = \begin{vmatrix} 0 & -z_{GF-geo,pos} & -y_{GF-geo,pos} \\ -z_{GF-geo,pos} & 0 & x_{GF-geo,pos} \\ y_{GF-geo,pos} & x_{GF-geo,pos} & 0 \end{vmatrix} \begin{vmatrix} \phi \\ \theta \\ \psi \end{vmatrix}$$
(3.26)

'Geo' is the geometrical position of the fixed part of the gripper frame relative to the rotation point of the vessel.

$$\begin{vmatrix} x_{GF-act,rot-NED} \\ y_{GF-act,rot-NED} \\ z_{GF-act,rot-NED} \end{vmatrix} = |R_n^b(\Theta_{nb})| \begin{vmatrix} x_{GF-act,rot-b} \\ y_{GF-act,rot-b} \\ z_{GF-act,rot-b} \end{vmatrix}$$
(3.27)

Position of the gripper frame due to linear offset b-frame relative to NED origin described in section 2.4.2.:

$$dN = \frac{d\mu}{atan(\frac{1}{R_M})} \tag{3.28}$$

And:

$$dE = \frac{dl}{atan(\frac{1}{R_N cos\mu_0})}$$
 (3.29)

The reference LAT $(d\mu)$ / LON (dl) is the LAT/LON offset of the vessel based on the DP set point position of the vessel.

Gripper frame position in NED frame:

$$\begin{vmatrix} x_{GF-act-NED} \\ y_{GF-act-NED} \\ (-) \end{vmatrix} = \begin{vmatrix} x_{GF-act,rot-NED} \\ y_{GF-act,rot-NED} \\ z_{GF-act,rot-NED} \end{vmatrix} + \begin{vmatrix} dN \\ dE \\ (-) \end{vmatrix}$$
(3.30)

Velocity The NED velocity calculation shows similarities with the position calculation. Linear gripper frame velocities caused by rotational vessel velocities and linear gripper frame velocities causes by linear vessel velocities are calculated separately, added and given in NED frame via the rotation matrix. Body fixed linear velocity due to body fixed angular velocity constructed from equation 2.35:

$$\begin{vmatrix} u_{GF-act,rot-b} \\ v_{GF-act,rot-b} \\ w_{GF-act,rot-b} \end{vmatrix} = \begin{vmatrix} 0 & -z_{GF-geo,pos} & -y_{GF-geo,pos} \\ -z_{GF-geo,pos} & 0 & x_{GF-geo,pos} \\ y_{GF-aeo,pos} & x_{GF-geo,pos} & 0 \end{vmatrix} |\omega_{b/n}^{b}|$$
(3.31)

Total linear body fixed velocity gripper frame:

$$\begin{vmatrix} u_{GF-act-b} \\ v_{GF-act-b} \\ w_{GF-act-b} \end{vmatrix} = \begin{vmatrix} u_{GF-act,rot-b} \\ v_{GF-act,rot-b} \\ w_{GF-act,rot-b} \end{vmatrix} + \begin{vmatrix} u_{vessel-act,lin-BF} \\ v_{vessel-act,lin-BF} \\ (-) \end{vmatrix}$$
(3.32)

Gripper frame velocity in NED frame:

$$\begin{vmatrix} u_{GF-act-NED} \\ v_{GF-act-NED} \\ w_{GF-act-NED} \end{vmatrix} = \left| R_n^b(\Theta_{nb}) \right| \begin{vmatrix} u_{GF-act-b} \\ v_{GF-act-b} \\ w_{GF-act-b} \end{vmatrix}$$
(3.33)

Offset from set point The offset (position and velocity) of the gripper frame from it set point in NED frame:

$$\begin{vmatrix} x_{GF-offset-NED} \\ y_{GF-offset-NED} \\ u_{GF-offset-NED} \\ v_{GF-offset-NED} \end{vmatrix} = \begin{vmatrix} x_{MP-set-NED} \\ y_{MP-set-NED} \\ u_{MP-set-NED} \\ v_{MP-set-NED} \end{vmatrix} - \begin{vmatrix} x_{GF-act-NED} \\ y_{GF-act-NED} \\ u_{GF-act-NED} \\ v_{GF-act-NED} \end{vmatrix}$$
(3.34)

NED to body fixed block The gripper frame is physically connected to the vessel. For that reason, the forces in x and y direction applied by the gripper frame are exactly in the vessel body fixed frame. Monopile NED x and y off set needs to be recalculated to a vessel body fixed frame. Small pitch and roll angles are assumed so the rotation is only done in the horizontal plane according figure 3.5. x_2 and y_2 are body fixed vectors and x_3 and y_3 are in NED frame:

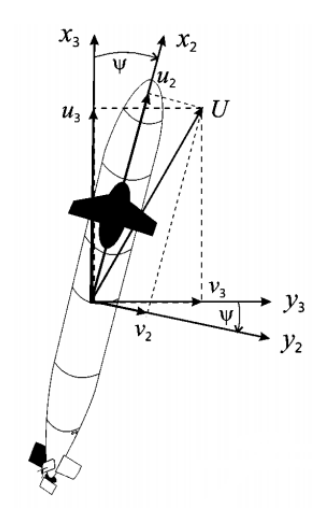


Figure 3.5: Rotation over yaw [20]

The rotation matrix is given by matrix 2.26. Position and velocity offset in body fixed frame:

$$\begin{vmatrix} x_{GF-offset-BF} \\ y_{GF-offset-BF} \\ u_{GF-offset-BF} \\ v_{GF-offset-BF} \end{vmatrix} = \begin{vmatrix} cos\psi & -sin\psi & 0 & 0 \\ sin\psi & cos\psi & 0 & 0 \\ 0 & 0 & cos\psi & -sin\psi \\ 0 & 0 & sin\psi & cos\psi \end{vmatrix} \begin{vmatrix} x_{GF-offset-NED} \\ y_{GF-offset-NED} \\ u_{GF-offset-NED} \\ v_{GF-offset-NED} \end{vmatrix}$$
(3.35)

3.2.3. Hydraulic gripper frame model

Layout Several types of monopile gripper frames layouts are available on the market or currently under development. These layout is depended on the used type of vessel. See chapter one. For jack-up vessel it is sufficient to use a fixed gripper frame in which the monopile is clamped by three of four hydraulic cylinders, see figure 3.6.



Figure 3.6: Example Fixed monopile gripper frame [17]

This cylinders have an rotational orientation of 120 or 90 degrees relative to each other. By moving all the cylinders simultaneous, in the right direction and with a certain ratio, the monopile can be moved inside the gripper frame. This could be necessary to correct for an inclination offset. But due to the continuous relocation of the connection between cylinders and monopile, only a small range can be achieved. It is assumed that a larger range is necessary because of the relative large footprint of a DP vessel. The motion compensated gripper

frame is modeled as a fixed part rigid connected to the vessel and a dynamic part connected to the monopile, sliding relative to the fixed part. This sliding movement is achieved by hydraulic cylinders with two degrees of freedom, namely in vessel body fixed x and y direction. The x and y direction are respectively related to vessel surge and sway direction. Parameters of the gripper frame are given in appendix D. The monopile is clamped inside the dynamic part of the gripper frame with another set of hydraulic cylinder. This hydraulic cylinder are not modeled. A rigid connection between the monopile and the dynamic part of the gripper frame is assumed.

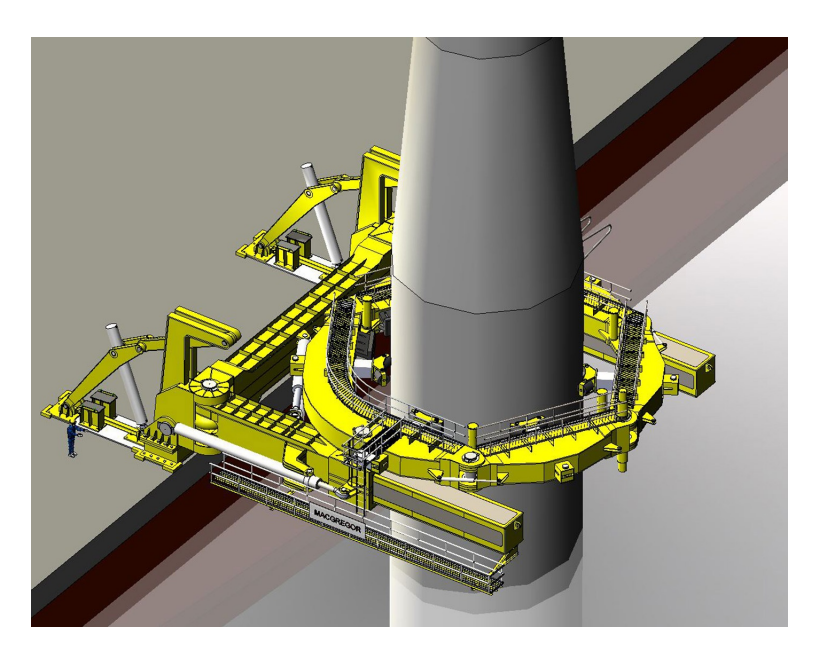


Figure 3.7: Example Motion Compensated Gripper Frame [32]

Two controller are added to control the gripper frame. An induced vessel motion compensation controller which apply inverse motion to counteract the vessel motions and a inclination controller which maintain the upright position of the monopile under influence of environmental forces.

Hydraulic model overview A position controlled hydraulic system model is build. The hydraulic cylinders are able to apply forces on the mechanical system (movable part of the gripper frame and the monopile) to control the position. Figure 3.8 shows an overview of the components involved.

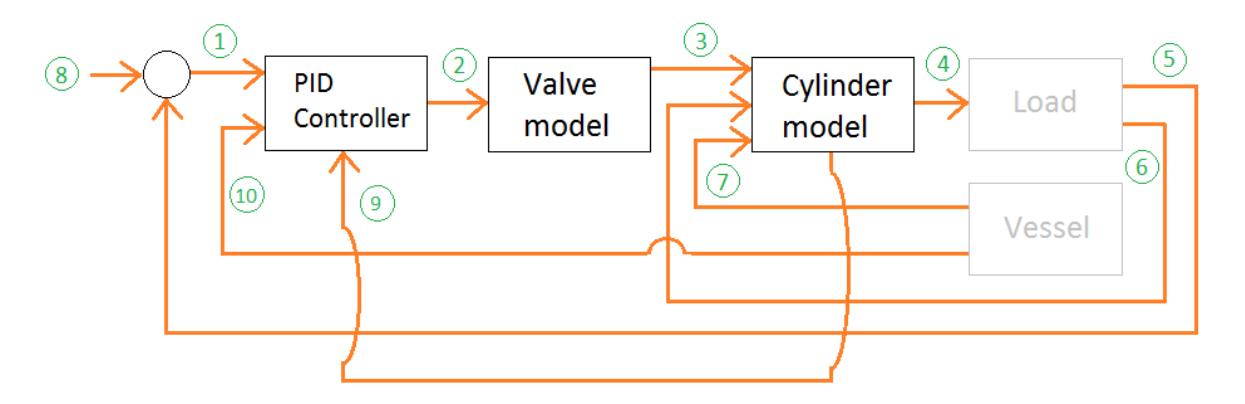


Figure 3.8: Overview hydraulic system

1 X _{MP-err-BF}	Location	n Variables	Description
2	1	X _{MP-err-BF}	North direction position error MP vessel body fixed
3 Q _{I,x} load flow x direction Q _{I,y} load flow y direction 4 F _{x,GF-MP} vessel body fixed force from GF to MP in surge direction F _{y,GF-MP} vessel body fixed force from GF to MP in sway direction vessel body fixed force from GF to MP in sway direction North direction position MP vessel body fixed y _{MP-BF} East direction position MP vessel body fixed v _{MP-BF} North direction velocity MP vessel body fixed v _{MP-BF} East direction velocity MP vessel body fixed v _{MP-BF} North direction position MP vessel body fixed y _{MP-BF} East direction position MP vessel body fixed y _{MP-BF} East direction position MP vessel body fixed		y _{MP-err-BF}	East direction position error MP vessel body fixed
3 Q _{I,x} load flow x direction Q _{I,y} load flow y direction 4 F _{x,GF-MP} vessel body fixed force from GF to MP in surge direction F _{y,GF-MP} vessel body fixed force from GF to MP in sway direction 5 X _{MP-BF} North direction position MP vessel body fixed y _{MP-BF} East direction position MP vessel body fixed V _{MP-BF} East direction velocity MP vessel body fixed x _{MP-BF} North direction position MP vessel body fixed x _{MP-BF} North direction position MP vessel body fixed y _{MP-BF} East direction position MP vessel body fixed y _{MP-BF} East direction position MP vessel body fixed	2	U _{contr-x}	control signal body fixed surge direction
Q _{I,y} load flow y direction 4 F _{x,GF-MP} vessel body fixed force from GF to MP in surge direction vessel body fixed force from GF to MP in sway direction 5 X _{MP-BF} North direction position MP vessel body fixed y _{MP-BF} East direction velocity MP vessel body fixed v _{MP-BF} East direction velocity MP vessel body fixed x _{MP-BF} North direction velocity MP vessel body fixed x _{MP-BF} North direction position MP vessel body fixed y _{MP-BF} East direction position MP vessel body fixed y _{MP-BF} East direction position MP vessel body fixed y _{MP-BF} East direction position MP vessel body fixed		u _{contr-y}	control signal body fixed sway direction
4 F _{x,GF-MP} vessel body fixed force from GF to MP in surge direction vessel body fixed force from GF to MP in sway direction 5 x _{MP-BF} North direction position MP vessel body fixed East direction position MP vessel body fixed 6 u _{MP-BF} North direction velocity MP vessel body fixed V _{MP-BF} East direction velocity MP vessel body fixed North direction position MP vessel body fixed North direction position MP vessel body fixed V _{MP-BF} East direction position MP vessel body fixed East direction position MP vessel body fixed	3	$Q_{l,x}$	load flow x direction
4 F _{x,GF-MP} vessel body fixed force from GF to MP in surge direction vessel body fixed force from GF to MP in sway direction 5 x _{MP-BF} North direction position MP vessel body fixed East direction position MP vessel body fixed 6 u _{MP-BF} North direction velocity MP vessel body fixed V _{MP-BF} East direction velocity MP vessel body fixed North direction position MP vessel body fixed North direction position MP vessel body fixed V _{MP-BF} East direction position MP vessel body fixed East direction position MP vessel body fixed		$Q_{l,y}$	load flow y direction
5 X _{MP-BF} North direction position MP vessel body fixed y _{MP-BF} East direction position MP vessel body fixed 6 U _{MP-BF} North direction velocity MP vessel body fixed v _{MP-BF} East direction velocity MP vessel body fixed x _{MP-BF} North direction position MP vessel body fixed y _{MP-BF} East direction position MP vessel body fixed	4		
y _{MP-BF} East direction position MP vessel body fixed u _{MP-BF} Vorth direction velocity MP vessel body fixed v _{MP-BF} East direction velocity MP vessel body fixed x _{MP-BF} North direction position MP vessel body fixed y _{MP-BF} East direction position MP vessel body fixed		$F_{y,GF-MP}$	•
6 U _{MP-BF} North direction velocity MP vessel body fixed V _{MP-BF} East direction velocity MP vessel body fixed North direction position MP vessel body fixed y _{MP-BF} East direction position MP vessel body fixed	5	X _{MP-BF}	North direction position MP vessel body fixed
V _{MP-BF} East direction velocity MP vessel body fixed x _{MP-BF} North direction position MP vessel body fixed y _{MP-BF} East direction position MP vessel body fixed		y_{MP-BF}	East direction position MP vessel body fixed
x _{MP-BF} North direction position MP vessel body fixed y _{MP-BF} East direction position MP vessel body fixed	6	u _{MP-BF}	North direction velocity MP vessel body fixed
y _{MP-BF} East direction position MP vessel body fixed		v_{MP-BF}	
		x_{MP-BF}	North direction position MP vessel body fixed
7 UCE RE North direction velocity fixed part GF vessel body fixed		У мР-ВF	· · · · · · · · · · · · · · · · · · ·
agr-br iteration releasely interaction records and	7	u _{GF-BF}	North direction velocity fixed part GF vessel body fixed
v _{GF-BF} East direction velocity fixed part GF vessel body fixed		v_{GF-BF}	East direction velocity fixed part GF vessel body fixed
8 x _{MP-set} North direction position MP set point (=0)	8	X _{MP-set}	North direction position MP set point (=0)
y _{MP-set} East direction position MP set point (=0)		y _{MP-set}	East direction position MP set point (=0)
9 Q _{L-x} Load flow hydraulic fluid in body fixed surge direction	9	Q_{L-x}	, , ,
Q _{L-y} Load flow hydraulic fluid in body fixed sway direction		Q_{L-y}	
10 x _{GF-BF} North direction position fixed part GF vessel body fixed	10	X _{GF-BF}	
y _{GF-BF} East direction position fixed part GF vessel body fixed		y _{GF-BF}	East direction position fixed part GF vessel body fixed

Table 3.7: Block outputs

Physics of a hydraulic system The structure of a hydraulic cylinder seems to be relatively simple but the system response can be quite complex when considering all the system dynamics. A model of a hydraulic system is given in [15] and described below. The model of a hydraulic cylinder has to contain at least a coupling between force and velocity at one hand and pressure and volume flow at the other hand. Different setups can be chosen to control the position and the force of the cylinder applied on the system. A constant pressure pump with a controllable valve is chosen in the simulation model. In order to maintain a constant supply pressure (P_s) and supply flow (Q_s) a high pressure relief valve is added to the system. The supplied hydraulic pressurized fluid flow to the four way valve and is depended on the position of the spool (x) and pressure difference between the cylinder chambers distributed to one of the cylinder chambers or/and back to the reservoir. The pump uses the hydraulic oil of the reservoir to supply the system with the above described pressurized hydraulic fluid. The system a is closed loop system. No fluid will leave or enter the system.

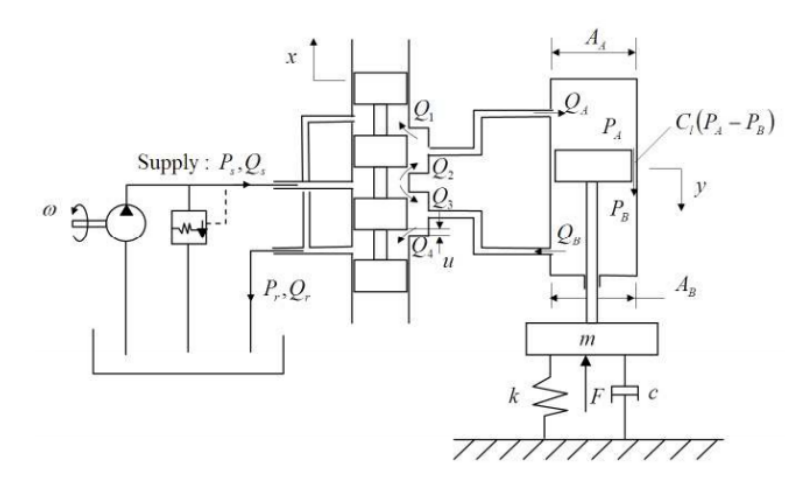


Figure 3.9: Schematic overview of a hydraulic system with a four way valve [15]

Load flow The load flow is the flow which enter the hydraulic cylinder. The general flow formulation through an orifice, depended on pressure difference over the orifice, can be set up with the principles founded by Bernoulli [15].

$$Q = AC_D \sqrt{\frac{2}{\rho} \Delta P}$$
 (3.36)

With:

- A is discharge flow area (m²)
- Cd is discharge coefficient (-)
- ρ is fluid density (kg/m^3)
- Δ P is pressure difference over the valve (Pa or N/m²)
- Q is fluid flow (m^3/s)

The discharge coefficient is found to be Cd = 1 from the continuity equation and Bernoulli's equation. In practice, there will be some loss of energy, and the cross section of the flow will be somewhat smaller than the cross section A. This will reduce the discharge coefficient Cd to be in the range 0.60 - 0.65 for orifices with sharp edges, and in the range 0.8 - 0.9 when the edges are rounded. A discharge coefficient of 0.67 is assumed [15].

This formula can be used in case of a turbulent flow. The Reynolds number for a flow is given by:

$$Re = \frac{D}{Av}Q\tag{3.37}$$

With:

- D is the diameter of the restriction (m)
- A is the cross sectional area of the flow (m^2)
- v is the kinematic viscosity (m^2/s)
- Q volumetric flow (m^3/s)
- Re is Reynolds number (-)

The flow, given by equation 3.36 may assumed to be turbulent for Reynolds numbers larger than 1000 and therefore given by equation 3.36 [15].

For the valve the assumption of a symmetric four way valve is made according figure 2.21:

$$A_a(x_v) = A_d(x_v) = A_b(-x_v) = A_c(-x_v)$$
(3.38)

With:

• x_v is the position of the spool (m)

The port areas for specific spool positions are given by the following formulations:

$$A_a(x_v) = A_d(x_v) = \begin{cases} 0, x_v \le 0 \\ bx_v, x_v \ge 0 \end{cases}$$
 (3.39)

$$A_b(x_v) = A_c(x_v) = \begin{cases} -bx_v, x_v \le 0\\ 0, x_v \ge 0 \end{cases}$$
 (3.40)

So, no leakage in the valve is assumed.

When the valve is matched and symmetric:

$$Q_A = Q_B \tag{3.41}$$

In this case, compressibility effects are not taken into account. Literature points out that the transfer function between spool position and flow represents the dynamics of the system with an accuracy which is sufficient enough [15].

The matched condition, orifice equation and symmetric load results in the following equations:

$$Q_1 = Q_4, Q_2 = Q_3 (3.42)$$

$$p_{s} + p_{r} = p_{A} + p_{B} {3.43}$$

With:

- p_s is the supply pressure (N/m²)
- p_r is the return pressure (N/m²)
- p_A is the pressure in cylinder chamber A (N/m^2)
- p_B is the pressure in cylinder chamber B (N/m²)

The load pressure is defined by:

$$p_l = p_A - p_B \tag{3.44}$$

The load flow by:

$$Q_l = \frac{1}{2}(Q_A + Q_B) {(3.45)}$$

 p_r is small relative to p_s and assumed to be zero. This implies:

$$p_A = \frac{p_s + p_l}{2}, p_B = \frac{p_s - p_l}{2}$$
 (3.46)

The load flow through the valve is found by:

$$Q_{l} = C_{d}A_{a}(x_{v})\sqrt{\frac{2}{\rho}*p_{B}} - C_{d}A_{b}(x_{v})\sqrt{\frac{2}{\rho}*p_{A}}$$
(3.47)

Which results in:

$$Q_l = C_d b x_v \sqrt{\frac{1}{\rho} (p_s - sgn(x_v)p_l)}$$
(3.48)

In non-dimensional form:

$$\frac{Q_l}{C_d b x_{v,max} \sqrt{\frac{1}{\rho} p_s}} = \frac{x_v}{x_{v,max}} \sqrt{1 - sgn(x_v) \frac{p_l}{p_s}}$$
(3.49)

Which can be written in a normalized function as:

$$Q_l^* = x_v^* \sqrt{1 - sgn(x_v)p_l^*}$$
 (3.50)

This gives the following plotted valve characteristic:

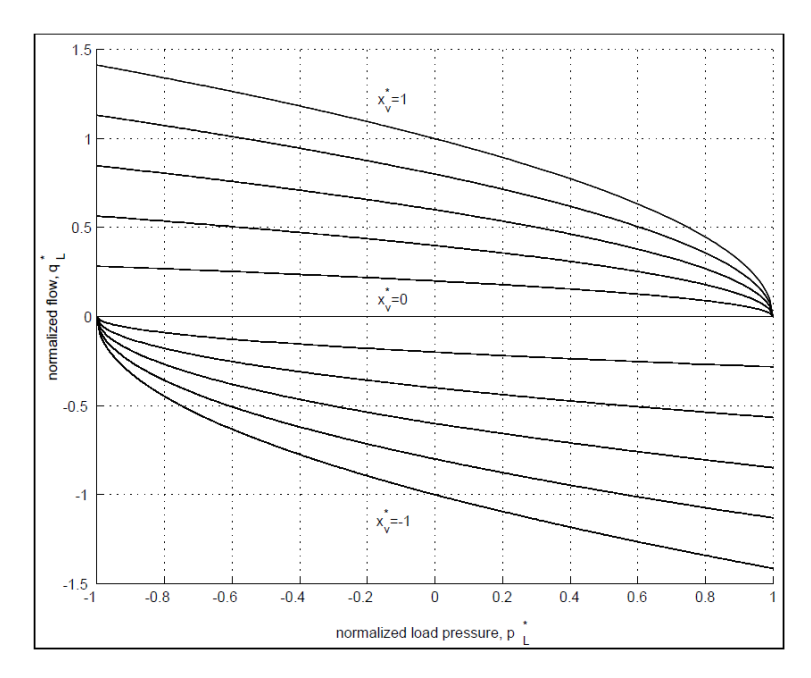


Figure 3.10: Valve characteristics [15]

Figure 3.10 shows the flow-pressure curves for different spool (x_v) positions. The normalized flow, pressure and spool positions are plotted.

The characteristic of the valve can be linearized [15]:

$$Q_l = K_q x_v - K_c p_l \tag{3.51}$$

With:

$$K_q = C_d b \sqrt{\frac{1}{\rho} (p_s - sgn(x_v)p_l)}$$
(3.52)

And:

$$K_{c} = \frac{C_{d}bx_{v}\sqrt{\frac{1}{\rho}(p_{s} - sgn(x_{v})p_{l})}}{2(p_{s} - sgn(x_{v})p_{l})}$$
(3.53)

Pressure analysis The relation between ρ and $d\rho$ which models the significant compressibility effects in the cylinder, is given by:

$$\frac{d\rho}{\rho} = \frac{dP}{\beta} \tag{3.54}$$

With:

• ß is the bulk modulus (N/m^2)

Mass balance for a volume:

$$\frac{d}{dt}(\rho V) = \rho q_{in} - \rho q_{out} \tag{3.55}$$

Combining equation 3.54 and equation 3.57, the mass balance of a hydraulic volume is given by:

$$\frac{V}{\beta}\dot{p} + \dot{V} = q_{in} - q_{out} \tag{3.56}$$

When considering both chambers in the hydraulic cylinder:

$$\dot{V_a} + \frac{V_a}{\beta} \dot{p_a} = -C_l (p_a - p_b) + Q_A \tag{3.57}$$

$$\dot{V_b} + \frac{V_b}{\beta} \dot{p_b} = -C_l (p_b - p_a) - Q_B \tag{3.58}$$

Combining mass balance formulations 3.57 and 3.58, this leads to one mass balance depended on load flow and load pressure:

$$\frac{V_t}{4\beta}\dot{p}_l = -C_l p_l - A_p \dot{x}_p + Q_l \tag{3.59}$$

With:

- V_t is $V_a + V_b$ (m^3)
- \bullet C₁ is the leakage coefficient across the piston (m⁴*s/kg)

Furthermore, based on figure 2.21, a load analysis can be made.

$$m\ddot{x}_p = -B_p\dot{x}_p + A_pp_l - F_l \tag{3.60}$$

With:

- m is the mass of the load (kg)
- \ddot{x}_{p} is the acceleration of the piston/load (m/s²)
- \dot{x}_p is the velocity of the piston/load (m/s)
- A_p is the piston area (m^2)
- \bullet F_1 is external force on the load (N)
- \bullet $B_{\rm p}$ is the internal viscous friction coefficient of the cylinder (Ns/m)

$$B_p = 4A_p \zeta_h \sqrt{\frac{\beta m}{V_t}} \tag{3.61}$$

With:

 \bullet ζ_h is the relative damping

The relative damping is set to 0.1. According [15] this parameter is typically in the range of 0.1-0.5.

Valve position The dynamics of the spool, i.e. the position of the valve (x_v) as function of a input signal from the controller is given by a second order transfer function [36].

$$X(s) = \frac{x_v(s)}{u(s)} = \frac{\omega_v^2}{s^2 + 2\zeta_v \omega_v s + \omega_v^2}$$
(3.62)

With:

- $x_v(s)$ is valve position
- u(s) is input signal
- ω_v -> natural frequency (rad/sec)
- ζ_v -> damping ratio

Constant	Value
ω_{v}	20 Hz
$\zeta_{ m v}$	0.75

Table 3.8: Constants valve [12]

The valve position is limited to a position of +/-0.025 meters.

Friction model The interaction between the movable and fixed part of the gripper frame and the interaction inside movable and fixed hydraulic cylinder parts influence the system behavior. This interaction is modeled as friction. Several types of friction can be distinguish. Stick slip, stribeck, coulomb and viscous friction. Only the velocity depended, viscous friction force is modeled. This force is depended on the friction coefficient and the relative velocity between vessel and monopile.

$$F_{fric} = \mu_v * (\dot{x}_v - \dot{x}_{mp}) \tag{3.63}$$

The friction coefficient is given in appendix D. A rigid connection between vessel and fixed part of the gripper frame is assumed.

Required load flow and load pressure Based on the maximum environmental force on the FB24, the required maximum load pressure (p_l) in the cylinder is preliminary determined to be 300 bar. To linearize the system around this required load pressure and to avoid saturation, the pump pressure (p_s) needs to be 1.5 times the load pressure [15] and is therefore determined to be 450 bar.

The required load flow (Q₁) at maximum load pressure is related to the roll and pitch motions of the vessel. The load flow is required to apply motion compensation of the moving vessel.

Roll +/- (deg)	Horizontal dist. (m)	T _p (s)	Velocity (m/s)	Q _{I,max} (m ³ /s)
1	0.45	7	0.125	0.015

Table 3.9: Required load flow

Power hydraulic pump The power of a hydraulic pump is depended on the pressurization and flow of the hydraulic fluid through the valve [15].

$$P_{pump} = p_l * Q_l \tag{3.64}$$

Gripper frame controllers Two factors are influencing the behavior of the monopile gripper frame combination. The gripper frame is connected to a moving base (vessel) and environmental forces are acting on the monopile. Two controllers are used to reduce the influence on the motions of the monopile. An inclination controller which maintain the upright position of the monopile under environmental load and induced vessel motion controller applies inverse motions compensation the compensate for the moving base.

Inclination controller The inclination controller maintain the upright position of the monopile. The inclination controller uses the inclination error of the monopile as an input. When the monopile have an inclination angle from the zero degree (upright) position, the gripper frame applies a force on the monopile in opposite direction to correct for this inclination error. The controller is tuned with the Matlab/Simulink linearization toolbox. The inclination controller is given a step input. The controller is tuned for a smooth response on this step input

To guarantee stability of the dual controlled system (DP vessel and Gripper frame-Monopile) and to avoid resonance interaction between both controlled systems it is required to separate the bandwidth of both controllers. The DP vessel controller is a black box so the bandwidth of the DP controller vessel combination is a given in this research. Based on the bandwidth of the DP controller, the minimum bandwidth of the inclination controller can be determined. The bandwidth of a controlled system can be determined with the rule of thumb [9].

Bandwidth (Hz) =
$$\frac{0.35}{RT}$$
 (3.65)

With:

• RT is 10%-90% rise time

The bandwidth of a dynamic positioning system in the controlled directions is typically in the range of 0.1 rad/sec [20]. This means a minimum fluctuating period of around 60 seconds. This bandwidth is chosen to maintain sufficient separation with the typical frequency of the first order force and to have the ability to counteract lower frequency forces such as second order wave forces and variation in wind forces.

In the past, several dual actuating control systems are designed to be applied, for example, in a hard disk drive. A relative high inertia, low bandwidth Voice Coil Motor is used with a large range and a relative low inertia, high frequency bandwidth piezoelectric microactuator to increase the overall bandwidth of the system to increase the tracking ability and to compensate for higher frequency noise. See for a description and modeling of such a system [29] and [2].

A bandwidth separation between both system in the range of 4 is observed. The systems are tested and no stability issues are observed. Applying these knowledge into this thesis, the inclination controller is tuned to have a bandwidth which is 4 times higher than the bandwidth of the DP vessel controller. The inclination controller will be tuned with the linearization toolbox to have a RT of 5.25 secs.

Induced vessel motion controller The induced vessel motion controller is used to compensate for the moving vessel to which the gripper frame is connected. The control action is based on the required flow of hydraulic fluid due to the moving vessel and the actual flow of hydraulic fluid. The controller reacts on the offset between both flows. When the required flow due to vessel motion matches perfectly the actual flow of hydraulic oil, the upright position of the monopile is perfectly maintained. However, in practice, also due to a delay in

the sensors, there will be an offset between those value. The monopile will slightly move with the motion of the vessel. The controller values are determined with the Matlab linearization toolbox. A trade off is made between maximum performance of the induced vessel motion controller and smooth motions of the monopile. The fastest system response is chosen for which the motions of the monopile are still smooth.

3.2.4. Overall model

Combining simulation blocks The separate blocks described above are combined in a overall simulation model. The blue blocks represents physical components, the orange blocks represents the controller algorithms.

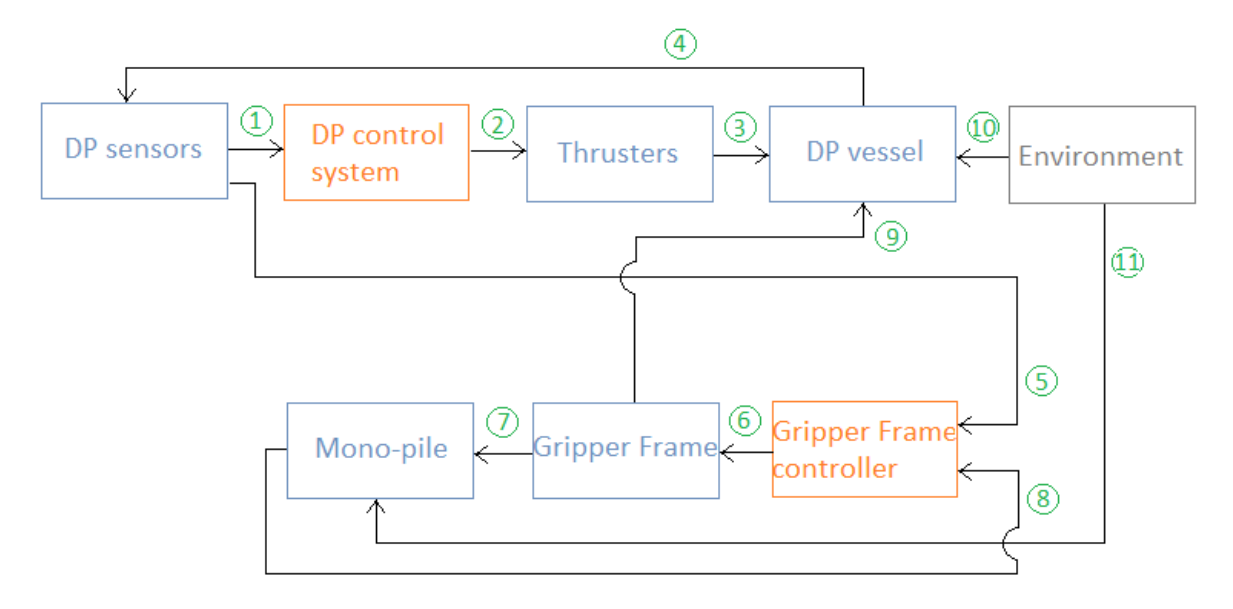


Figure 3.11: Overview simulation blocks

Location	Variables	Description
1	Vessel states	Position and velocity vessel
2	Control signals	-
3	Force	Provided by several thrusters
4	Location sensors on vessel	-
5	Vessel states	Position and velocity vessel
6	Control signals	-
7	Force on monopile	In surge and sway direction
8	Monopile states	Position and velocities
9	Reaction force on vessel	In surge and sway direction
10	Environmental force on vessel	Wind, wave and current force
11	Environmental force on monopile	Wind, wave and current force

Table 3.10: Overall simulation block out- and inputs

Two modes of operation can be distinguished. Monopile gripper frame on or off, mode 1 and mode 2. When the gripper frame is on, the interaction between vessel and monopile is the hydraulic monopile gripper frame. When the gripper frame is off, vessel and monopile forms one rigid body. In other words, the motions of the monopile are induced by the motions of the vessel. In the other way around, the motions of the vessel are restricted by the interaction of the monopile with the soil. Mode 2 is used to verify the induced vessel motion block.

Simulation frequency The hydraulic system will be the most governing simulation block with respect to resonance due to the high bulk modulus of the hydraulic fluid. The resonance frequency is depended on the size of the cylinder and the mass attached to the cylinder. Equation 3.66 gives the resonance frequency [25].

$$HRF = \frac{1}{\pi} \sqrt{\frac{A\beta}{ML_s}} \tag{3.66}$$

With:

- β = bulk modulus
- A = area of both sides of the cylinder
- M = mass of the load
- L_s = length of the cylinder

A resonance frequency of 2Hz is calculated. A good rule of thumb is a the sampling frequency chosen to be at least 30 times larger than closed loop bandwidth frequency [19]. The closed loop bandwidth frequency is likely to be larger than the resonance frequency. The simulation frequency is determined to be 100Hz.

3.3. Model verification

Several tests are carried out to verify the simulation model. The hydrodynamic model of the vessel, the station keeping performance of the 'clean' vessel, the falling behavior of the monopile, the behavior of the gripper frame and the behavior of the monopile-gripper frame combination are checked.

3.3.1. Surge and sway motions under environmental load

Test	Current (m/s)	Direction to (deg)			
1	2.0	180			
2	2.0	90			

Table 3.11: Environmental conditions surge and sway comparison

Appendix B shows surge and sway behavior plots under environmental load. A current of 2 m/s is acting on the bow in the surge behavior test and from port side in the sway behavior test. Both plots shows the velocity of the vessel in a time domain plot. In both plots, an error between the simulation model and the data from Boskalis is observed. The velocity, in the low velocity range, is lower compare to the data from Boskalis and higher in the high velocity range. This implies a overestimation of the damping in the low velocity range and an underestimation in the high velocity range. Dynamic positioning is a low velocity application [20], so the performance of the system might be overestimated due to the higher assumed damping. Comparing both surge and sway plot, the adaption of the velocity of the vessel to the applied current velocity is faster in sway direction compare to surge direction. In the low vessel velocity range, the inertia of the vessel is dominant with respect to the damping force of the vessel. A larger force is acting on the vessel in sway direction compare to surge direction due to the larger frontal area. This is implies that a larger forces is available in sway direction for the acceleration of the vessel. In the higher velocity range, where the drag force becomes more important, an earlier flatting of the sway velocity curve is observed.

3.3. Model verification 61

3.3.2. Roll and pitch motions vessel under wave load

The roll and pitch motions due to wave load of the RH Marine vessel model is compared to data from Boskalis. The verification is carried out for two environmental conditions:

Test	Hs (m)	Tp (s)	Direction from (deg)
1	2.5	7	330
2	2.5	9	330

Table 3.12: Environmental conditions roll-pitch comparison

The probability plots can be found in appendix B. Key values of the plots are listed below.

Test	R. min	R. max	R. mean	R. st. dev.	P. min	P. max	P. mean	P. st. dev.
RH Marine	-0.163	0.174	0.000	0.070	-0.250	0.253	0.000	0.130
Boskalis	-0.287	0.324	-0.002	0.068	-0.390	0.362	-0.008	0.094

Table 3.13: Test 1 roll and pitch (deg) comparison RH marine simulator with Boskalis data Hs 2.5m, Tp 7s

Test	R. min	R. max	R. mean	R. st. dev.	P. min	P. max	P. mean	P. st. dev.
RH Marine	-0.375	0.426	-0.000	0.175	-0.594	0.590	0.002	0.316
Boskalis	-0.761	0.572	-0.014	0.176	-0.850	0.789	-0.007	0.217

Table 3.14: Test 2 roll and pitch (deg) comparison RH marine simulator with Boskalis data Hs 2.5m, Tp 9s

When comparing both data sets, similarities and differences are observed. The values of the roll and pitch motions are in both environmental conditions in the same order. However, the maximum and minimum value of the roll and pitch angle are larger in the Boskalis data set. This is due to the fact that the waves applied in the Boskalis simulation model is based on a wave spectrum. This imply that also wave with an higher and lower wave period and wave height is acting on the vessel. In the RH Marine vessel model, the first order waves are modeled as a perfect sinus wave. This results in lower minimum and maximum angle values and relative a wider spread between the values. However, both values are in the same order so the RH Marine vessel model is assumed to be valid with respect to roll and pitch motions.

3.3.3. Station-keeping performance vessel

The station-keeping performance plots of the 'clean' vessel under environmental load can be found in appendix B. The minimum, maximum, mean and standard deviation values for surge and sway direction are given in table 3.16.

Test	current	waves	wind	Direction
1	2.5 kn	Hs 2.5 meters, Tp 7.0 sec	19 kn	330 deg
2	2.5 kn	Hs 2.5 meters, Tp 9.0 sec	19 kn	330 deg
3	2.5 kn	Hs 2.5 meters, Tp 9.0 sec	19 kn	000 deg

Table 3.15: Vessel footprint tests conditions

Test	S. min	S. max	S. st. dev.	Sw. min	Sw. max	Sw. st. dev.
1	-0.45	0.40	0.17	-0.79	1.24	0.32
2	-0.49	0.50	0.19	-0.88	1.44	0.35
2	-0.52	0.43	0.17	-0.51	0.56	0.23

Table 3.16: DP footprint 'clean' vessel under environmental load

The vessel is able to achieve a station-keeping situation under environmental conditions with a realistic footprint. A larger footprint is observed in case of wave with an higher wave

period. Waves with an higher Tp implies higher first order wave forces. This explains the larger footprint. Furthermore, a larger envelope is observed comparing sway to surge motions. In general, the hydrodynamic damping in sway direction is much larger compare to surge direction. However, since this damping is velocity depended and a DP operation is a low velocity application [20]. The inertia of the mass plays a larger roll in low velocity operation. The inertia of the vessel mass is the same in surge and sway direction. Beside that, a larger environmental force is acting on the vessel in sway direction. This could cause a large envelope. The DP controller design also have influence on the DP footprint. However, the DP controller is a black box in this research.

Comparing the case of the direction of the environmental force from 330 and 000, a comparable footprint is observed in surge direction and a significant smaller footprint in sway direction. The environmental force in surge direction is higher although, the thruster can almost fully be used to counteract the force in surge direction. Less azimuth rotation is necessary. This reduce the footprint.

The footprint of the vessel under environmental conditions is acceptable taking into account the mass and size of the vessel.

3.3.4. Falling behavior monopiles

In appendix B, the behavior of the unstable monopile is compared with data provided from Boskalis. 4 tests are carried out. Both monopiles (FB16 and FB24) are given an inclination offset (0.1° and 1.0°). The falling behavior of the simulated monopile is compared to simulation data obtained from Boskalis.

Monopile	1s	2s	3s	4s	5s	6s	7s	8s	9s	10s	11s	12s	13s	14s	15s
FB16	0	0	0	0	0	0	0	0	0.5	1	2	5	6.5	7.5	10
FB24	0	0	0	0	0	3	8	10	10	10	10	10	5	3	2

Table 3.17: Angle error between simulation and Boskalis data in (%), default inclination 0.1°

Monopile	1s	2s	3s	4s	5s	6s	7s	8s	9s	10s
FB16	0	0	4	9	7	10	10	7	5	5
FB24	0	0	2	5	7.5	7.5	6	4	2	0

Table 3.18: Angle error between simulation and Boskalis data in (%), default inclination 1.0°

Table 3.17 and 3.18 shows an error between the output of the simulation model and the data provided by Boskalis. For small angles, the error is relative low. When the inclination offset of the monopile becomes larger, the error increases. This is possibly caused by the linearization of the goniometric equations of the monopile model. During the simulation, it is necessary to achieve a low monopile inclination error to avoid saturation of the vessel thrusters. For the low angle range, the fit is good enough to assume the simulation model of the monopile as valid.

3.3.5. Induced vessel motion test

Testing transformation of vessel motion into monopile motions and the correct coupling of the reaction force of the gripper frame/monopile on the vessel.

Situation Motion compensated gripper frame off (vessel and monopile are one rigid body), high penetration depth of the monopile (in other words, the monopile is relative fixed to the earth. Monopile rotations requires high forces), Stationary current force on the vessel from a certain direction.

Expected behavior The vessel will rotate around the monopile, in a relative perfect circular motion because of the fixed monopile into the soil and the vessel - monopile which acts as one rigid body, till a certain equilibrium position and orientation of the vessel is reached. The

3.3. Model verification 63

positive moment and the negative moment around the rotation point of the vessel due to the reaction force from the gripper frame on the vessel is in balance. The total moment is zero so the vessel has reach a new equilibrium.

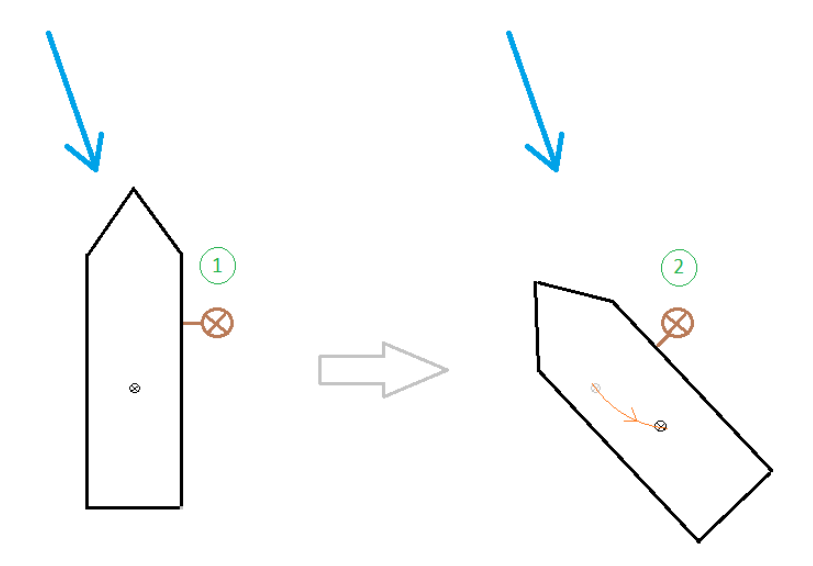


Figure 3.12: Example of expected behavior inverse kinematic test

Simulation variables The system configuration is given in table 3.19.

Variable	Description	Number	Unit
pos. MP-x	Relative to vessel rotation point	20	m
pos. MP-y	Relative to vessel rotation point	30	m
MP diameter	-	10	m
MP penetration depth	-	16	m
current velocity	-	2.0	kn
current direction test 1	-	120	deg
current direction test 2	-	300	deg

Table 3.19: Variables inverse kinematic test

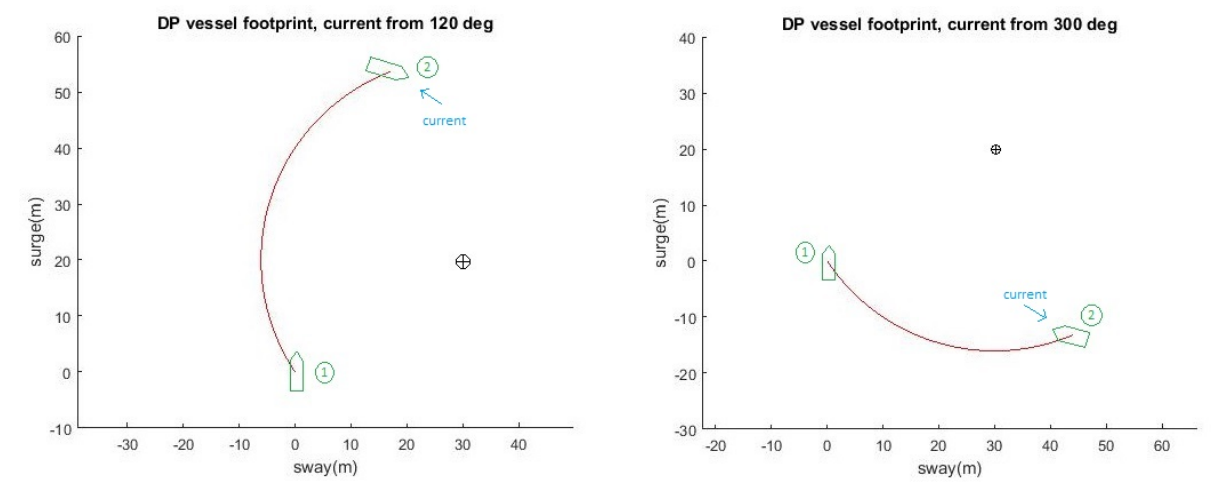


Figure 3.13: Equilibrium behavior test 1

Figure 3.14: Equilibrium behavior test 2

The vessel reach a equilibrium position based on expectations and a circular motion around the monopile is observed in figure 3.13 and 3.14.

The equilibrium yaw angle in test 1 is 101.5 degrees. The angle between current direction and yaw angle is 18.5 degrees. The equilibrium yaw angle in test 2 is 281.5 degrees. The angle between current direction and yaw angle is in this case also 18.5 degrees. In both tests, the same equilibrium between current direction and yaw angle is observed. A correct coupling between motions of the vessel, motions of the monopile and interaction forces between vessel and monopile is verified.

3.3.6. Hydraulic gripper frame

As mentioned before, in the hydraulic cylinder, a load flow and load pressure is translated into a force and velocity of a system coupled to the hydraulic cylinder. The relation between both is depended on the geometrical properties of the cylinder. The system is designed to deliver a certain load flow under maximum load pressure. These values are given in section 3.2.3. According the linearized equation of the load flow as function of the spool position and load pressure, equation 3.51 and the requirements in paragraph 'Required load flow and load pressure' the load flow can be determined. Three relations between load pressure, spool position and load flow are verified.

Spool pos.	Load pres. (bar)	Load force (kN)	Req. load flow (m ³ /s)	Req. load vel. (m/s)	
+0.5*max	0	0	0.012	0.099	
+max	300	3594	0.015	0.125	
-max	-300	-3594	-0.015	-0.125	

Table 3.20: Load flow as function of load pressure

The gripper frame is verified by applying a force on a damped and undamped mass. To verify the case in which the load pressure is positive or negative, the damping have a positive value. In case of verifying the zero load pressure case, the value of the damping is zero.

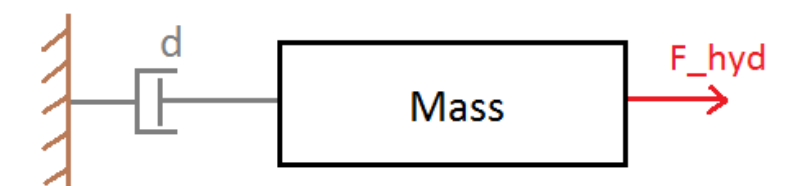


Figure 3.15: Damped mass

The damping in the test is corresponding to the tested load force and load velocity. In case when the maximum velocity at zero load pressure case is tested, the damping in the system is zero. The hydraulic cylinder needs to accelerate the mass to a maximum velocity corresponding to the maximum flow at zero load pressure. After reaching the maximum velocity, the resulting force reduce to zero so the mass does not accelerate anymore. For the test to investigate the load flow at maximum load pressure, a damping is chosen which relate the maximum load pressure to the required maximum load flow. The plots of the tests are given in appendix D.

Analyzing the plot, a velocity of the mass is observed which corresponds to the load pressure shown in table 3.20. So the assumption is made that the relation between spool position, load pressure and load flow is simulated correctly.

3.3.7. Hydraulic gripper frame-monopile behavior

This section shows some preliminary simulation results to study the performance of the hydraulic gripper frame. The main objective of the gripper frame is to maintain an upright position of the unstable monopile under dynamic environmental conditions (moving vessel and environmental force on the monopile). 4 scenario's are studied:

3.3. Model verification 65

• Test 1: a relative fast fluctuating base (platform to which the gripper frame is connected) to simulate the tracking ability of vessels fast pitch and roll motions. The base fluctuate with a frequency of 0.25 Hz (Tp 4s) and an amplitude of 0.15 meter.

- ullet Test 2: a relative slow fluctuating base to simulate second order drift motions of the vessel. The base fluctuate with a frequency of 0.02 Hz and an amplitude of 1.5 meter.
- Test 3: a constant force is applied on the monopile at gripper frame level to investigate the ability of the gripper frame of maintaining upright position under a constant environmental load. A load of 500 kN is applied on the FB24 monopile and 200 kN is applied on the FB16 monopile. The force is applied from 0 to maximum force in 10 secs.
- Test 4: the monopile is given a default offset of 1.0 deg. to investigate the ability of the gripper frame to recover an inclined monopile back to the upright position.

Visualization of the tests:

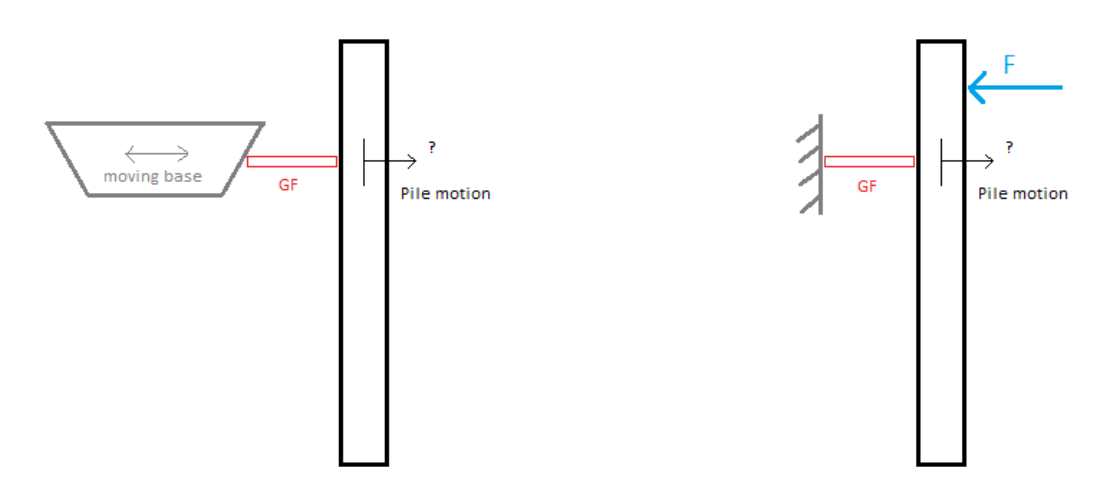


Figure 3.16: Visualization

The results are plotted for both the FB16 and FB24 monopile. The tests are carried out in one degree of freedom. The plots are presented in appendix C.

Test 1 and 2 The gripper frame is able to apply motion compensation for high and low frequency induced motions of the vessel. In both cases the upright position of the monopile is maintained and the motion of the monopile at gripper frame level is smaller than the motions of the vessel at gripper frame level.

Monopile	Freq. base (Hz)	Ampl. base (m)	Ampl. monopile (m)	Reduction in (%)
FB16	0.02	1.5	0.038	97%
FB16	0.25	0.15	0.071	53%
FB24	0.02	1.5	0.059	96%
FB24	0.25	0.15	0.084	44%

Table 3.21: Motion reduction gripper frame

Comparable motion reduction is observed for both monopiles. This might be strange when taking into account the large weight of the FB24 compare to the FB16. Values of I, d and k are in order of twice in magnitude. However, the distance from gripper frame is 1.5 times larger. This implies smaller angle offset for the FB24 with equal linear offset at gripper frame level. Furthermore, the moment applied by the gripper frame is 1.5 times larger in case of the larger monopile. Therefore, the similarity in motion reduction is logical. However, the motions of the larger monopile are still larger in magnitude due to the higher weight of the monopile.

A motion compensate pile gripper frame designed by the company TWD (www.TWD.nl) claims a reduction in surge and sway motion with respect to the monopile of 95%. For that reason, realistic performance of the vessel motion compensation ability of the hydraulic gripper frame is assumed.

Test 3 In the first 10 seconds of this test, a linear increasing environmental force is pushing against the compressibility of the hydraulic fluid in the cylinder due to the motion of the monopile. After 10 seconds, when the environmental force is constant, the gripper frame controller apply an extra force to compensate for the offset of the monopile. The FB16 monopile is faster recovered to its zero inclination angle compare to the FB24 monopile. This is due to the lower constant force and the lower weight of the monopile.

Test 4 For both pile, the gripper frame is able to recover an inclined monopile. From t=0 sec. to t=3 sec., the monopiles are hanging in the gripper frame. At t=3 sec., the controllers of the gripper frame are switched on and the gripper frame recover the monopile. Due to the lower weight of the FB16 monopile, a faster recovery is observed. The recovery of the FB16 monopile take in order of 7 sec. and the recovery of the FB24 monopile in order of 10 sec. Note: this is outside the bandwidth frequency range of the surge and sway motions of the vessel and is according the tuning of the inclination controller mentioned before.

3.3.8. Conclusion

The separate models are checked according data from Boskalis or expected behavior. The available simulation block (DP vessel model) is configured according vessel data from Boskalis. The DP controller keeps the position of the vessel under environmental load within acceptable limitations. The gripper frame is able to maintain upright position of the monopile in governing environmental conditions. The next chapter investigate the system behavior the the combined model blocks.

4

System analysis

This section presents the simulation results and provide an analysis on the system to declare the behavior. Four case are studied to investigate the sensitivity of changing variables.

4.1. Gripper frame force feed forward

Several studies are done on DP vessel operation with an large external installation force acting on the vessel. [43] And [4] propose a feed forward solution of the installation force into the Kalman filter for better state estimation of the vessel. The concept is successfully proven and described by [8] in case of a combined DP heavy lift operation. Wind force can lead to a drift of a DP vessel. Especially the wind force variation which is in frequency larger than the compensation ability of the Integral action of the PID controller and small enough in frequency to have a significant influence on the surge and sway motions of the vessel stated in [39]. [39] propose a Kalman feed forward solution to deal with these forces. "The measurements of wind speed and wind direction from the anemometers are fed into a wind force model from which are obtained estimates of the forces on the vessel in each axis, surge, sway and yaw. These forces are fed into the Kalman filter (KF) which is used to estimate vessel motions".

The Kalman feed forward solution is used in the simulation. Figure 4.1 shows in red (line 12) the extra connection in the simulation model. Forces from the gripper frame controller are fed into the DP control system. The force from the gripper frame in the vessel is not directly feed forward to the thruster allocation algorithm due to the assumption that the force profile also consists of high frequency (first order wave frequency) forces. The ramp up of the thrusters are limited so the thrusters can not follow these forces.

68 4. System analysis

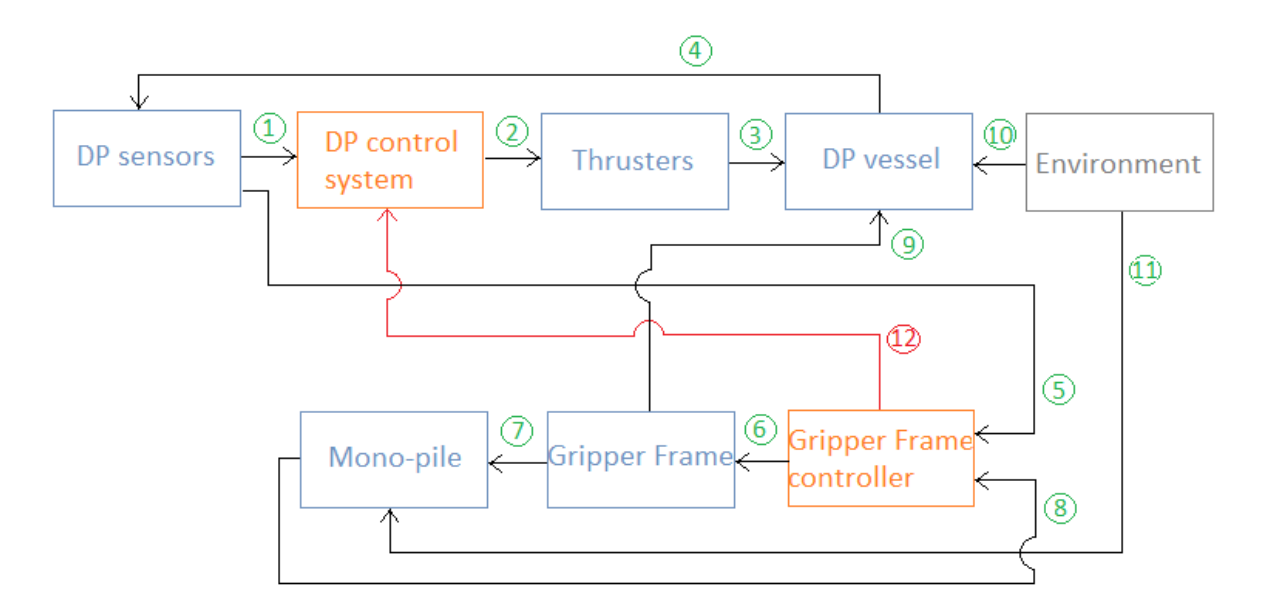


Figure 4.1: Overview simulation blocks with Kalman feed forward

The assumption is made that the forces applied by the hydraulic gripper frame can be measured with a pressure sensor inside the hydraulic cylinder. Pressure sensors are available on the market and widely used also for monitoring hydraulic systems and for alerting operators when the system is in danger. This pressure can be recalculated into the force applied by the gripper frame on the monopile and vessel. This calculated force is fed into the Kalman filter.

4.2. Envelope and capacity requirements by case studies

4.2.1. Simulation objectives

To achieve a safe operation the following have to be maintained or investigated.

Maintain:

- vessel stability in terms of dynamic positioning
- upright position of the unstable monopile

Investigate:

- the required range of the gripper frame
- the required power and force of the gripper frame

4.2.2. Variables and assumptions

Some simulation parameter are variable in the simulation. The other parameters are assumed to be fixed which does not mean that changing those parameter would not influence the simulation results. The influence of changing those parameter will be discussed in chapter 5. A recap of the assumptions and variables is given in table 4.1.

Assumptions	Variables
Vessel mass and water displacement, Bokalift1	Monopile dimensions, FB16 and FB24
Vessel power and thruster configuration, Bokalift1	Environmental conditions
Gripper frame hardware characteristics	Direction environmentals
Location of gripper frame	
Installation phase, pre-hammering	

Table 4.1: Assumptions and variables simulation

Simulation of all the combinations of variables are carried out for a total of 5 simulations.

4.2.3. Environmental conditions

The environmental conditions could limit the operation. The amplitude of the wave height and period of the wave influence the roll and pitch motions of the vessel. The magnitude of the current and wind force determine the load on the vessel. Carrying out the operation for sea state up to Hs 2.5 meter is typically for offshore lifting and installation operations [30] to maintain sufficient operability in which the operation can carried out. Up to 85% workability can be achieved in the North Sea are. A rule of thumb relation between the significant wave height and the peak period is given by [28]:

$$T_p \approx 5.3\sqrt{H_s} \tag{4.1}$$

This relation is comparable to the IMCA wind-wave relationship. The environmental conditions for which the simulations are carried out are shown in table 4.2 below.

Condition	current	waves	wind
1	2.5 kn	Hs 2.5 meters, Tp 7 sec	19 kn
2	2.5 kn	Hs 2.5 meters, Tp 9 sec	19 kn

Table 4.2: Environmental conditions

Two wave periods around the calculated wave period are chosen. Tp 7 secs and Tp 9 secs. For a higher wave period, the spectral density, or the energy of the wave is higher. A lower wave period is more governing in terms of the ability of the gripper frame to compensate for vessel motions (see the verification part of the gripper frame monopile combination).

4.2.4. Direction environmental force

Based on the DP capability of the vessel, a vessel have the highest capability to counteract environmental conditions from the bow or the stern. Due to the smaller frontal area, the force acting on the vessel is smaller for the same environmental condition compare to the case when the environment is acting on the side of the vessel.

The capability of the vessel is less when the environmental forces are acting with an angle from the bow. This implies that current wind and wave are also acting on the large side area of the vessel. This gives higher forces on the vessel for given environmental conditions which increase the required power of the thrusters to maintain position of the vessel.

Combining those two, gives the following environmental force directions: wind from 330 deg direction, wave from 330 deg direction and current to 150 deg direction. This is a worst case scenario with respect to the capability of the vessel. When the angle of the environmental forces with respect to the bow becomes larger during the operation, weathervaning can be applied to limit the environmental load on the vessel. Normally, the current forces is not acting in the same direction as the wave and wind forces. This is a worst case scenario and therefore assumed in the simulation. Furthermore, to investigate the governing requirements on the gripper frame in surge direction, a simulation is done with the environmental conditions from the bow. The directions are visualized in figure 4.2.

70 4. System analysis

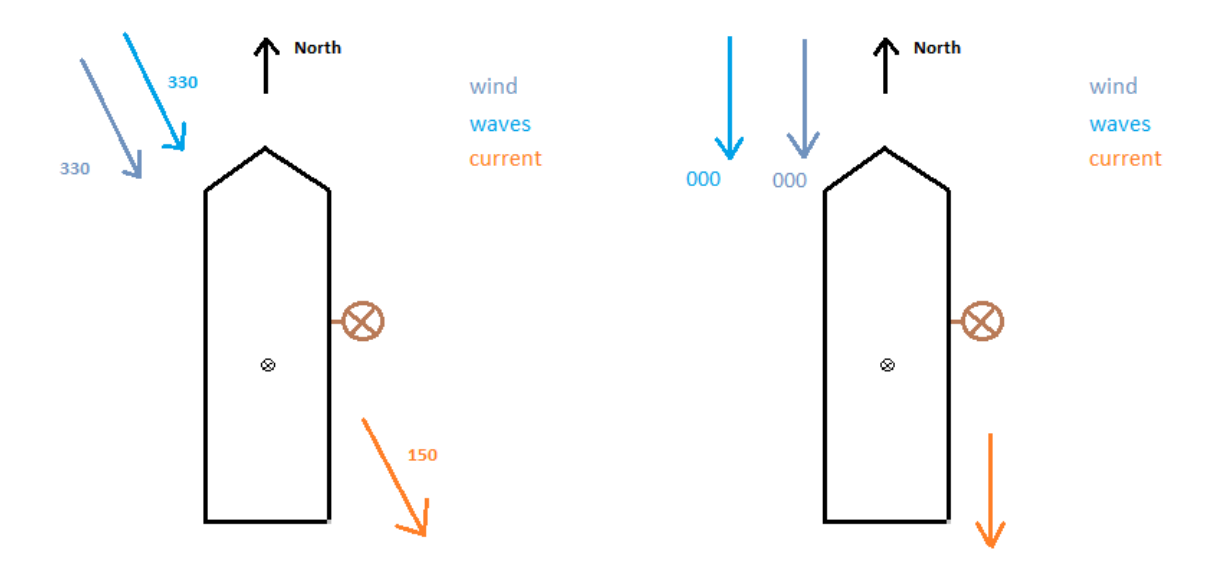


Figure 4.2: Direction environmental force on the vessel, case

Figure 4.3: Direction environmental force on the vessel, case

	Fw-x (kN)	Fc-x (kN)	Rel. F-x (%)	Fw-y (kN)	Fc-y (kN)	Rel. F-y (%)
Vessel	-270	-120		300	500	
FB16	-36.4	-41.6		21.0	24.0	
Relative			20			6
FB24	-61.3	-129.0		35.4	74.5	
Relative			49			14

Table 4.3: Relative magnitude stationary environmental force direction 330

In case of the FB24 monopile, the stationary force in surge direction on the pile is significant in relation to the stationary force on the vessel. There will be a possibility of a drift of the vessel when the forces on the monopile are acting on the vessel.

4.2.5. Simulation steps

At t=0, the environmental forces are applied on the vessel. The first 1500 seconds of the simulation are used to initiate the Kalman filter which estimates the stationary and slow varying forces acting on the vessel. From t=1500 to t=1600, the forces from the gripper frame are slowly introduced to the vessel. This represents the lowering process of the monopile. Equation 4.2 give the ramp up function:

$$f_{ramp} = u^3 (6u^2 - 15u + 10) (4.2)$$

The applied force on the vessel is normalized with the ramp up function. 'u' increase linear in 100 sec. from 0 to 1. After 100 sec, the ramp up function is one. After 100 sec, the total force is acting on the vessel.

From (s)	Till (s)	Description
0	1500	Initialization DP controller
1500	1600	Lowering process monopile
1600	12300	Early hammering phase

Table 4.4: Simulation steps

The simulation results are presented from t=1500 to t=12300 sec. The 3-hour length was chosen because this is a typical test length used in ocean basins [40].

4.2.6. Simulation results

Simulation results are given for the variables given in section 4.1. The influence on the vessel performance of changing this variables can be studied by comparing the simulation results.

- Plot 1: Surge position vessel relative to its DP setpoint, (m)
- Plot 2: Surge position vessel relative to its DP setpoint, (m)
- Plot 3: Position dynamic part Gripper Frame relative to fixed part Gripper Frame in surge direction, (m)
- Plot 4: Position dynamic part Gripper Frame relative to fixed part Gripper Frame in sway direction, (m)
- Plot 5: Rotation of monopile around in surge direction, (deg)
- Plot 6: Rotation of monopile around in sway direction, (deg)
- Plot 7: Force Gripper frame applied on the vessel in surge direction, (kN)
- Plot 8: Force Gripper frame applied on the vessel in sway direction, (kN)
- Plot 9: Power hydraulic pump gripper frame in surge direction, (kW)
- Plot 10: Power hydraulic pump gripper frame in sway direction, (kW)

The simulation results can be found in appendix F.

4.2.7. Simulation analysis

This section presents the simulation results and provide an explanation of the results. The overall operation is simulated with different system variables. The simulation results can be found in appendix H. The influence of different system parameters are discussed below.

Increase in vessel footprint To investigate the influence of the combined operation on the DP vessel footprint, the footprint of the 'clean' vessel is compared to the DP footprint when the monopile is attached to the vessel.

Test	S. min	S. max	S. st. dev.	Sw. min	Sw. max	Sw. st. dev.
Base line						
1	-0.45	0.40	0.17	-0.79	1.24	0.32
2	-0.49	0.50	0.19	-0.88	1.44	0.35
2	-0.52	0.43	0.17	-0.51	0.56	0.23
With monopile						
1, FB16, Tp7	-0.58	0.41	0.21	-0.75	1.50	0.40
2, FB16, Tp9	-0.59	0.46	0.19	-0.75	1.67	0.44
3, FB24, Tp7	-0.79	0.67	0.22	-1.09	2.13	0.54
4, FB24, Tp9	-0.87	0.98	0.27	-1.34	2.28	0.54
5, FB24, Tp9	-0.55	0.45	0.19	-0.73	0.82	0.28

Table 4.5: Comparison vessel footprint 'clean' vessel and vessel with monopile (m)

72 4. System analysis

Test	Increase surge envelope	Increase sway envelope
1, FB16, Tp7	16%	11%
2, FB16, Tp9	6%	4%
3, FB24, Tp7	72%	60%
4, FB24, Tp9	87%	56%
5, FB24, Tp9	5%	40%

Table 4.6: Increase in footprint test with monopile compare to base case (%)

As expected, an increase in vessel footprint is observed due to the monopile added to the vessel. Table 4.6 shows the relative increase in footprint compare to the base case.

A major difference is observed when comparing the results of both monopile with each other. The environmental force on the FB24 monopile is larger compare to the FB16 monopile. As already mentioned, the monopile is lowered to the seabed in 100 sec. The forces starts to act on the vessel. Normally, the vessel will drift when forces are acting on the vessel and the Kalman filter estimates the forces before the thrusters can counteract the forces. In this case, the Kalman filter is fed with the forces from the gripper frame onto the vessel. In case of the FB16 monopile, the drift is within limited due to the feed forward. The thrusters can ramp-up fast enough to counteract for the forces. In case of the FB24 monopile, the thrusters have to ramp-up more, this takes more time and therefore the vessel will slightly drift. Due to the relative low footprint of the vessel in the base case, a drift of half a meter means a relative larger increase in footprint. After recovery from the drift, the typical footprint of the vessel with monopile is in the same order as the footprint of the vessel in the base case.

The expectation was that the vessel should be more stable in sway direction compare to surge direction. A note need to be made that this is also depended on the settings of the DP controller. However, comparable increase in envelope is observed in surge and sway direction. The increase in envelope is slightly larger in surge direction. This could be explained by the direction of environmental force. Comparable behavior in surge and sway direction can be explained by the fact that DP is a low velocity application [20]. The inertia of the vessel is dominant relative to the hydrodynamic damping. The next chapter, a bode plot is made to compare the response on environmental forces on the motions in surge and sway direction.

Stability of the DP vessel The simulation results shown a significant increase in vessel footprint due to operation of installing a monopile with a DP vessel compare to a 'clean' vessel. The conclusion can be made that the force applied by the gripper frame on the vessel is responsible for the increase vessel footprint. The DP controller is designed and tuned for the 'clean' vessel. Adding the monopile to the vessel is an off-design condition for the DP controller. The gripper frame force also contribute to the yaw moment of the vessel which implies that the thrusters needs to counteract for this yaw rotations.

The force from the gripper frame on the vessel can can be divided into three types of forces. Namely:

- 1: High frequency forces due to the first order wave forces on the vessel and the fluctuating motion behavior of the monopile. The frequency of this force have the same frequency order as the first order wave forces.
- 2: Low frequency second order wave forces. These wave forces are typically is order of 0.01Hz [35].
- 3: Relative stationary current and wind force on the monopile is acting, via the gripper frame, on the vessel.

The influence of first order wave forces on surge and sway motions are relative small compare to second order wave forces. This is also stated by [26] and shown in figure 4.4 which shows the response of the vessel in surge and sway direction as function of the frequency of the applied load.

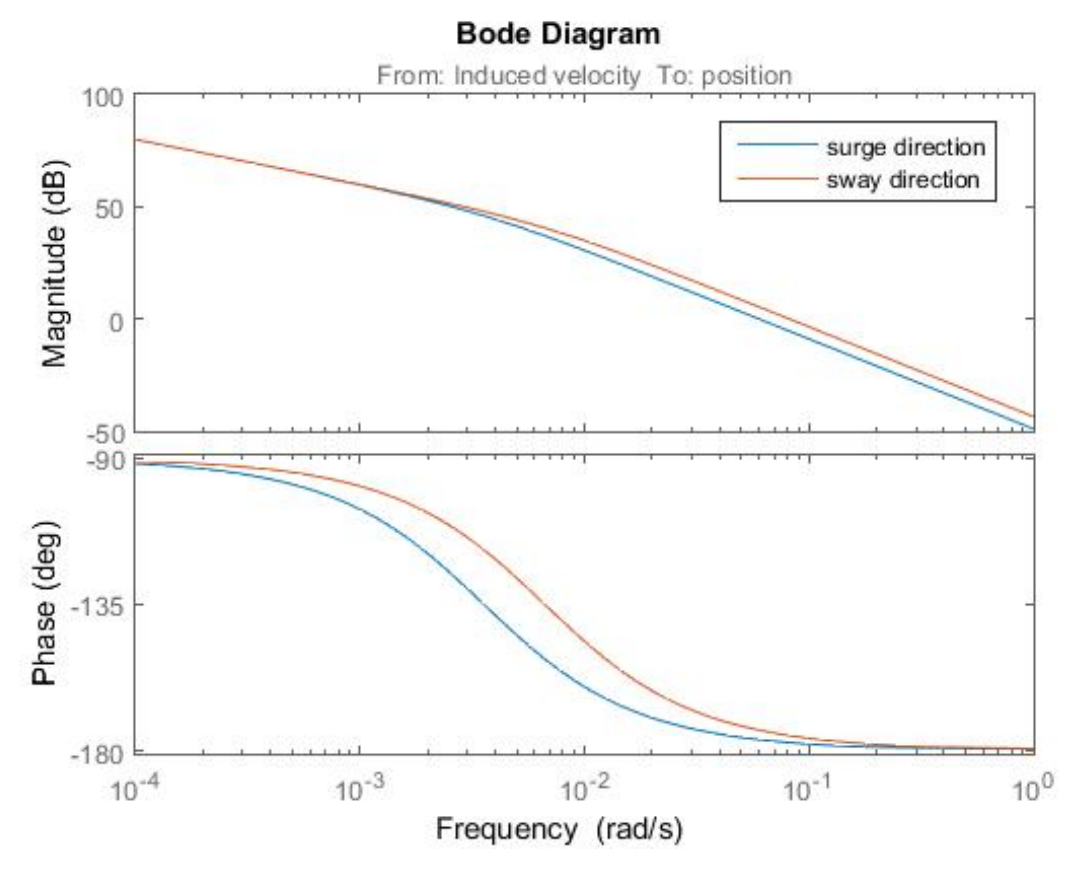


Figure 4.4: Bode plot induced velocity to surge and sway motions vessel

For a relative high frequency force, with a period of 9 sec, the bode plot shows a magnitude of -42.8dB for surge motions and -36.2dB for sway motions. For a relative low frequency force, with a period of 100 sec, the bode plot shows a magnitude of -0.97dB for surge motions and 5.67dB for sway motions. The induced velocity is the velocity towards the velocity of the vessel converge when the force is applied for a long period on the vessel.

$$F = c * v_{ind}^2 \tag{4.3}$$

$$v_{ind} = \sqrt{\frac{F}{c}} \tag{4.4}$$

The constant 'c' consists of the drag coefficient, the frontal water area and the water density. The value of 'c' is larger in sway direction compare to surge direction mainly due to the much large frontal water area.

First order force response The surge and sway response on forces with a period of 9 seconds is given in the following table.

Induced velocity surge	Surge amplitude	Induced velocity sway	Sway amplitude
5.69 m/s	0.039 m	2.16 m/s	0.032 m

Table 4.7: Surge and sway response for a sinus wave force with an amplitude of 3000 kN and Tp 9 sec

74 4. System analysis

Induced velocity surge	Surge amplitude	Induced velocity sway	Sway amplitude
3.28 m/s	0.023 m	1.25 m/s	0.019 m

Table 4.8: Surge and sway response for a sinus wave force with an amplitude of 1000 kN and Tp 9 sec

Second order force response The surge and sway response on forces with a period of 100 seconds is given in the following table.

Induced velocity surge	Surge amplitude	Induced velocity sway	Sway amplitude
1.80 m/s	1.61 m	0.68 m/s	1.30 m

Table 4.9: Surge and sway response for a sinus wave force with an amplitude of 300 kN and Tp 100 sec

Induced velocity surge	Surge amplitude	Induced velocity sway	Sway amplitude
1.04 m/s	0.93 m	0.39 m/s	0.74 m

Table 4.10: Surge and sway response for a sinus wave force with an amplitude of 100 kN and Tp 100 sec

The conclusion can be made that the high frequency forces do not amplify the vessel significantly. This is also a logical conclusion with respect to the wave forces on the vessel. These high frequency forces have an even larger magnitude and also those forces do not increase the footprint of the vessel significantly. Beside that, these forces are approximately mean zero so it is not necessary to react with the thrusters on these forces. As mentioned before, the vessel also not able to counteract for this first order wave forces because those forces are out of the bandwidth of the DP controller. When the monopile is continue fluctuating around its setpoint with the frequency of the first order wave force, this interaction force between vessel and monopile via the gripper frame will not decrease the stability of the vessel. Only a minor difference between surge and sway direction is observed in position response. The inertia of the vessel is dominant in the response for high frequency forces. This explain comparable response. Also for fluctuating forces with a period of 100 sec, still a minor difference is observed between surge and sway motions. Only for lower period fluctuating forces a major difference is observed between surge and sway response. The magnitude converge for low frequency applied forces so the response will show a difference because of the higher damping in sway direction.

The monopile fluctuate around its upright position. This is shown in the monopile rotation plots in appendix F. The rotation of the monopile is in order of 0.05-0.15 deg. depended on the monopile size and environmental conditions. The rotation is depended on the monopile size, the wave forces acting on the monopile and the roll and pitch motions of the vessel. The monopile rotation are in the same period as the first order roll and pitch motions of the vessel due to the high bandwidth of the inclination controller of the monopile (see for description chapter 3). The gripper frame force to counteract these motions are for that reason also in that frequency range. These forces only have minor influence on the surge and sway motions of the vessel (see table 4.7 and 4.8. Due to the difference in frequencies between the motions of the vessel and the motions of the monopile, the characteristic of the force from the monopile on the vessel is not comparable to the DP heavy lift incident where the vessel becomes unstable because of the additional installation force which was in the same period as the surge motion of the vessel, see figure 1.11. The conclusion is made that the fluctuating monopile will not decrease the stability margin of the DP vessel.

Envelope gripper frame The required envelope of the gripper frame is based on the footprint of the vessel, the yaw rotation and the monopile motions. The required envelope is given for the four simulation cases in table 4.11.

Test	S. min	S. max	S. st. dev.	Sw. min	Sw. max	Sw. st. dev.
1, FB16, Tp7	-0.47	0.89	0.27	-1.50	0.73	0.39
2, FB16, Tp9	-0.80	1.05	0.26	-1.81	0.77	0.43
3, FB24, Tp7	-0.93	1.37	0.34	-2.14	1.06	0.55
4, FB24, Tp9	-1.33	1.43	0.38	-2.34	1.60	0.56
5, FB24, Tp9	-0.60	0.88	0.26	-0.95	0.76	0.30

Table 4.11: Required gripper frame envelope (m)

The required envelope relative to the surge and sway footprint of the vessel is given in table 4.12.

Test	Rel. surge GF envelope to DP surge	Rel. sway GF envelope to DP sway
1, FB16, Tp7	37%	-1%
2, FB16, Tp9	76%	7%
3, FB24, Tp7	58%	-1%
4, FB24, Tp9	49%	9%
5, FB24, Tp9	48%	10%

Table 4.12: Relative GF envelope compare to DP vessel footprint

A larger gripper frame envelope is observed for surge direction relative to the DP surge offset compare to the sway direction. It is not really clear what causes this difference. It could be the case that extreme surge offset goes hand in hand with extreme yaw rotations. Half a degree of yaw rotation, typical a extreme yaw rotation value during the simulation, provide an extra 0.25 m of required gripper frame envelope. This is relative a large number to the relative small vessel surge envelope.

Force and power hydraulic gripper frame The following tables provide the extreme values of the power and force for which the gripper frame needs to be designed.

Test	P. S. min	P. S. max	P. S. st. dev.	P. Sw. min	P. Sw. max	P. Sw. st. dev.
1, FB16, Tp7	-80	116	17	-59	85	13
2, FB16, Tp9	-118	148	28	-99	82	15
3, FB24, Tp7	-135	246	35	-136	141	28
4, FB24, Tp9	-350	467	68	-246	270	36
5, FB24, Tp9	-515	507	80	-4	4	1

Table 4.13: Required hydraulic pump power (kW)

Test	F. S. min	F. S. max	F. S. st. dev.	F. Sw. min	F. Sw. max	F. Sw. st. dev.
1, FB16, Tp7	-1252	1036	345	-638	704	204
2, FB16, Tp9	-1160	1006	345	-649	698	204
3, FB24, Tp7	-2333	1997	657	-1118	1339	388
4, FB24, Tp9	-2693	2272	742	-1316	1511	432
5, FB24, Tp9	-3594	2472	842	-72	84	12

Table 4.14: Required hydraulic gripper frame force (kN)

The maximum force is determined by the maximum peak forces on the monopile. The maximum power is based on the load flow into the cylinder and the pressurization of the fluid in the cylinder at the same moment. For a higher wave period, the roll and pitch motions of the vessel have a larger amplitude. Beside that, the load pressure in the cylinder, when installing a FB24 monopile, is higher, so the higher required pump power and gripper frame force is when installing the larger pile (FB24) with the longer wave period (Tp9). Beside that, the required force and power is maximal when the environmental force on the monopile is in line with a direction of the gripper frame, which is test case 5.

76 4. System analysis

Lower sea state When the operation is performed in a lower sea state compare to the governing sea state in the simulation, the wind, current and wave forces on the vessel and monopile are lower. This results in a higher margin between the installed power on board of the vessel and the power used for station-keeping of the vessel. This decrease the possibility of drifting away from the set point and probably touching the boundaries of the gripper frame. In most cases, a lower sea state also mean lower wave periods. The roll and pitch periods are lower, however the amplitude of the roll and pitch motions are also lower. An investigation need to be made if the induced velocity of the fixed part of the gripper frame is within design limitations to conclude if the gripper frame is still able to compensate adequate for vessel motions.

4.2.8. Gripper frame requirements

Taking the governing results into account, the gripper frame minimal design criteria is given in table 4.15. For the envelope and required gripper frame force, 4 times the standard deviation + the mean offset from zero is taken. The shape of the required pump power distribution function do not match to the to the shape of a standard distribution function. For the requirement on the pump power of the gripper frame, the maximum value +10% is taken.

	Magnitude	Unit
Envelope gripper frame x direction	+/-1.8	m
Envelope gripper frame y direction	+/-2.6	m
Power hydraulic pump per direction	560	kW
Gripper frame force	3594	kN

Table 4.15: Design specifications gripper frame

4.3. Conclusion

After carrying out the simulation, the conclusion can be made that stability of the DP vessel is maintained during the monopile installation operation. The requirements on th gripper frame are considered to be acceptable in terms of magnitude. It is expected that a gripper frame with the required envelope can be constructed and beside that, hydraulic pumps with the required power are widely available. Furthermore, the construction of a gripper frame which can handle the loads presented above seams not to be an issue. Gripper frame in the past are also constructed and successfully used and those gripper frame also needs to handle the wave forces on the monopile and transfer those forces to the vessel.

Conclusions, recommendations and limitations

Conclusions and limitations about this research and recommendations for further research are given in this chapter.

5.1. Conclusions

Installing a monopile for an offshore wind turbine is studied in this thesis. The main question at the start of the research is 'How would the extra installation force influence the DP performance of the vessel and is the operation feasible and under what conditions'. Several steps are involved in installing a monopile. The earlier hammering phase is studied. The monopile is unstable and the upright position is maintained by the gripper frame. A simplified 1D model is build to study the stability of the system. Via the Lyapunov theory, the conclusion can be made for a mechanical system, when damping is added to the system, the total energy of the system decreasing within time and the system convergence to it equilibrium position. The hydrodynamic damping in sway direction is larger than in surge direction for a mono hull vessel. The vessel will be more stable in sway direction. The hydrodynamic damping of the monopile also adds damping to the overall system. The conclusion can be made that the overall system is stable. However, the real simulation model is much richer than the simplified model. In the simplified model, the proportional and damping term are directly related to the real state of the vessel. In the real simulation model, also thruster delay, state estimation, thrust allocation and sensor delay is incorporated. In other words, the applied thrust is not in all case directly related to the real vessel state. Delays in the system might introduce a phase delay which reduce the phase margin of the system. A reduction in phase margin can cause instable behavior. To study real case scenarios, a simulation model is build and governing test case are determined. Based on the simulation, the vessel can maintain stable behavior. The inclination controller of the gripper frame is tuned to have a higher bandwidth compare to the bandwidth of the DP vessel which is in order of 0.1 rad/sec. The gripper frame can maintain upright position without moving with the vessel in the same frequency range as the surge and sway motions of the vessel. This avoid leaning of the monopile on the vessel and a decrease in stability of the vessel. A bode plot a force as input on the vessel and the position of the vessel as output shows only minor influence of increased footprint due to the first order, high frequency, forces on the vessel. That means that the motions of the pile, which are typically in the same frequency order as the roll and pitch motions of the vessel do not significantly influence the footprint of the vessel and therefore do not have a large influence on the stability of the DP system. When the force would be in phase with the surge and sway motions of the vessel (in case of the DP heavy lift incident) the stability margin of the DP vessel is decreased. A significant enlarged footprint (87%) of the vessel is observed in case of the installing the 'large' FB24 monopile. This is due to the fact that the vessel slightly drift when applying the force from the gripper frame to the vessel. This is

not the case when installing the 'small' FB16 monopile (16%). The stationary forces on the monopile are responsible for this drift. This increase the requirement on the envelope of the gripper frame. The wave period only have minor influence on the DP footprint of the vessel. A increased vessel footprint in order of 10% is observed due to the higher first order wave forces in case of a larger wave period. For this type of vessel, this range of monopile sizes and feed forward of the installation force into the Kalman filter (for better state estimation) the conclusion can be made that stable vessel behavior can be maintained with an acceptable required range of the gripper frame. The requirements on gripper frame envelope, maximum force of the gripper frame and the power of the gripper frame are given in chapter 4.

5.2. Recommendations and limitations

Installing a monopile with a DP vessel is based on the results of this report promising for the future. Further investigation need to be done to achieve information about the technical and economical feasibility of the combined operation. Several assumptions are made in this research so the validity of the simulation results are bounded by limitations.

The friction in the hydraulic system is not modeled in advanced. Only a linear viscous friction component is involved in the model. Stribeck friction, stick slip friction and a static friction is not taken into account. This can possible lead to different behavior of the gripper frame and monopile.

The model of the monopile is a simplified representation of reality. The frequency depend mass and damping coefficients are not modeled. The rotational damping is assumed to be linear and only the trapped mass is modeled as added mass. The frequency depended wave making radiation term could be incorporated. This influence the dynamic behavior under environmental load.

The forces of the gripper frame acting on the monopile (and therefore the reaction forces on the vessel) are assumed to be known exactly. In the real world, these forces are known with a certain uncertainty. The forces from the gripper frame which are fed into the Kalman filter have for that reason a uncertainty which is not modeled. The performance of the state estimator is overestimated. The overestimation will probably decrease the requirements on the envelope of the gripper frame.

The monopile is modeled as a inverted pendulum with an hinge in the soil. In real life, the monopile will have marginal stability because of the vertical soil interaction. However, to study the worst case scenario during the early hammering phase it is better to assume no monopile-soil interaction. When installing the monopile in a dense sand seabed, the self penetration is limited. This increase the unstable behavior of the monopile which gives more governing results.

The angle offset of the monopile is assumed to be know exactly. This is not realistic in the real world. The angle offset of the monopile is the input for the inclination controller of the gripper frame. The performance of the gripper frame in the real world will probably be worser due to the uncertainty in angle offset of the monopile. Furthermore, the induced vessel motion compensation controller based its control actions on the real states of the vessel. In the real world, these real states are not known. The vessel states are estimated by the Kalman filter. The ability of compensating for the motions of the vessel might be overestimated in this research. This will lead to an increase in pile rotation and a larger force on the vessel. This larger force will increase the footprint of the vessel.

The starting point of this research was the Bokalift1. The validity of the results are not guaranteed for other DP vessels. Different mass and hydro dynamic parameter, controller settings of the DP control system and thruster configuration might influence the DP perfor-

mance and the DP stability margin of the vessel.

Only one step of the installation steps is analyzed. Crane operations could also have a considerable effect on the DP performance of the vessel. Furthermore, when the monopile become fixed to the soil during the hammering phase and the monopile is still attached to the vessel via the gripper frame, probably a large mooring stiffness, due to the monopile soil interaction, is added to the vessel. This is comparable to the problem which occur in DP heavy lift. Instability of the DP vessel can occur.

The operation is assumed to be a DP2 operation. In DP2 requires no loss of position in case of a failure of an active component. However, re-initialization of the DP controller might cause an increase in vessel footprint. The boundaries of the gripper frame can be touched. The worst case failure need to be investigate and the effect need to be analyzed.

The influence of a failure of the gripper frame needs to be investigated. The instable tendency of the monopile, normally compensate by the gripper frame, could cause large forces on the vessel in the direction of motion of the vessel. The monopile could lean on the vessel and insufficient power of the vessel to counteract the gravity force from the monopile could lead to a drift of the vessel.

In this research, the decision is made to feed forward the forces from the gripper frame on the vessel into the Kalman filter to prevent drift of the vessel during lowering of the monopile to the seabed. An investigation could be made if it is also possible to direct feed forward the force from the gripper frame into the thrust allocation algorithm of the DP controller. Probably a low pass filter need to be added to filter the high frequency forces due to first order wave force on the monopile and the force necessary for the rotation of the monopile



P-y curves

The p-y curves are plotted for respectively a 10m and 7.4m diameter mono-pile. Curve between load (p) and horizontal pile displacement (y) due to pile rotation is given for every meter till a soil depth of 16m. The following soil parameters are used:

Variable	Value	Unit
Effective soil weight	10	kN/m3
Angle of internal friction (0 -> -5)	33.0	deg.
Angle of internal friction (-5 -> -14)	35.0	deg.
Angle of internal friction (-14 -> -16)	38.5	deg.
Factor for cyclic load	0.9	(-)

Table A.1: Soil parameters [27]

82 A. P-y curves

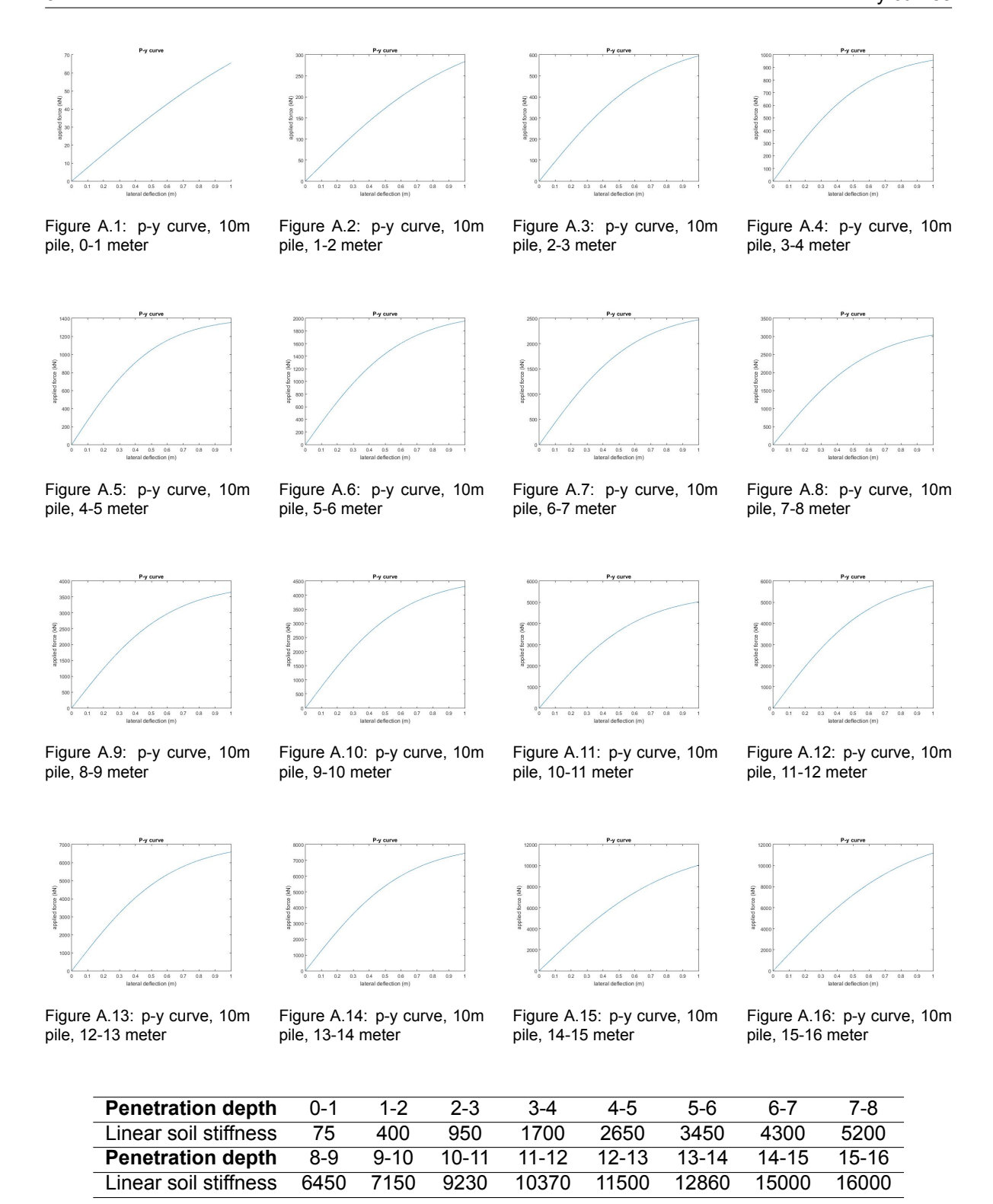


Table A.2: Linear soil stiffness mono-pile, 10m diameter, (kN/m)

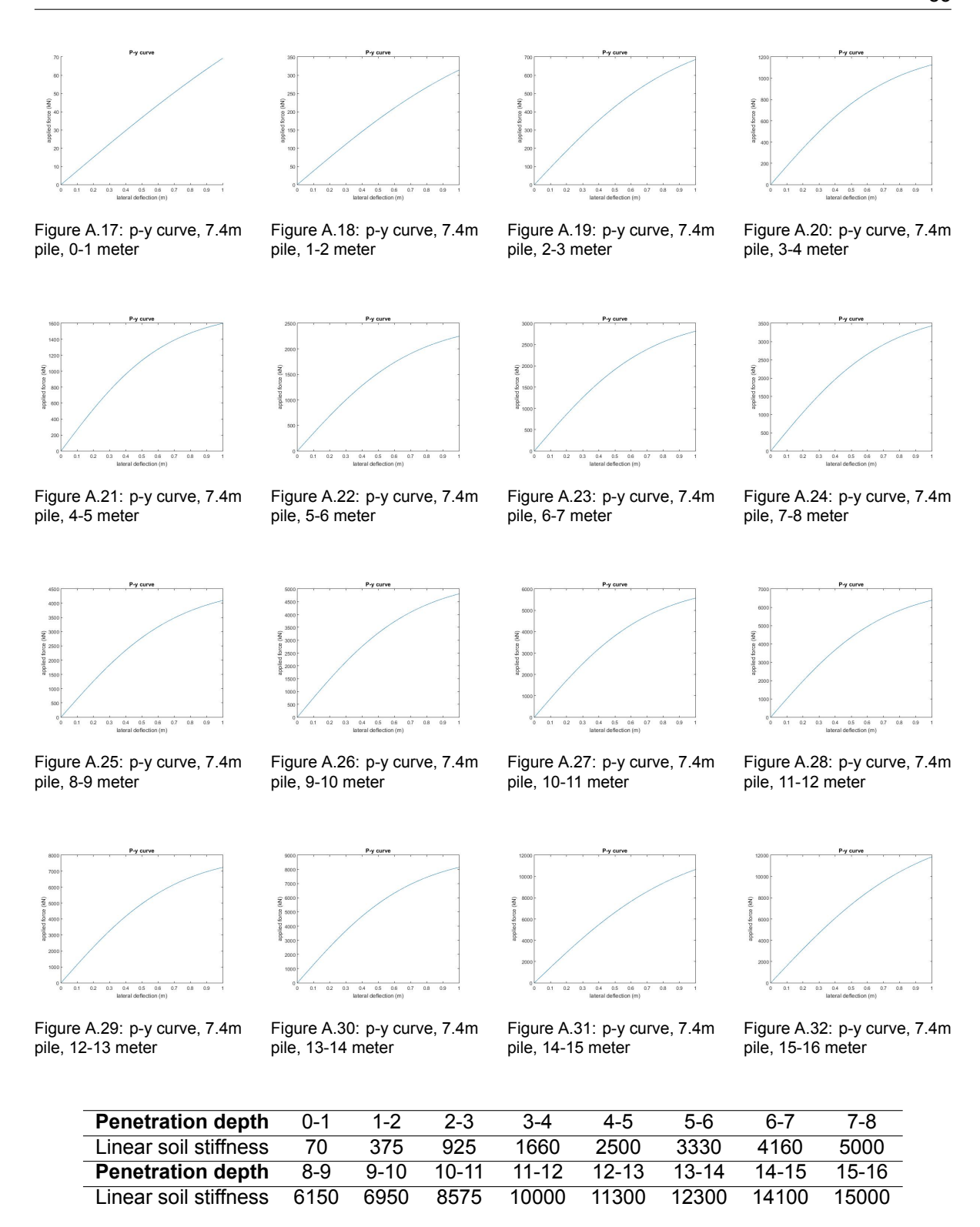


Table A.3: Linear soil stiffness mono-pile, 7.4m diameter, (kN/m)



Vessel details

B.0.1. Vessel specifications

Some important vessel parameters are given which determine the DP capability and to see weather the results of the reports also count for similar construction vessel.

Vessel main particular		
Detail	Value	unit
Length o.a.	216.70	m
Length b.p	212.13	m
Breadth	43	m
Draught for simulations	8	m

Table B.1: Vessel main particular

Hydrostatic and Mass properties		
Detail	Value	unit
Displacement	53924	m3
Radii of gyration - roll	19.4	m
Radii of gyration – pitch	54.7	m
Water plane area	7787	m2
Metracentric height (transverse) w.r.t. water plane	12.4	m
Metracentric height (longitudinal) w.r.t. water plane	407.0	m
Drag coefficient surge (C-d,surge)	0.526	(-)
Drag coefficient sway (C-d,sway)	0.742	(-)
Under water area surge (A-surge)	344	m2
Under water area sway (A-surge)	1782	m2

Table B.2: Hydrostatic and Mass properties

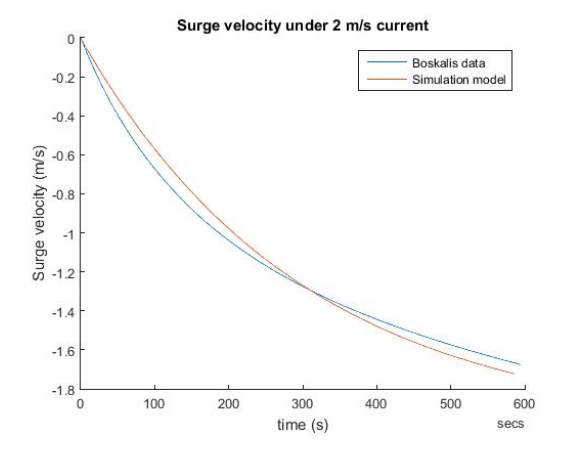
86 B. Vessel details

Component Detail Value unit Bow thruster 1 FWD AFT Type Tunnel - (x,y) 197.0,0 m Max. Thrust 160 kN RPM rate 10 %/sec Bow thruster 1 FWD AFT Type Tunnel - (x,y) 200.2,0 m Max. Thrust 160 kN RPM rate 10 %/sec Azimuth 1 AFT SB Type Azimuth - (x,y) 49.76,-14.88 m Max. Thrust 665 kN RPM rate 4.5 %/sec Angle rate 6 deg/sec Azimuth 2 AFT PS Type Azimuth - (x,y) 49.76,-14.88 m m Max. Thrust 665 kN RPM rate 4.5 %/sec Azimuth 3 FWB SB Type Azimuth - (x,y) 150.56,-14.88 m Max. Thrust 665	Bow thruster 1 FWD AFT	Type (x,y) Max. Thrust RPM rate	Tunnel	-
(x,y)		(x,y) Max. Thrust RPM rate		
Max. Thrust 160 kN RPM rate 10 %/sec		Max. Thrust RPM rate	197.0,0	100
RPM rate		RPM rate		ΙΠ
Bow thruster 1 FWD AFT			160	kN
(x,y) 200.2,0 m Max. Thrust 160 kN RPM rate 10 %/sec Max. Thrust 160 kN RPM rate 10 %/sec Max. Thrust 665 kN RPM rate 4.5 %/sec Angle rate 6 deg/sec Azimuth 2 AFT PS Type Azimuth - (x,y) 49.76,14.88 m Max. Thrust 665 kN RPM rate 4.5 %/sec Angle rate 6 deg/sec Azimuth 3 FWB SB Type Azimuth - (x,y) 150.56,-14.88 m Max. Thrust 665 kN RPM rate 4.5 %/sec Angle rate 6 deg/sec Azimuth 4 FWB PS Type Azimuth - (x,y) 150.56,-14.88 m Max. Thrust 665 kN RPM rate 4.5 %/sec Angle rate 6 deg/sec Azimuth 4 FWB PS Type Azimuth - (x,y) 150.56,14.88 m Max. Thrust 665 kN RPM rate 4.5 %/sec Angle rate 6 deg/sec Main propeller 1 AFT SB Type Main Propeller - (x,y) 3.94,-7.0 m Max. Power 5250 kW			10	%/sec
(x,y) 200.2,0 m Max. Thrust 160 kN RPM rate 10 %/sec Azimuth 1 AFT SB Type Azimuth - (x,y) 49.76,-14.88 m Max. Thrust 665 kN RPM rate 4.5 %/sec Angle rate 6 deg/sec Azimuth 2 AFT PS Type Azimuth - (x,y) 49.76,14.88 m Max. Thrust 665 kN RPM rate 4.5 %/sec Angle rate 6 deg/sec Azimuth 3 FWB SB Type Azimuth - (x,y) 150.56,-14.88 m Max. Thrust 665 kN RPM rate 4.5 %/sec Angle rate 6 deg/sec Azimuth 4 FWB PS Type Azimuth - (x,y) 150.56,14.88 m Max. Thrust 665 kN RPM rate <td>Bow thruster 1 FWD AFT</td> <td>Type</td> <td>Tunnel</td> <td>-</td>	Bow thruster 1 FWD AFT	Type	Tunnel	-
RPM rate		(x,y)	200.2,0	m
Azimuth 1 AFT SB Type (x,y) 49.76,-14.88 Max. Thrust 665 kN RPM rate 4.5 %/sec Angle rate 6 deg/sec Azimuth 2 AFT PS Type Azimuth (x,y) 49.76,14.88 Max. Thrust 665 kN RPM rate 4.5 %/sec Angle rate 6 deg/sec Azimuth 3 FWB SB Type Azimuth (x,y) 150.56,-14.88 Max. Thrust 665 kN RPM rate 4.5 %/sec Angle rate 6 deg/sec Azimuth 4 FWB PS Type Azimuth (x,y) 150.56,-14.88 Max. Thrust 665 kN RPM rate 4.5 %/sec Angle rate 6 deg/sec Azimuth 4 FWB PS Type Azimuth (x,y) 150.56,14.88 Max. Thrust 665 kN RPM rate 4.5 %/sec Angle rate 6 deg/sec Main propeller 1 AFT SB Type Main Propeller (x,y) 3.94,-7.0 Max. Power 5250 kW		Max. Thrust	160	kN
(x,y) 49.76,-14.88 m Max. Thrust 665 kN RPM rate 4.5 %/sec Angle rate 6 deg/sec Azimuth 2 AFT PS Type Azimuth - (x,y) 49.76,14.88 m Max. Thrust 665 kN RPM rate 4.5 %/sec Angle rate 6 deg/sec Azimuth 3 FWB SB Type Azimuth - (x,y) 150.56,-14.88 m Max. Thrust 665 kN RPM rate 4.5 %/sec Angle rate 6 deg/sec Max. Thrust 665 kN RPM rate 4.5 %/sec Angle rate 6 deg/sec Main propeller 1 AFT SB Type Main Propeller (x,y) 3.94,-7.0 m Max. Power 5250 kW		RPM rate	10	%/sec
Max. Thrust 665 kN kN RPM rate 4.5 %/sec Angle rate 6 deg/sec Azimuth 2 AFT PS Type Azimuth Type Azimuth - (x,y) 49.76,14.88 m m Max. Thrust 665 kN kN RPM rate 4.5 %/sec Angle rate 6 deg/sec Azimuth 3 FWB SB Type Azimuth (x,y) 150.56,-14.88 m m Max. Thrust 665 kN kN RPM rate 4.5 %/sec Angle rate 6 deg/sec Max. Thrust 665 kN Max. Thrust 665 kN RPM rate 4.5 %/sec Angle rate 6.5 kN RPM rate 4.5 %/sec Angle rate 6 deg/sec Main propeller 1 AFT SB Type Main Propeller (x,y) 3.94,-7.0 m Max. Power 5250 kW	Azimuth 1 AFT SB	Туре	Azimuth	-
RPM rate		(x,y)	49.76,-14.88	m
Azimuth 2 AFT PS Type (x,y) 49.76,14.88 Max. Thrust 665 kN RPM rate 4.5 Angle rate 6 deg/sec Azimuth 3 FWB SB Type Azimuth Azimuth 3 FWB SB Type Azimuth (x,y) 150.56,-14.88 Max. Thrust 665 kN RPM rate 4.5 %/sec Angle rate 6 deg/sec Azimuth 4 FWB PS Type Azimuth Azimuth 4 FWB PS Type Azimuth Azimuth Azimuth 4 FWB PS Type Azimuth Azimu		Max. Thrust	665	kN
Azimuth 2 AFT PS Type		RPM rate	4.5	%/sec
(x,y)		Angle rate	6	deg/sec
(x,y) 49.76,14.88 m Max. Thrust 665 kN RPM rate 4.5 %/sec Angle rate 6 deg/sec Azimuth 3 FWB SB Type Azimuth - (x,y) 150.56,-14.88 m Max. Thrust 665 kN RPM rate 4.5 %/sec Angle rate 6 deg/sec Max. Thrust 665 kN RPM rate 4.5 %/sec Angle rate 6 deg/sec Main propeller 1 AFT SB Type Main Propeller - (x,y) 3.94,-7.0 m Max. Power 5250 kW	Azimuth 2 AFT PS	Туре	Azimuth	-
RPM rate			49.76,14.88	m
Angle rate 6 deg/sec Azimuth 3 FWB SB Type Azimuth - (x,y) 150.56,-14.88 m Max. Thrust 665 kN RPM rate 4.5 %/sec Angle rate 6 deg/sec Azimuth 4 FWB PS Type Azimuth - (x,y) 150.56,14.88 m Max. Thrust 665 kN RPM rate 4.5 %/sec Angle rate 665 kN RPM rate 4.5 %/sec Angle rate 6 deg/sec Main propeller 1 AFT SB Type Main Propeller - (x,y) 3.94,-7.0 m Max. Power 5250 kW		Max. Thrust	665	kN
Azimuth 3 FWB SB Type (x,y) 150.56,-14.88 Max. Thrust RPM rate Azimuth 4 FWB PS Type Azimuth 4 FWB PS Type (x,y) 150.56,14.88 Max. Thrust (x,y) 150.56,14.88 Max. Thrust 665 KN RPM rate 4.5 Max. Thrust 665 KN RPM rate 4.5 Mysec Angle rate 6 Main propeller 1 AFT SB Type Main Propeller (x,y) 3.94,-7.0 Max. Power 5250 KW		RPM rate	4.5	%/sec
(x,y) 150.56,-14.88 m Max. Thrust 665 kN RPM rate 4.5 %/sec Angle rate 6 deg/sec Azimuth 4 FWB PS Type Azimuth - (x,y) 150.56,14.88 m Max. Thrust 665 kN RPM rate 4.5 %/sec Angle rate 6 deg/sec Main propeller 1 AFT SB Type Main Propeller - (x,y) 3.94,-7.0 m Max. Power 5250 kW		Angle rate	6	deg/sec
Max. Thrust 665 kN RPM rate 4.5 %/sec Angle rate 6 deg/sec Azimuth 4 FWB PS Type Azimuth - (x,y) 150.56,14.88 m Max. Thrust 665 kN RPM rate 4.5 %/sec Angle rate 6 deg/sec Main propeller 1 AFT SB Type Main Propeller - (x,y) 3.94,-7.0 m Max. Power 5250 kW	Azimuth 3 FWB SB	Туре	Azimuth	-
RPM rate		(x,y)	150.56,-14.88	m
Angle rate 6 deg/sec Azimuth 4 FWB PS Type Azimuth - (x,y) 150.56,14.88 m Max. Thrust 665 kN RPM rate 4.5 %/sec Angle rate 6 deg/sec Main propeller 1 AFT SB Type Main Propeller - (x,y) 3.94,-7.0 m Max. Power 5250 kW		Max. Thrust	665	kN
Azimuth 4 FWB PS Type		RPM rate	4.5	%/sec
(x,y) 150.56,14.88 m Max. Thrust 665 kN RPM rate 4.5 %/sec Angle rate 6 deg/sec Main propeller 1 AFT SB Type Main Propeller - (x,y) 3.94,-7.0 m Max. Power 5250 kW		Angle rate	6	deg/sec
Max. Thrust 665 kN RPM rate 4.5 %/sec Angle rate 6 deg/sec Main propeller 1 AFT SB Type Main Propeller - (x,y) 3.94,-7.0 m Max. Power 5250 kW	Azimuth 4 FWB PS	Туре	Azimuth	-
RPM rate A.5 %/sec deg/sec Angle rate 6 deg/sec Main propeller 1 AFT SB Type Main Propeller - (x,y) 3.94,-7.0 m Max. Power 5250 kW		(x,y)	150.56,14.88	m
Main propeller 1 AFT SB Type (x,y) Main Propeller (x,y) - Max. Power 5250 kW		Max. Thrust	665	kN
Main propeller 1 AFT SB Type Main Propeller (x,y) 3.94,-7.0 Max. Power 5250 kW		RPM rate	4.5	%/sec
(x,y) 3.94,-7.0 m Max. Power 5250 kW		Angle rate	6	deg/sec
Max. Power 5250 kW	Main propeller 1 AFT SB	Туре	Main Propeller	-
		(x,y)	3.94,-7.0	m
RPM rate 1 %/sec		Max. Power	5250	kW
1 W 14 C 1 /0/3CC		RPM rate	1	%/sec
Main propeller 1 AFT PS Type Main Propeller -	Main propeller 1 AFT PS	Туре	Main Propeller	-
(x,y) 3.94,7.0 m		(x,y)	3.94,7.0	m
Max. Power 5250 kW		Max. Power	5250	
RPM rate 1 %/sec		RPM rate	1	%/sec
Durdon Apple note CO destruction	Rudder	Angle rate	2.3	deg/sec

Table B.3: Thruster and rudder particulars

B.0.2. Surge and sway behavior plots

The surge and sway behavior of the simulated vessel in the RH marine simulator is verified with data from Boskalis. A current of 2 m/s is acting on the bow in the surge behavior test and a current from port side is acting on the vessel in the sway behavior test.



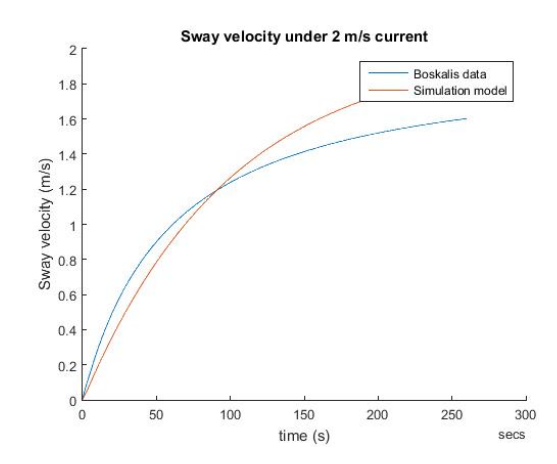


Figure B.1: Surge behavior

Figure B.2: Sway behavior

88 B. Vessel details

B.0.3. Roll and pitch behavior plots

Test	Hs (m)	Tp (s)	Direction (deg)
1	2.5	7	330
2	2.5	9	330

Table B.4: Environmental conditions roll-pitch comparison

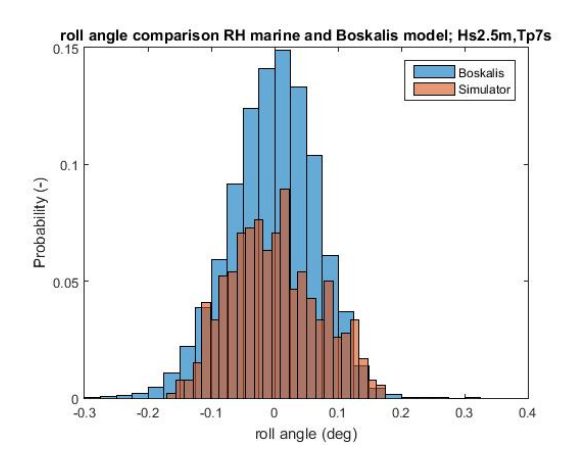


Figure B.3: Roll behavior test 1

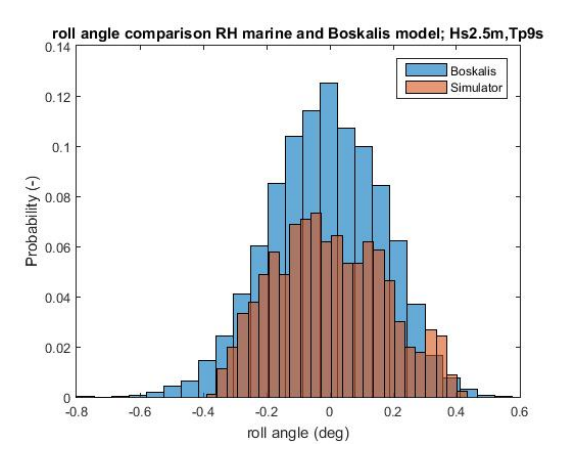


Figure B.5: Roll behavior test 2

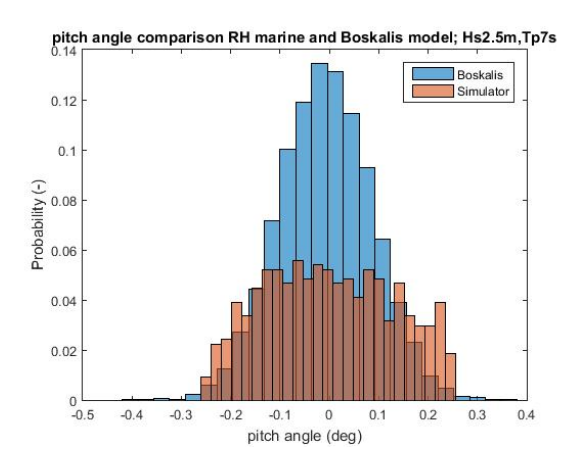


Figure B.4: Pitch behavior test 1

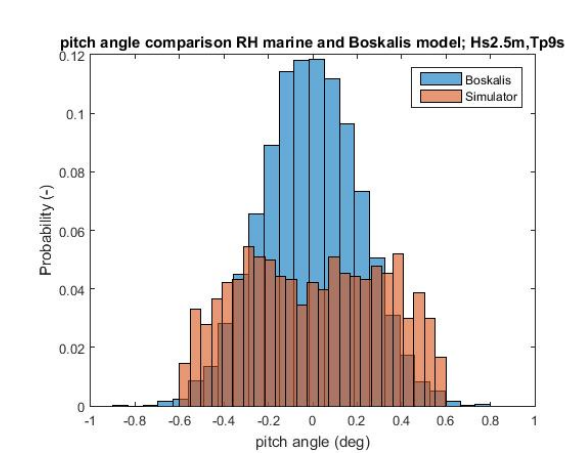


Figure B.6: Pitch behavior test 2

B.0.4. Vessel footprint plots

The dynamic DP capability off the vessel is checked for several cases.

Test	current	waves	wind	Direction
1	2.5 kn	Hs 2.5 meters, Tp 7.0 sec	19 kn	330 deg
2	2.5 kn	Hs 2.5 meters, Tp 9.0 sec	19 kn	330 deg
3	2.5 kn	Hs 2.5 meters, Tp 9.0 sec	19 kn	000 deg

Table B.5: Vessel footprint tests

The tests are carried out in time domain simulation of 12300 sec. The first 1500 sec are used for initialization of the vessels control system. In other words: to estimate the stationary environmental forces by the Kalman filter. The station keeping plots are from t=1500 to t=12300.

Test 1 DP vessel behavior

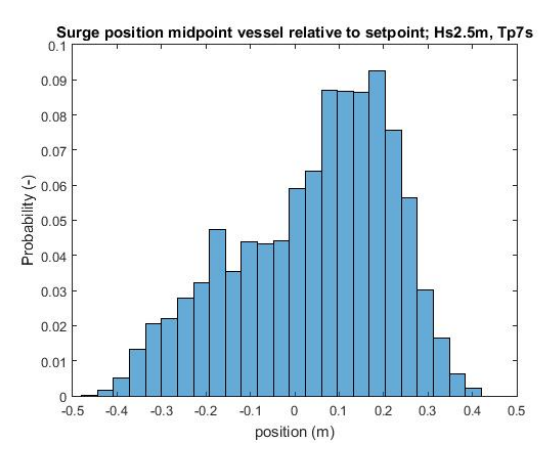


Figure B.7: Dynamic surge behavior test 1

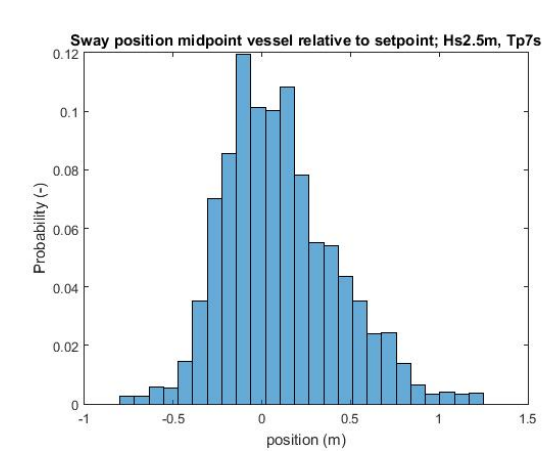


Figure B.8: Dynamic sway behavior test 1

Test 2 DP vessel behavior

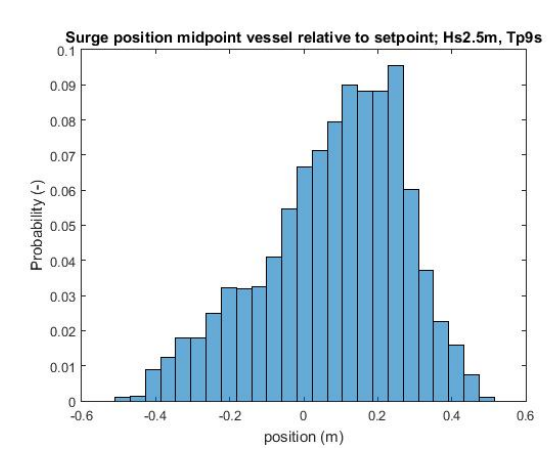


Figure B.9: Dynamic surge behavior test 2

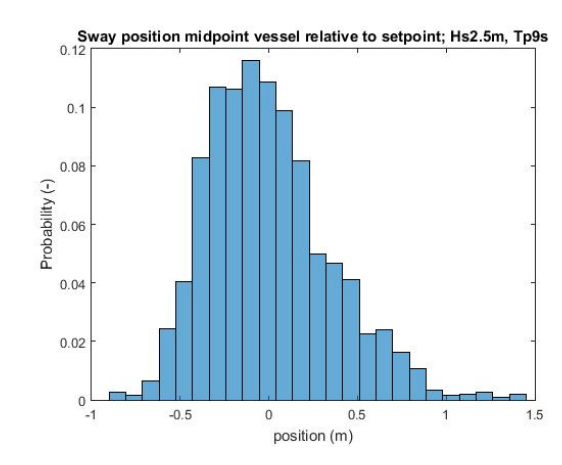
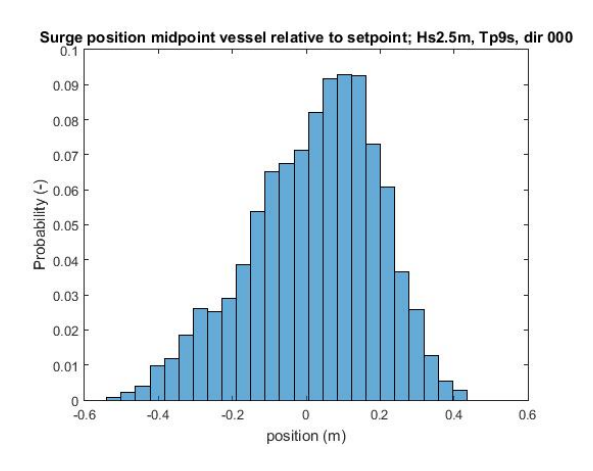
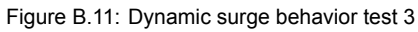


Figure B.10: Dynamic sway behavior test 2

90 B. Vessel details

Test 3 DP vessel behavior





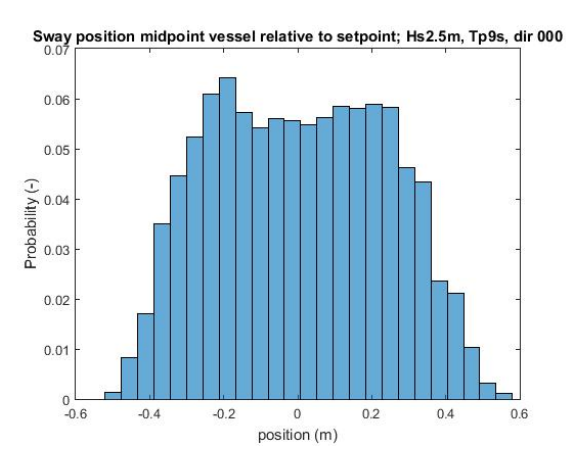


Figure B.12: Dynamic sway behavior test 3



Hydraulic Gripper Frame details

C.0.1. Gripper frame specifications

Detail	Value	unit
Cylinder diameter	0.3	m
Rod diameter	0.25	m
Number of cylinders per direction	2	(-)
Max valve position	+/-0.025	m
Natural frequency	20	Hz
Damping ratio	0.75	(-)
Valve gain	0.0025	V/m
Position x relative to vessel rotation point	20	m
Position y relative to vessel rotation point	30	m

Table C.1: Gripper frame specifications [Boskalis]

C.0.2. Model verification hydraulic gripper frame

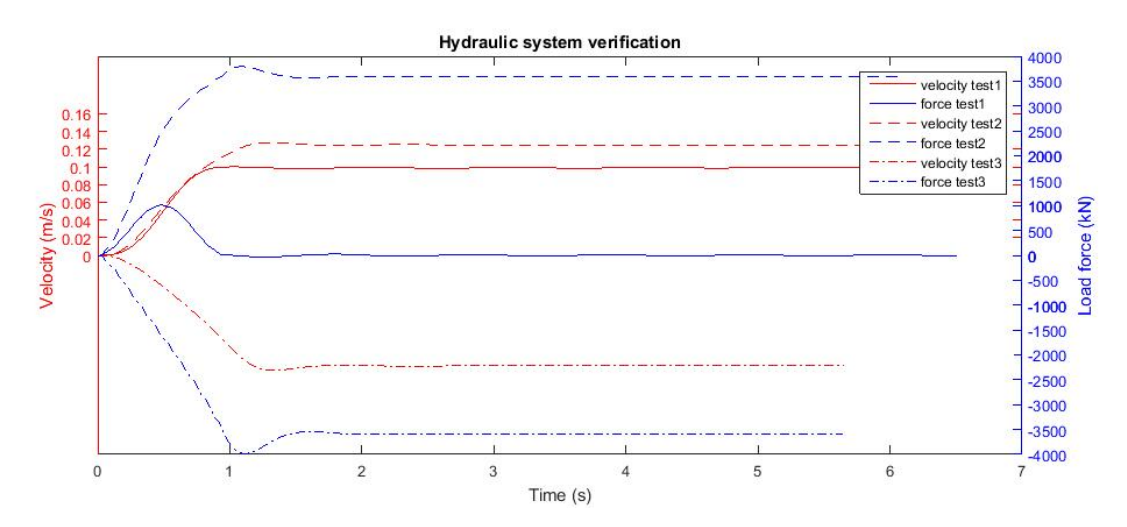
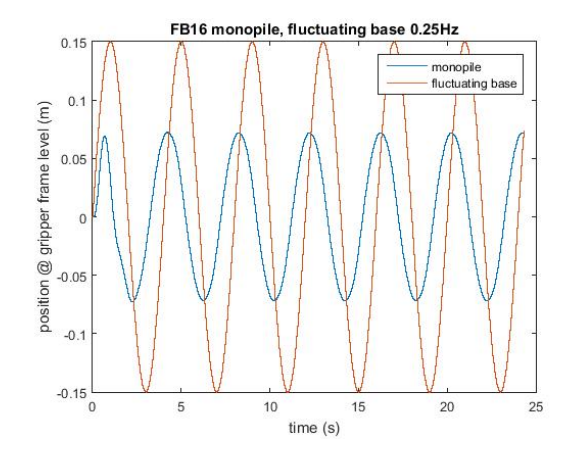


Figure C.1: Hydraulic system verification

C.0.3. Model verification hydraulic gripper frame-monopile combination FB16 $\,{ m Plots}$



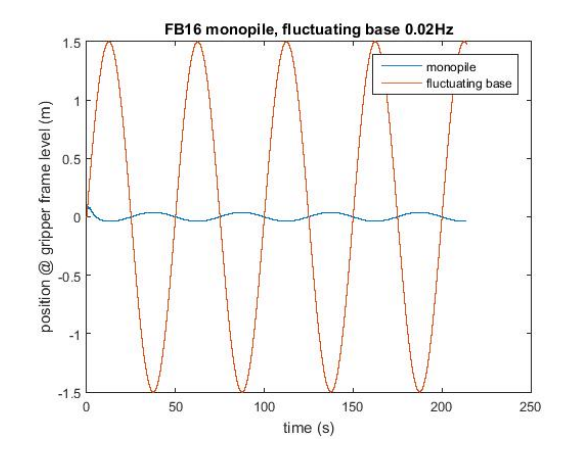


Figure C.2: FB16 gripper frame test 1

Figure C.3: FB16 gripper frame test 2

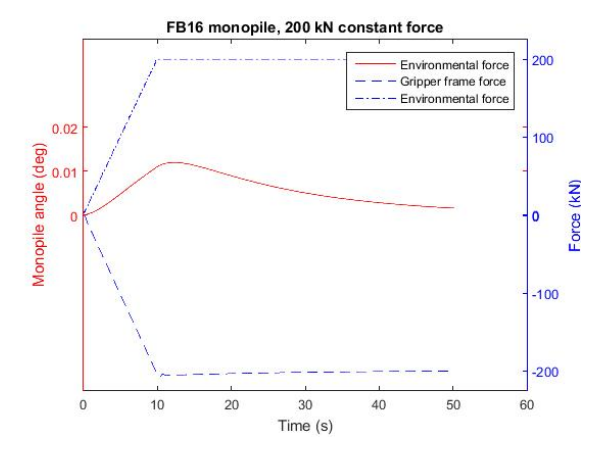


Figure C.4: FB16 gripper frame test 3

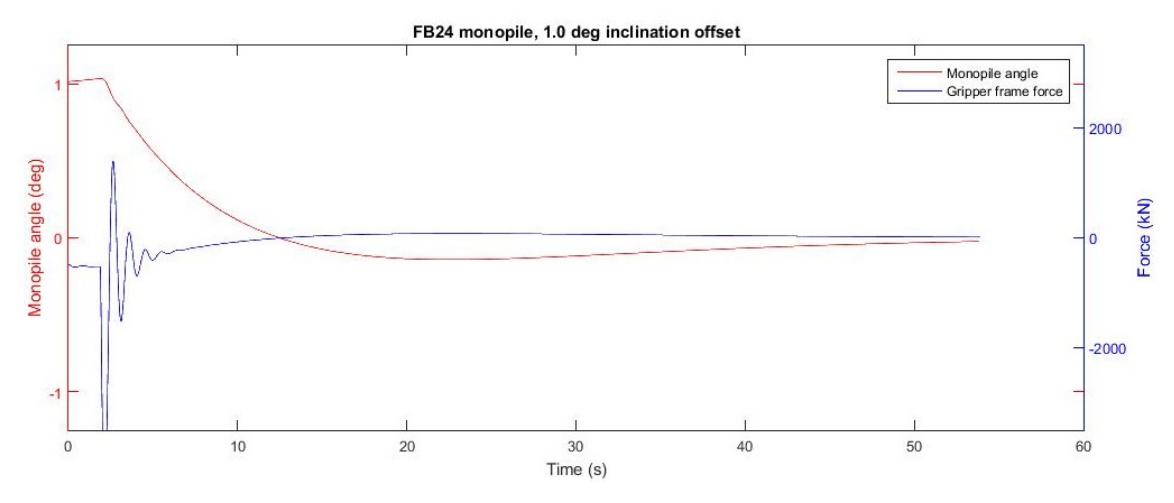
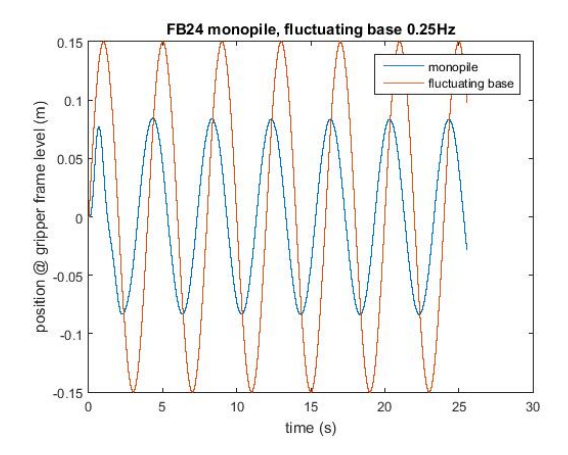


Figure C.5: FB16 gripper frame test 4

FB24 Plots



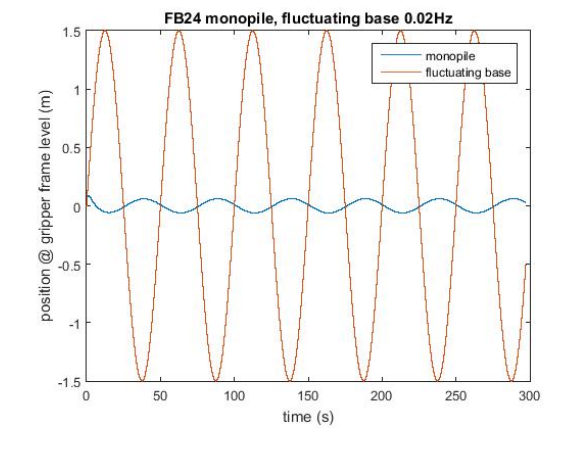


Figure C.6: FB24 gripper frame test 1

Figure C.7: FB24 gripper frame test 2

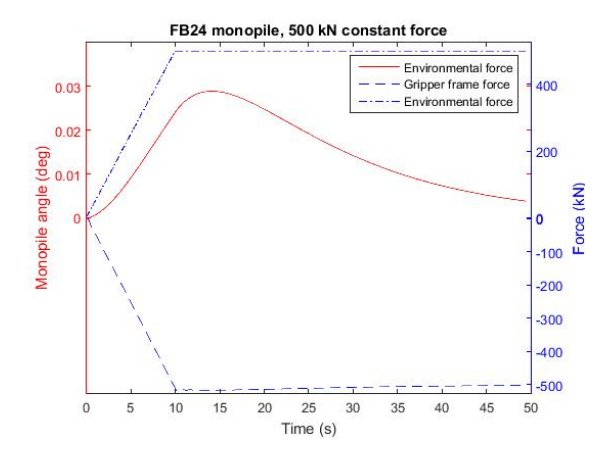


Figure C.8: FB24 gripper frame test 3

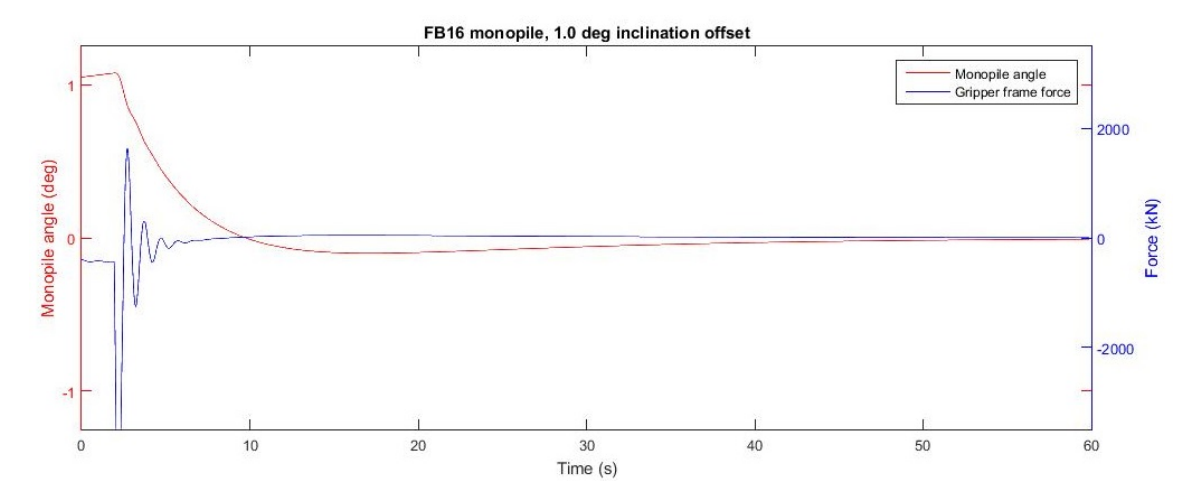
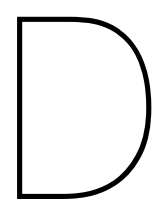


Figure C.9: FB24 gripper frame test 4



Monopile details

D.0.1. Monopile propertiesMonopile properties according figure 3.1:

FB24 main properties			
Designation	Symbol	Magnitude	Magnitude
Total length	L6	m	97
External diameter	D _{e-24}	m	10.0
Radius of gyration	L5	m	28.24
Mass monopile	M _{mp-24}	mT	1653.0
Mass trapped water	M_{tw-24}	mT	3170.0
Soil penetration depth	L1	m	4
Distance soil to point of rotation	L2	m	3.2
Water depth	L3	m	41
Transverse CoG monopile	L4	m	45.1
Transverse CoG Hydro hammer	L7	m	105.9
Distance Gripper Frame above water level	L8	m	13
Distance monopile above water level	L9	m	52

Table D.1: FB24 main specifications

FB16 main properties			
Designation	Symbol	Magnitude	Magnitude
Total length	L6	m	67
External diameter	D _{e-16}	m	7.4
Radius of gyration	L5	m	19.52
Mass	M _{mp-16}	mT	870.0
Mass trapped water	M _{tw-16}	mT	886.0
Soil penetration depth	L1	m	3
Distance soil to point of rotation	L2	m	2.4
Water depth	L3	m	21
Transverse CoG monopile	L4	m	32.3
Transverse CoG Hydro hammer	L7	m	75.9
Distance Gripper Frame above water level	L8	m	13
Distance monopile above water level	L9	m	43

Table D.2: FB16 main specifications

96 D. Monopile details

D.0.2. Monopile verification plots

Both monopile are given an inclination offset of 0.1 and 1 degree. The monopile is free falling. Simulation data is check with data from Boskalis.

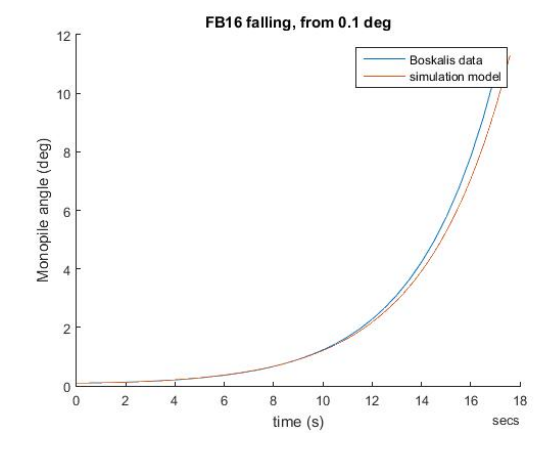


Figure D.1: 870 mT monopile falling from 0.1 deg

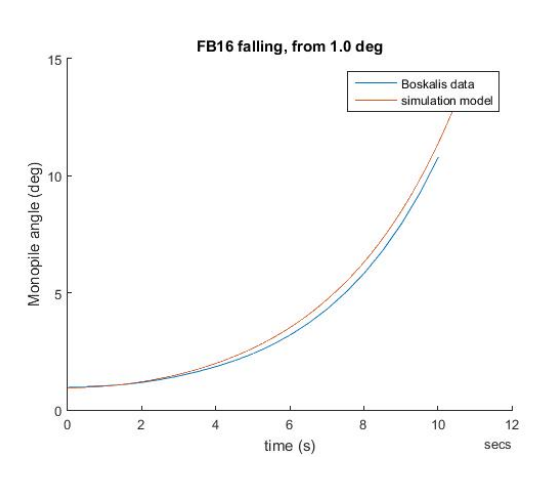


Figure D.2: 870 mT monopile falling from 1.0 deg

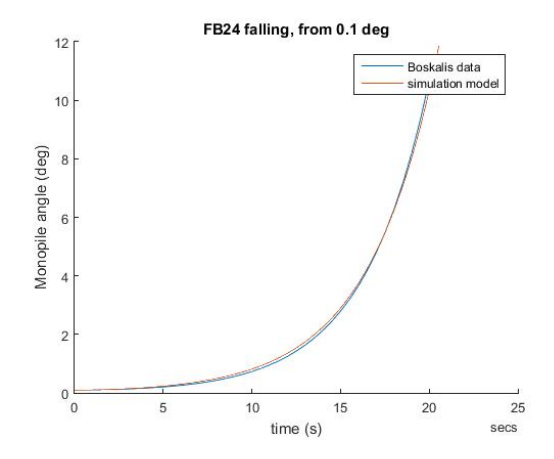


Figure D.3: 1653 mT monopile falling from 0.1 deg

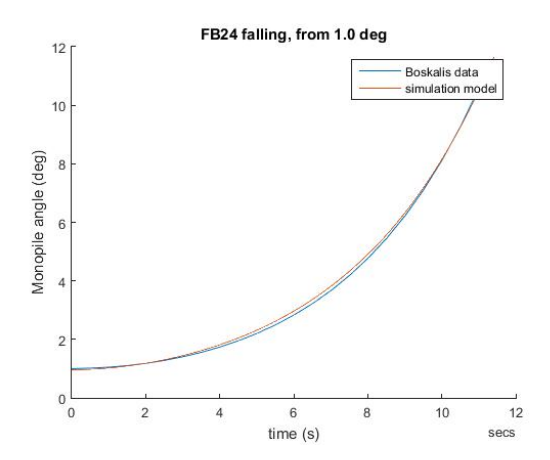
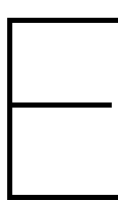


Figure D.4: 1653 mT monopile falling from 1.0 deg



Hydro hammer details

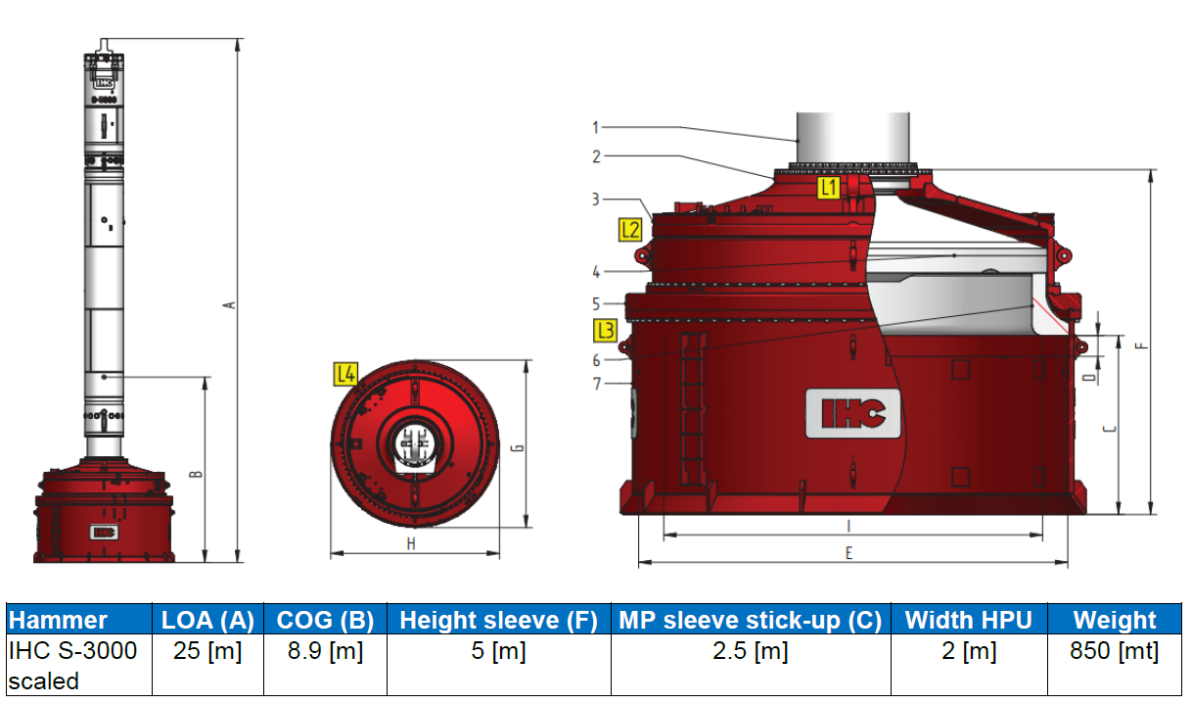
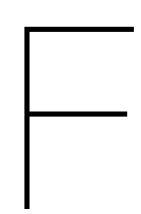


Figure E.1: Drawing and details of the 850 mT hydro hammer



Simulation results

Detail	Value	unit
Current direction	150 to	deg.
Wave direction	330 from	deg.
Wind direction	330 from	deg.

Table F.1: Environmental force direction case 1-4

Test case	Mono-pile	Waves	Current	Wind
1	FB16	Hs2.5, Tp7	2.5 kn	19 kn
2	FB16	Hs2.5, Tp9	2.5 kn	19 kn
3	FB24	Hs2.5, Tp7	2.5 kn	19 kn
4	FB24	Hs2.5, Tp9	2.5 kn	19 kn

Table F.2: Overview test cases 1-4

Detail	Value	unit
Current direction	180 to	deg.
Wave direction	000 from	deg.
Wind direction	000 from	deg.

Table F.3: Environmental force direction case 5

Test case	Mono-pile	Waves	Current	Wind
5	FB24	Hs2.5, Tp9	2.5 kn	19 kn

Table F.4: Overview test case 5

The state of the s

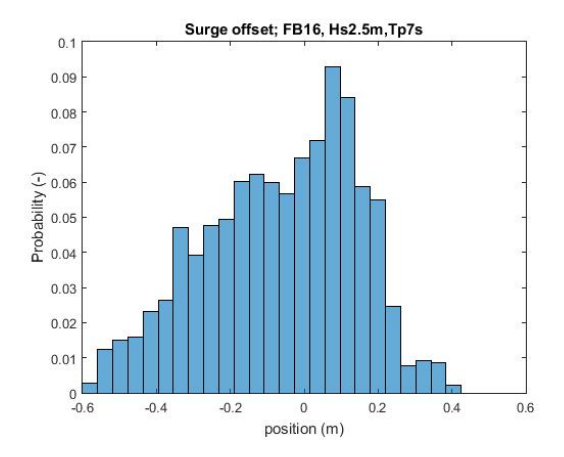


Figure F.1: FB16, case 1, plot 1

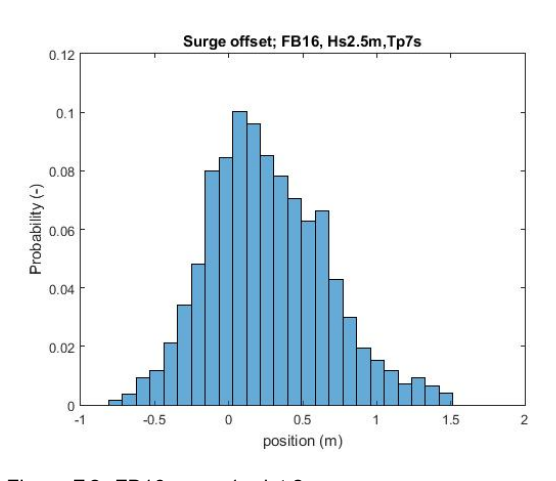


Figure F.2: FB16, case 1, plot 2

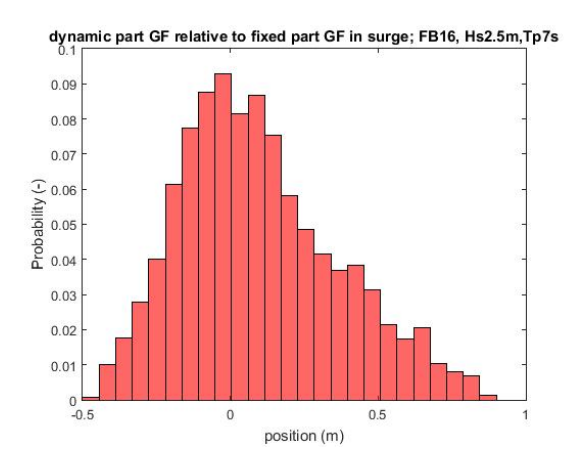


Figure F.3: FB16, case 1, plot 3

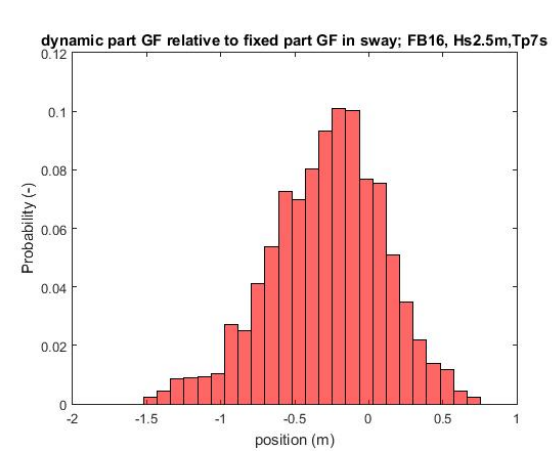


Figure F.4: FB16, case 1, plot 4

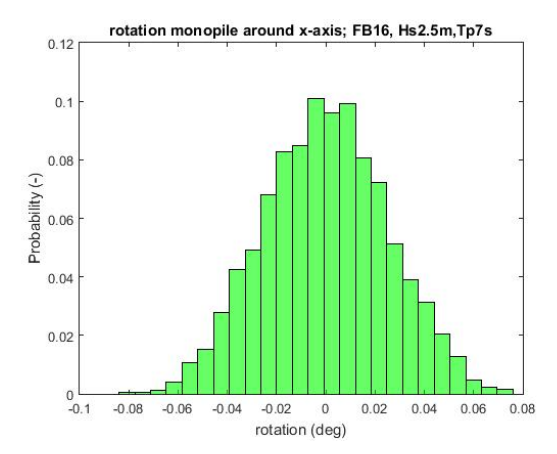


Figure F.5: FB16, case 1, plot 5

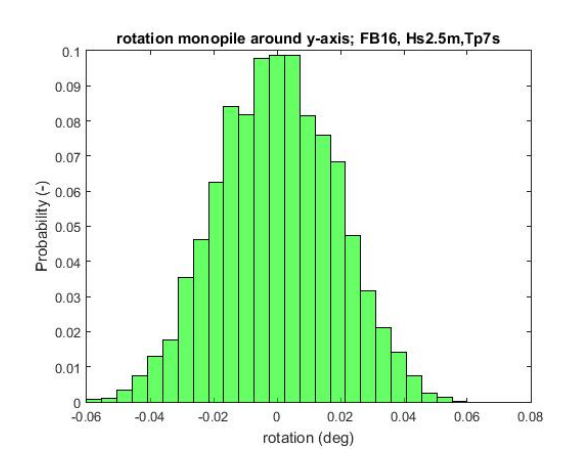


Figure F.6: FB16, case 1, plot 6

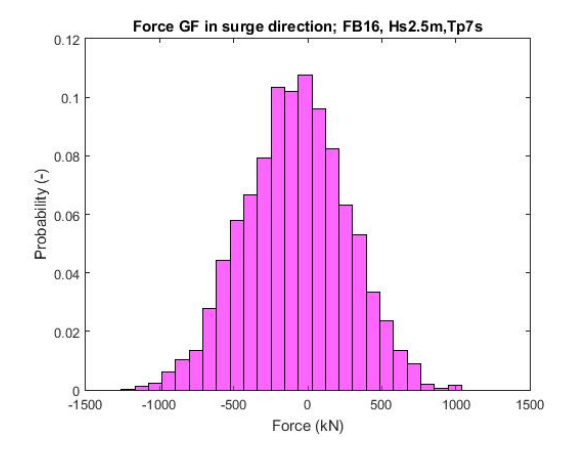


Figure F.7: FB16, case 1, plot 7

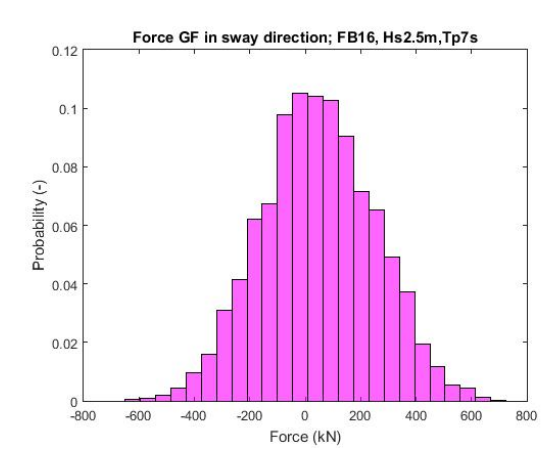


Figure F.8: FB16, case 1, plot 8

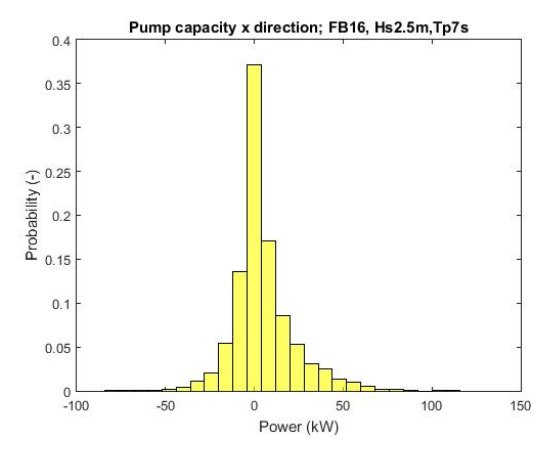


Figure F.9: FB16, case 1, plot 9

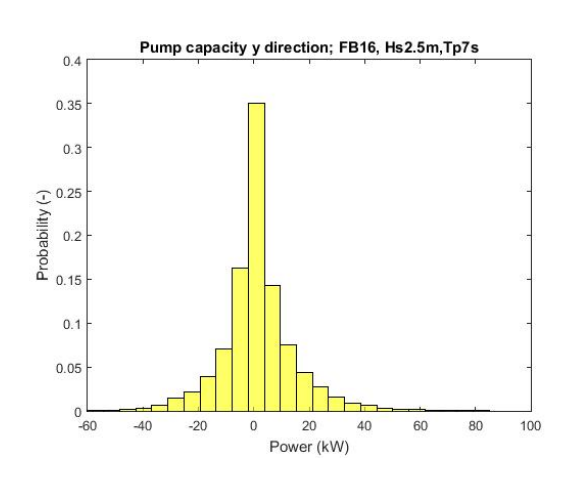


Figure F.10: FB16, case 1, plot 10

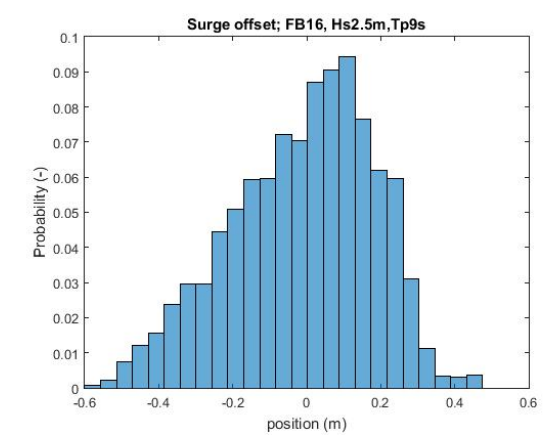


Figure F.11: FB16, case 2, plot 1

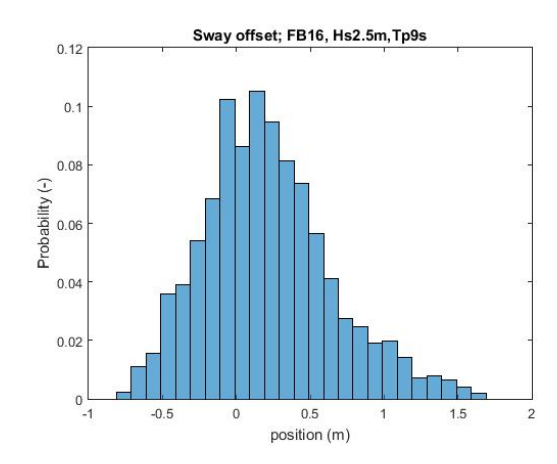


Figure F.12: FB16, case 2, plot 2

102 F. Simulation results

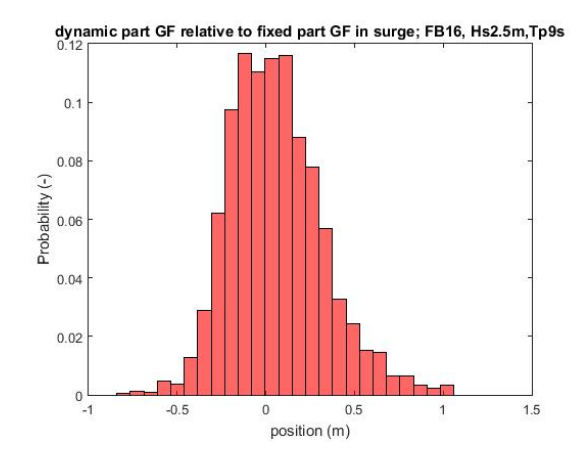


Figure F.13: FB16, case 2, plot 3

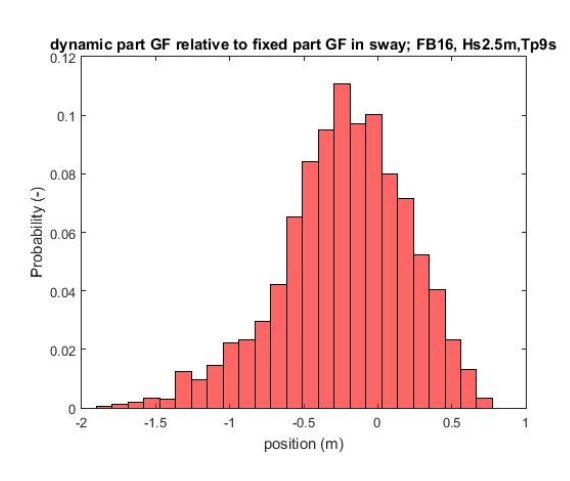


Figure F.14: FB16, case 2, plot 4

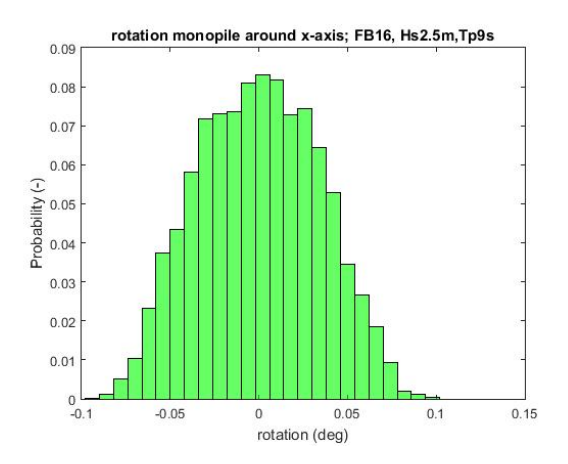


Figure F.15: FB16, case 2, plot 5

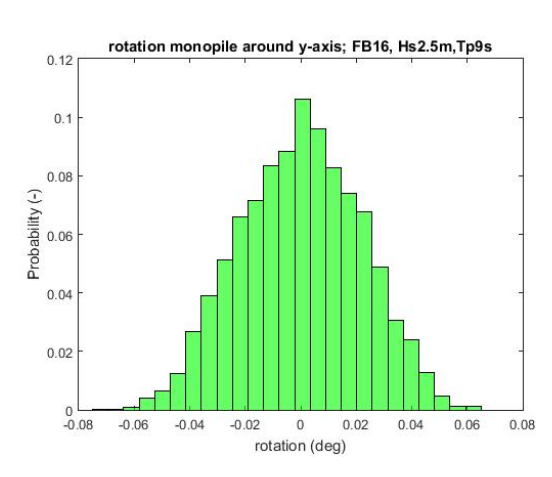


Figure F.16: FB16, case 2, plot 6

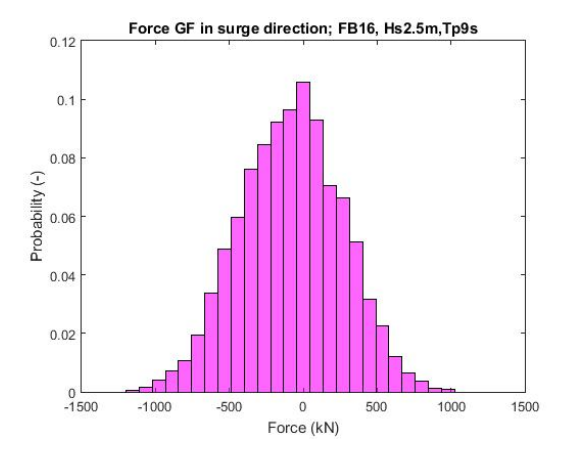


Figure F.17: FB16, case 2, plot 7

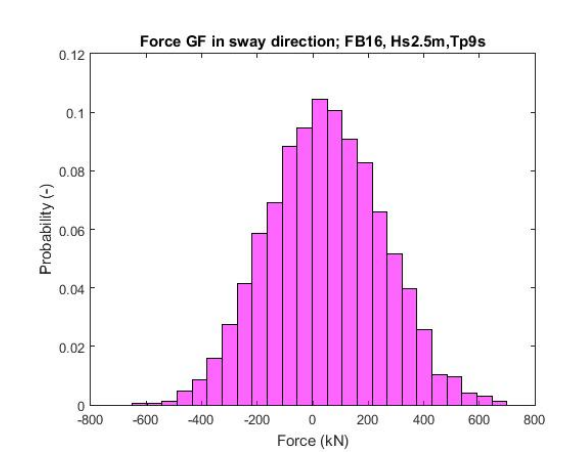


Figure F.18: FB16, case 2, plot 8

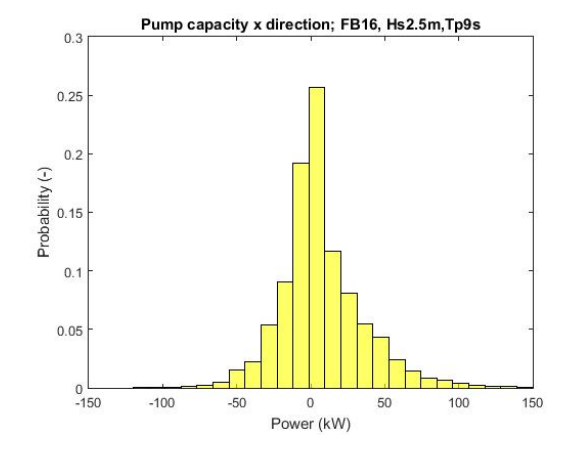


Figure F.19: FB16, case 2, plot 9

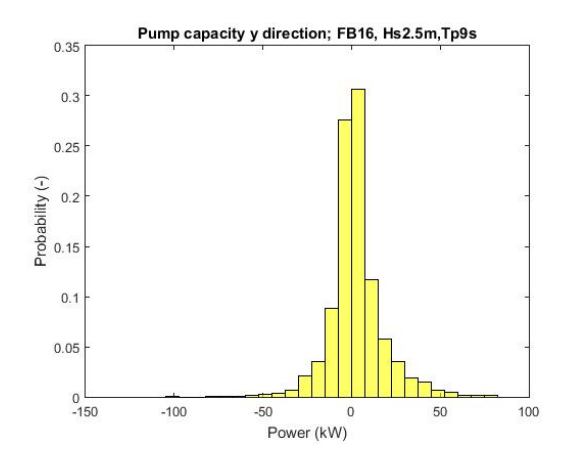


Figure F.20: FB16, case 2, plot 10

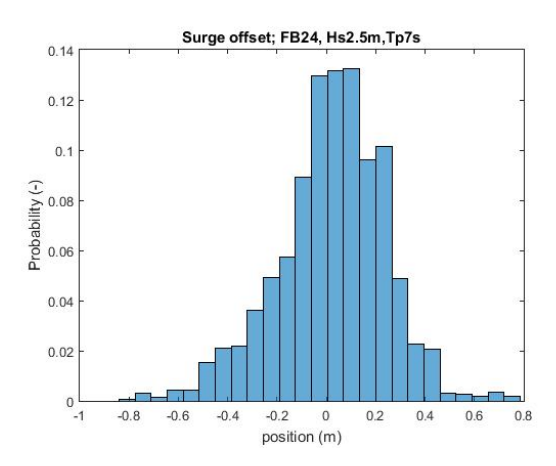


Figure F.21: FB24, case 3, plot 1

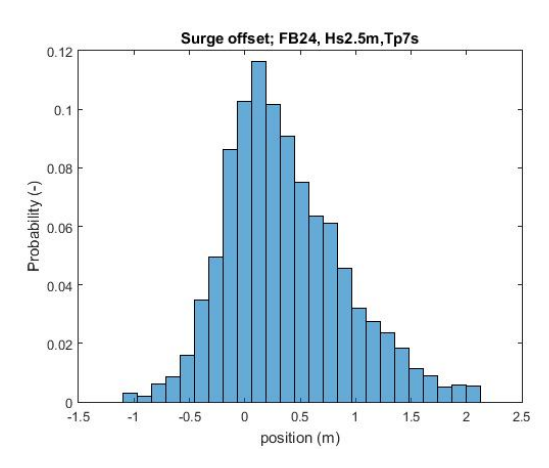


Figure F.22: FB24, case 3, plot 2

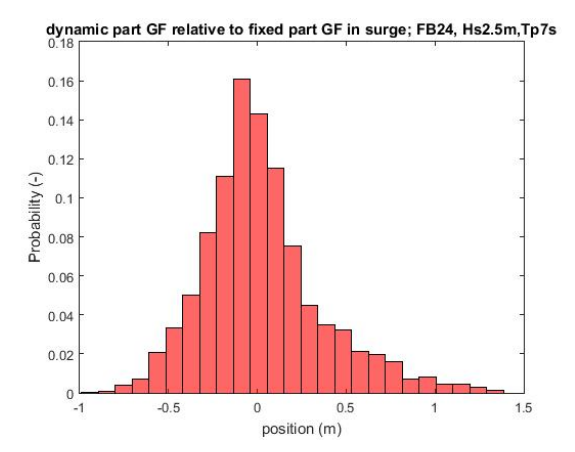


Figure F.23: FB24, case 3, plot 3

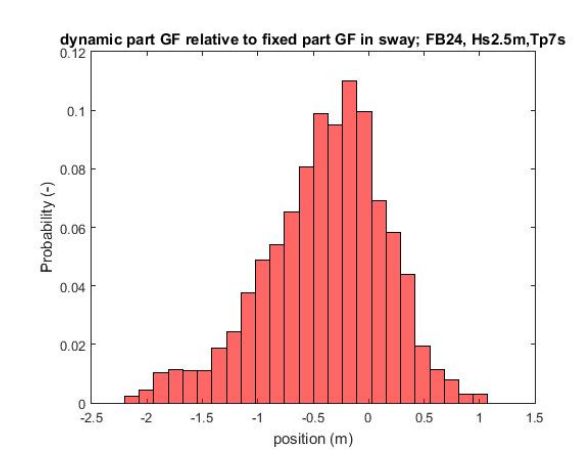


Figure F.24: FB24, case 3, plot 4

104 F. Simulation results

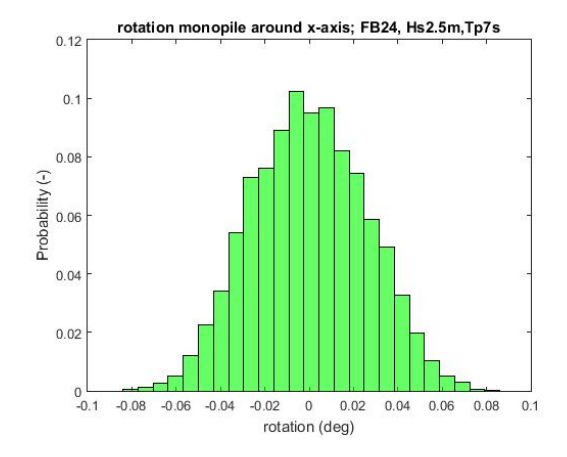


Figure F.25: FB24, case 3, plot 5

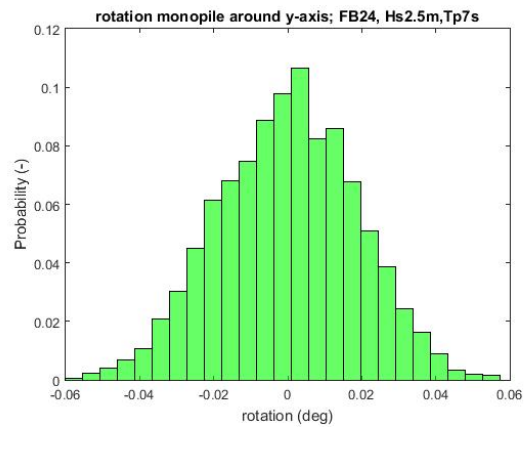


Figure F.26: FB24, case 3, plot 6

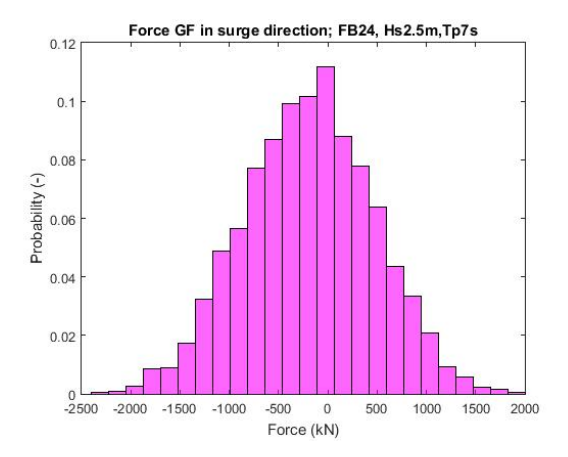


Figure F.27: FB24, case 3, plot 7

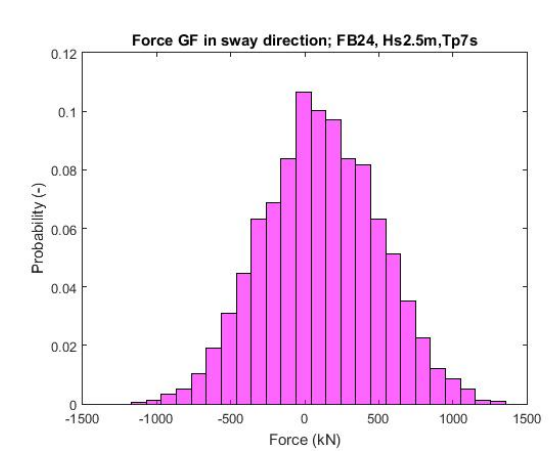


Figure F.28: FB24, case 3, plot 8

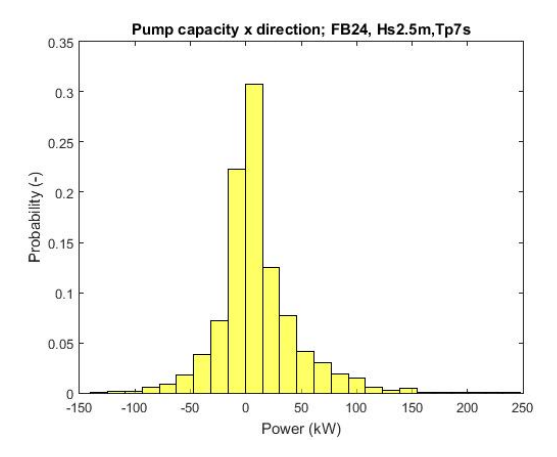


Figure F.29: FB24, case 3, plot 9

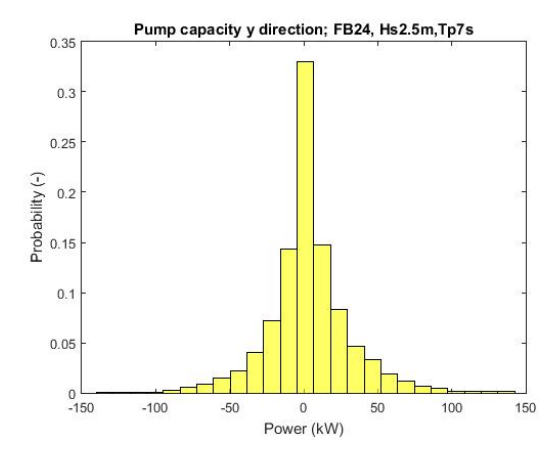


Figure F.30: FB24, case 3, plot 10

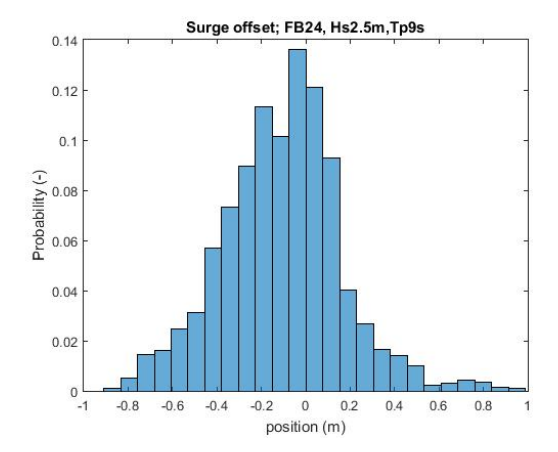


Figure F.31: FB24, case 4, plot 1

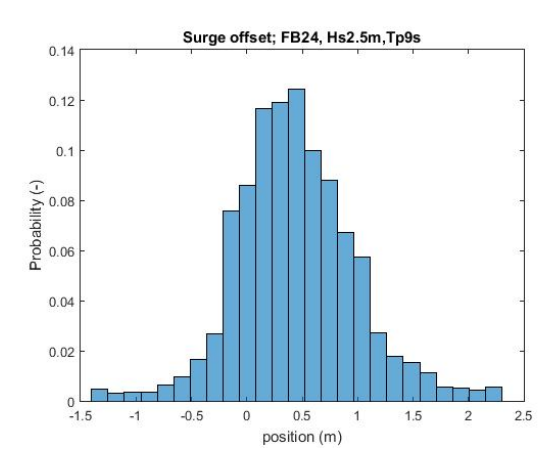


Figure F.32: FB24, case 4, plot 2

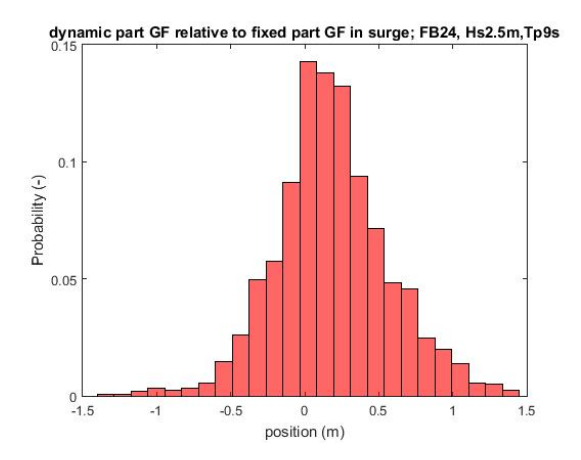


Figure F.33: FB24, case 4, plot 3

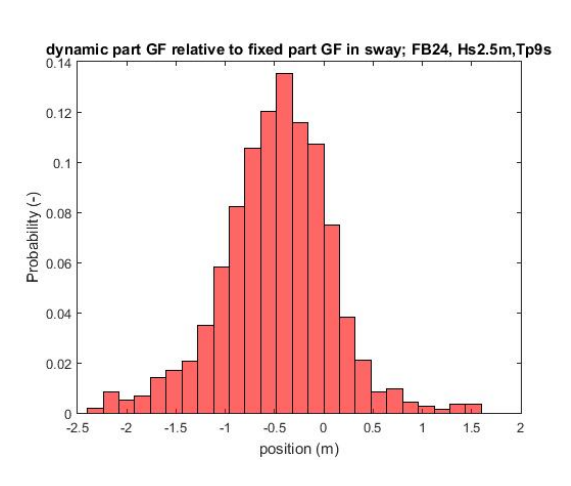


Figure F.34: FB24, case 4, plot 4

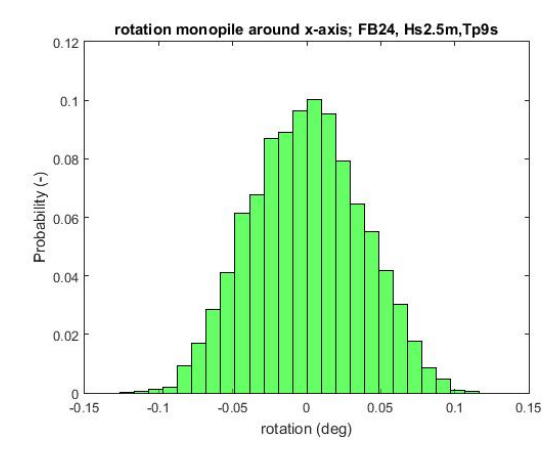


Figure F.35: FB24, case 4, plot 5

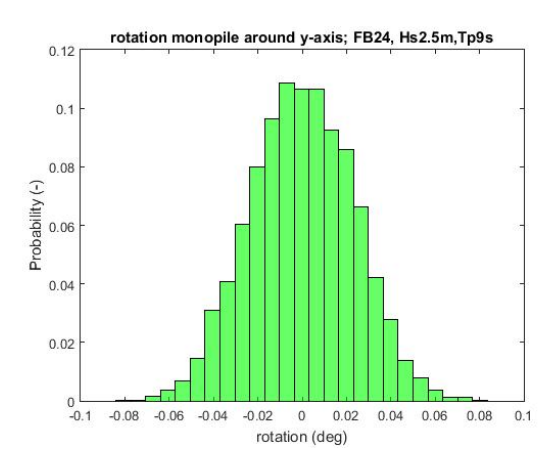


Figure F.36: FB24, case 4, plot 6

106 F. Simulation results

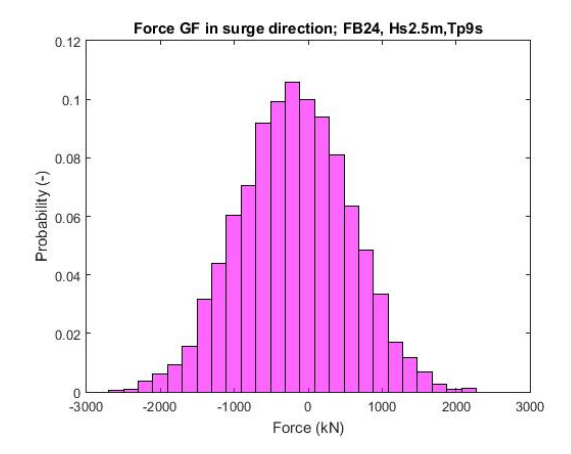


Figure F.37: FB24, case 4, plot 7

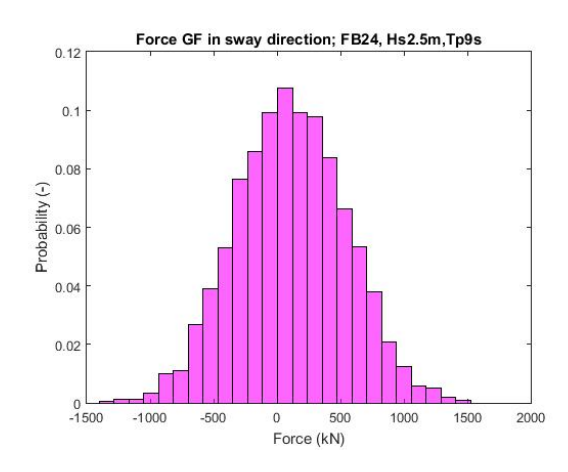


Figure F.38: FB24, case 4, plot 8

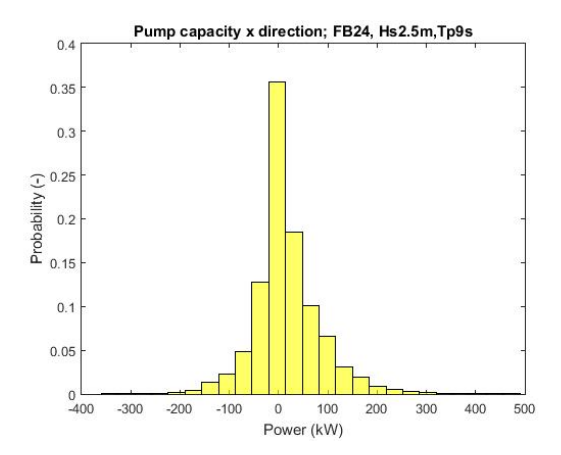


Figure F.39: FB24, case 4, plot 9

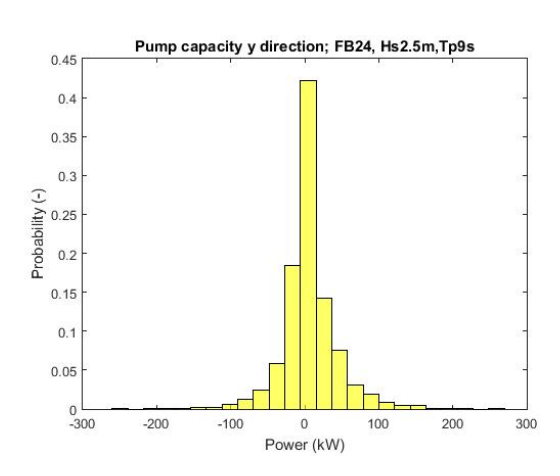


Figure F.40: FB24, case 4, plot 10

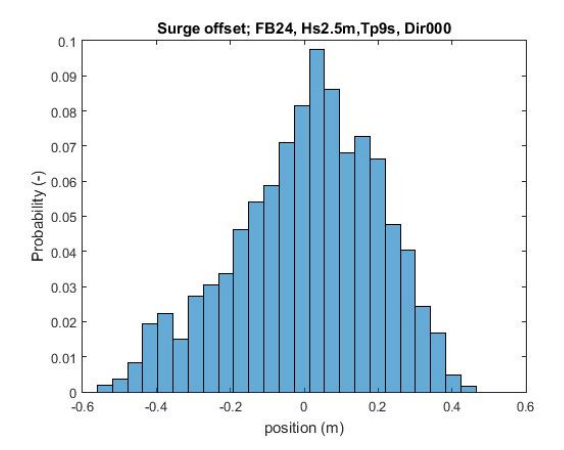


Figure F.41: FB24, case 4, plot 1

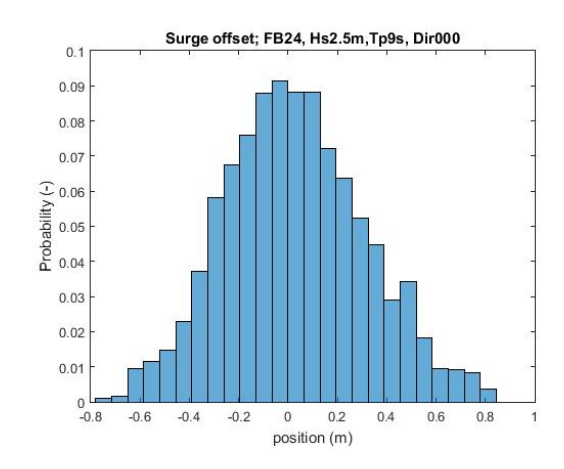


Figure F.42: FB24, case 4, plot 2

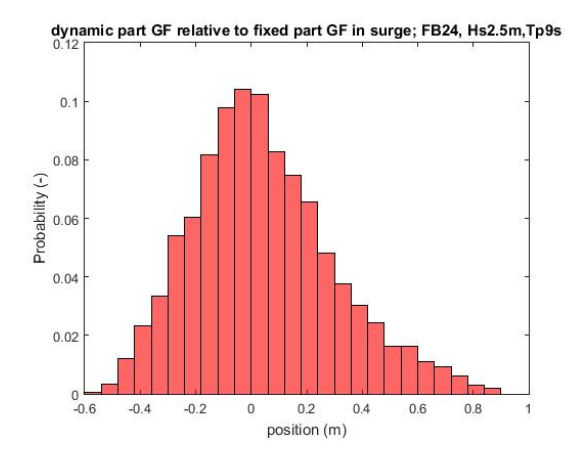


Figure F.43: FB24, case 4, plot 3

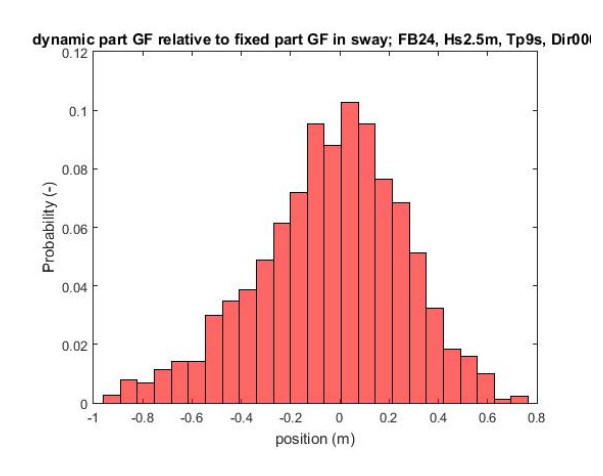


Figure F.44: FB24, case 4, plot 4

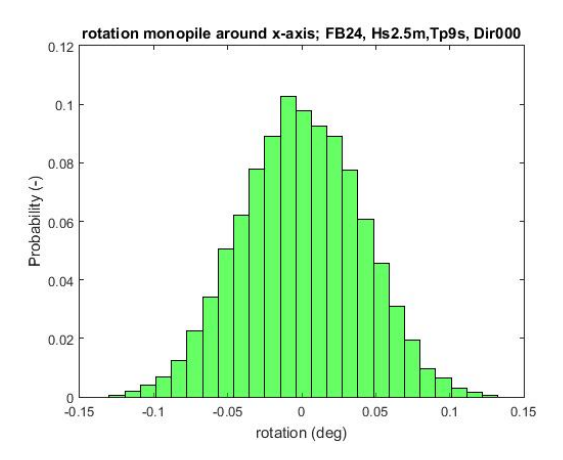


Figure F.45: FB24, case 4, plot 5

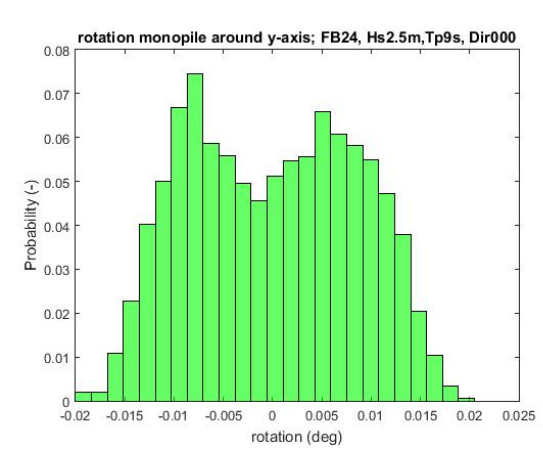


Figure F.46: FB24, case 4, plot 6

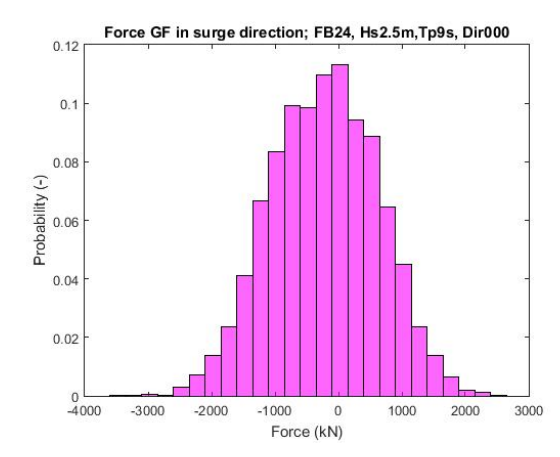


Figure F.47: FB24, case 4, plot 7

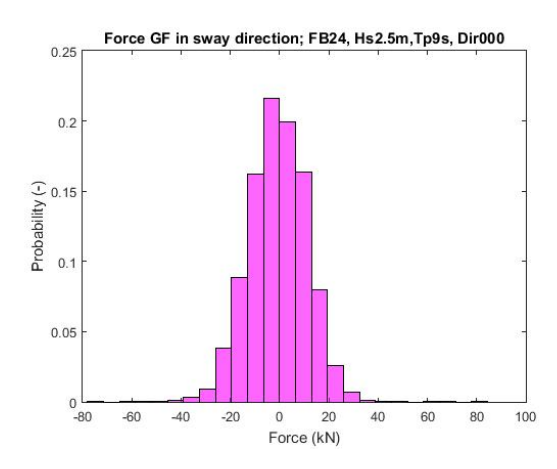
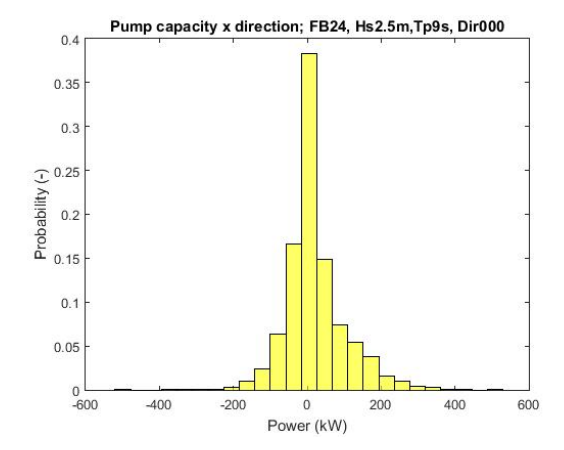
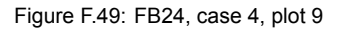


Figure F.48: FB24, case 4, plot 8

To F. Simulation results





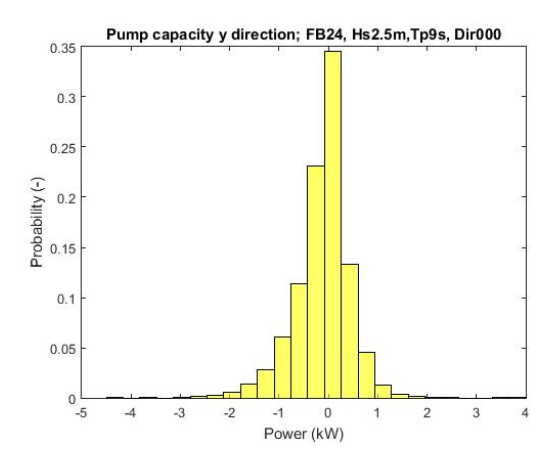


Figure F.50: FB24, case 4, plot 10

Bibliography

- [1] DNV 2014. Design of offshore wind turbine structures. may 2014.
- [2] A. Al-Mamun. Design of controller for the dual-stage actuator in hard disk drive using internal model approach. *National University of Singapore*, 2002.
- [3] E. A. Alderlieste. Experimental modelling of lateral loads on large diameter mono-pile foundations in sand. 2011. doi: uuid:2dc40e3f-d333-4d23-ad4f-24187aeae03d.
- [4] Elena Ambrosovskaya Andrey Loginov, Anton Proskurnikov and Dmitry Romaev. Dp systems for track control of dredging vessels. 9th IFAC Conference on Manoeuvring and Control of Marine Craft, The International Federation of Automatic Control, September 19-21, 2012. Arenzano, Italy, 2012.
- [5] Det Norske Veritas Classication A/S. Foundations classification notes no 30.4. 1992.
- [6] Nederlandse WindEnergie Associatie. Nwea visie 2030, 2018. URL http://www.nwea.nl/images/PDFs/NWEA-Visie-2030.pdf. Last accessed 13 August 2018.
- [7] Karl Johan Astrom. Feedback systems, an introduction for scientists and engineers. *Lund University*, 2007.
- [8] F.C. Bakker. A conceptual solution to instable dynamic positioning during offshore heavy lift operation. *Repository TU Delft*, 2015.
- [9] Eric Bogatin. Rule of thumb 1: Bandwidth of sigfrom time, 2013. URL nal its rise https://www.edn. com/electronics-blogs/bogatin-s-rules-of-thumb/4424573/ Rule-of-Thumb--1--The-bandwidth-of-a-signal-from-its-rise-time. Last accessed 25 September 2018.
- [10] K.T. Brødbæk. Review of p-y relationships in cohesionless soil. *Aalborg University, DCE Technical Report No.* 57, 2009.
- [11] L.G. Buitendijk. Floating installation of offshore wind turbine foundations. *TU Delft, The Netherlands*, 2016.
- [12] Martin CHOUX and Geir HOVLAND. Design of a hydraulic servo system for robotic manipulation. *University of Agder Department of Engineering Sciences/Mechatronics*, 2008.
- [13] Dynamic Positioning Committee. Dp operations guidance. *Marine Technology Society*, 2015.
- [14] DNVGL. Dynamic positioning vessel design philosophy guidelines, recommended practice. 2015.
- [15] Olav Egeland and Jan Tommy Gravdahl. Modeling and simulation for automatic control. *Marine Cybernetics AS*, 2002. doi: ISBN82-92356-01-0.
- [16] E. el Amam. Dp control systems, guest lecture oe5663 dynamic positioning. *TU Delft, Offshore Engineering*, 2015.
- [17] Eneco. Animatie van transport- en installatieschip aeolus, 2018. URL https://www.youtube.com/watch?v=JV9PykR5bHo. Last accessed 31 August 2018.

110 Bibliography

[18] esru.strath. Installation of mono-piles, 2018. URL http://www.esru.strath.ac.uk/ EandE/Web_sites/14-15/XL_Monopiles/technical.html. Last accessed 10 March 2018.

- [19] Control Tuturials for Matlab/Simulink. Inverted pendulum: Digital controller design, 2018. URL http://ctms.engin.umich.edu/CTMS/index.php?example= InvertedPendulum§ion=ControlDigital. Last accessed 31 August 2018.
- [20] Thor I. Fossen. Handbook of marine craft hydrodynamics and motion control. *Marine Cybernetics AS*, 2011. doi: ISBN 978-1-119-99149-6.
- [21] National Geographic. Effect of global warming, 2018. URL https://www.nationalgeographic.com/environment/global-warming/global-warming-effects/. Last accessed 4 March 2018.
- [22] Poulus H. and Hull T. The role of analytical geomechanics in foundation engineering. *In Foundation Eng.: Current principles and Practices*, pages 1578–1606, 1989.
- [23] E. Frickel H. Cozijn. Past, present and future of hydrodynamic research for dp applications. *Maritime Research Institute Netherlands (MARIN)*, 2015.
- [24] J. Brinch Hansen. The ultimate resistance of rigid piles against transversal forces,. Akademiet for de Tekniske Videnskaber, Geoteknisk Institut, Geo-technical Institute Denmark, Bulletin no. 12, Copenhagen., 1961.
- [25] Hydraulics and Pneumatics. Hydromechanical resonant frequency and cylinder speed, 2018. URL https://www.hydraulicspneumatics.com/cylinders-amp-actuators/hydromechanical-resonant-frequency-and-cylinder-speed. Last accessed 31 August 2018.
- [26] W.W. Massie J.M.J. Journée and R.H.M.Huijsmans. Offshore hydromechanics, third edition. 2015.
- [27] J. Jonkman and W. Musial. Offshore code comparison collaboration (oc3) for iea task 23 offshore wind technology and deployment. *Technical Report*, NREL/TP-5000-48191, 2010.
- [28] M. Karsten. Statistical description of wave parameters, 2007. URL http://www.coastalwiki.org/wiki/Statistical_description_of_wave_parameters. Last accessed 28 September 2018.
- [29] Peng Kemao. Dual-stage actuator design for hdd systems via cnf control. *University of Singapore*, *Singapore* 11 75 76, 2002.
- [30] Lin Li. Dynamic analysis of the installation of monopiles for offshore wind turbines. *Norwegian University of Science and Technology*, pages 24–25, 2016. doi: ISBN 978-82-326-1616-9.
- [31] A. M. Lyapunov. The general problem of the stability of motion, doctoral dissertation. *Univ. Kharkov*, 1892.
- [32] Macgregor. Combined expertise cuts wind turbine installation times, 2018. URL https://www.macgregor.com/news-insights/news-articles/2018/combined-expertise-cuts-wind-turbine-installation-times/. Last accessed 31 August 2018.
- [33] United Nations. Adoption of the paris agreement. pages 1–32, 2015. doi: FCCC/CP/2015/L.9/Rev.1.
- [34] Maritime Research Institute Netherlands. Dynamic positioning. URL http://www.marin.nl/web/Research-Topics/Manoeuvring-DP/Dynamic-Positioning.htm. Last accessed 14 August 2018.

Bibliography 111

[35] J.A. Pinkster. Low frequency second order wave exciting forces on floating structures. *University of Agder*, 2017.

- [36] Michael Ruderman. Full- and reduced-order model of hydraulic cylinder for motion control. *University of Agder*, 2017.
- [37] Moné C. Maples B. Hand M. Simith, A. 2013 cost of wind energy review. *National Renewable Energy Laboratory (NREL), CO, USA.*, 2015. doi: TechnicalReportNREL/TP-5000-63267.
- [38] T. Staal. Monopile installation with a dynamically positioned vessel and motion compensated outrigger. *Delft University of Technology*, 2016.
- [39] Dr. Richard I. Stephens. Wind feedforward: blowing away the myths. *DYNAMIC POSI-TIONING CONFERENCE*, 2011.
- [40] René Huijsmans Tim Bunnik. Identification of quadratic responses of floating structures in waves. *Maritime Research Institute Netherlands*, 2006.
- [41] H.K. Veldkamp and J. van der Tempel. Influence of wave modelling on the prediction of fatigue for offshore wind turbines. *Wind Energy*, 2005.
- [42] American Petroleum Institute. Washington D.C. Recommended practice for planning, designing, and constructing fixed offshore platforms working stress design. 1993. doi: APIRP2A-WSD,21.edition.
- [43] R. Wouts. Heavy lifting on dp, and the role of simulators. Imca seminar paper, 2015.
- [44] Wiser R. Hand M. Hohmeyer O. Ineld D. Jensen P. H. Nikolaev V. O'Malley M. Sinden G. Zervos A. Yang, Z. Ipcc special report on renewable energy sources and climate change mitigation. *National Renewable Energy Laboratory (NREL)*, CO, USA., 2011.